Paper T35

Born Statistics, Local Records, and Entanglement in Holosphere Theory

Connected loading, protected circulation, and reciprocal readout

Michael John Sarnowski
Independent Researcher, Holosphere Theory Project
ORCID: 0009-0005-4210-6027
thilel@charter.net

October 21, 2026
Comprehensive derivation edition 2.1
Wording revised October 28, 2026

Abstract

This paper assembles the retained Holosphere Born-rule and entanglement arguments into explicit derivation chains. Reversible two-sided histories select a squared positive mode under a stated measure. A separate occupied-contact Hamiltonian gives conserved inventories, reciprocal energy transfer, protected circulation, and a connected finite-time loading and external-readout mechanism. Supporting derivations distinguish finite partner selection from mechanical binding, carried phase from analyzer rotation, two-mode compression from a closed physical receiver, and stationary traffic from first records. Matched receiving channels and capacity competition provide a conditional route from amplitudes to event fractions; the native tetrahedral comparison and feeder experiment establish different, explicitly bounded physical results. The entanglement account derives the supplied joint-state benchmark, its classical alternatives, complete Bell accounting, rotating-contact event measures, conservative repair, and the additional premises of a guidance-based completion. Each argument is given one substantive location and linked to its dependencies. The work preserves genuine model-level preparation, memory, loading and reading results without treating an assigned reference measure, tensor state, or recording protocol as an autonomous microscopic derivation. Autonomous reference generation, a physical arbitrary-axis analyzer, persistent external recording, and the complete native two-wing law remain separate connections. Controlled, calibrated tests could establish whether measurement and event-selection effects cause an apparent Bell violation in a specified apparatus; that empirical attribution remains open. The complete common-solver Python program and Windows runner are retained unchanged in this derivation-focused edition.

Keywords and meanings

Term	Meaning in this paper
Born-like statistics	Squared mode fractions under stated preparation and recording conditions.
Native dynamics	Consequences of the declared contact Hamiltonian, not an experimentally verified constituent theory.
Loading	Inventory and phase information arriving through evolving contacts from outside the recording core.
Protected circulation	A signed loop field unable to cross its zero boundary while a specified energy inequality holds.
External native reader	Additional occupied sites and fields, outside the core, that react under the same equations.
Complete trial	Every launched preparation, including ties, unresolved signals, and later failures.
Entanglement benchmark	An explicitly supplied quantum joint-state calculation, distinguished from native derivation.

1 Plain-language summary and the physical question

The paper follows the reasoning from source preparation and admissible histories to receiving modes, physical records, and joint measurements. Its two probability routes remain separate: counting matched histories explains a square under a stated measure, while a signal–reference comparison explains record fractions under a stated preparation. They are not multiplied together or presented as if either had supplied the other's physical assumptions.

The most developed connected physical segment is a loading-and-reading experiment in the model. A prepared pattern begins on four feeder sites, not in the recording core. The contact dynamics carry that pattern inward. The core then develops a circulation whose direction depends on the actual signal and reference fractions. Two side contacts, already connected and allowed to react, develop a field difference that reports the same direction during an initial operating interval. Energy and population changes in the feeders, core, side contacts, and remaining host are all retained.

This is stronger than initializing a finished record, reading a variable inside it, and assuming that a future loader and instrument will preserve the result. The new calculation includes loading and reader reaction in one trajectory. It is also narrower than a permanent detector. The side signal later changes sign in some runs, and the local protection budget can be lost. The useful result is a finite protected loading-and-reading interval, not a settled memory after all loading has ended.

The earlier T14 result answers a different question: why a square can arise in a population of histories. A complete history has an allowed approach and an allowed continuation. When their profiles match, their product is a square. That conditional mathematical result is retained. So are T35's prepared-memory protection theorem, the restricted all-time internal-current theorem, and the earlier three-path writing/readout mechanism. Their assumptions are not silently transferred to the new attached-reader experiment.

The remaining preparation problem is now more precise. The feeder states have fixed inventory, specified relative phase, and an explicitly supplied reference distribution. The new equations transport those data; they do not create the required distribution from an independently operating source. Likewise, the side-contact field difference is a physical variable of the model, but it is not yet a calibrated voltage or a permanent digital event. An autonomous phase-setting and launch process, followed by a reliable macroscopic record, still needs to be derived.

The selected-event examples in Section 8 and Appendix H illustrate how measurement and event-selection effects can create a false impression of nonlocality. What remains unestablished is whether they do so in actual Bell experiments, especially those designed to close the relevant loopholes. The

proposed tests could establish that explanation for a specified protocol if a calibrated local mechanism predicts its apparent violation together with the complete outcome, no-detection and timing records. Observing detector memory alone would establish a detector effect; connecting it to the Bell inference requires a joint experiment or a sufficiently complete reanalysis of its raw records.

One intuitive analogy

Imagine a small wheel with four feeder arms and two side gauges. Earlier calculations placed the wheel in a prepared state and showed that its direction could be protected. The new calculation starts the prepared material in the feeder arms. Its arrival turns the wheel, while the side gauges draw from and react on the same machinery. For a useful interval, the wheel's direction and the gauges agree. Later, returning motion can move a gauge the other way. A correct account must therefore specify when the reading occurs and keep track of the motion stored outside the wheel. Counting every gauge reading is also different from counting only the clearest ones. Two wheels can share an earlier preparation, but their full paired readings still need a separate calculation. The analogy explains those jobs; it adds no friction, latch, random choice, or unmodeled energy sink.

What is established

The paper supplies conditional square-law mathematics, native protected preparations, and a connected short-time loading–protection–external-response theorem. The new reader is included dynamically. Correct permanent quantum-record probabilities, autonomous generation of the reference ensemble, and a native explanation of complete entangled laboratory statistics are not claimed. Calibrated experiments or sufficiently complete raw-data tests could determine whether measurement and selection account for an apparent violation in a specified protocol.

How to follow the derivation chains

The main text develops the common native model, its strongest record results, and their physical interpretation. The appendices carry the distinct supporting arguments that would otherwise interrupt that sequence. A result in one row does not discharge an assumption in another unless the stated mathematical map connects them.

Step	Premises and conclusion	Derivation location
Native action	The declared contact Hamiltonian gives currents, energy exchange and conserved Gauss data.	Section 2 and Appendix E.
Source pairing	A finite registry and supplied costs give robust matching and controlled selection; actual pair amplitudes are retained.	Appendix B.
Mechanical binding	Same-sector energy comparison, host response and relaxed curvature give conditional binding and separation-work results.	Appendix B.
History square	A primitive reversible history kernel and two boundary weights give the squared interior law and finite-depth control.	Section 3 and Appendix D.
Analyzer geometry	The source generator gives an exact contrast compression, omitted-mode correction and half-angle eigenline; a material setting law is additional.	Appendix C.

Step	Premises and conclusion	Derivation location
Loading to first events	A declared matched receiver plus a capacity preparation and interlock gives conditional first-record fractions.	Appendices C and D.
Protected comparison	A neutral tetrahedral ground family gives nonreversing circulation and an internal sign-reading current.	Section 4.
Connected apparatus	Prepared feeder states and the reacting reader give a finite protected loading/read interval and complete error accounting.	Section 5.
Reference and clock	Native dimer motion supplies quadrature; clock and transferred-inventory measures differ. Norm and launch remain physical requirements.	Section 6 and Appendix D.
Other memory routes	Triangular force, paid neutral completion, prepared storage and reciprocal probes have distinct hypotheses.	Section 7 and Appendix E.
Event geometry	Stationary crossings, first crossings and conserved-label mixtures yield different conditional laws.	Appendix F.
Repair and coherence	Lossless export contracts a stated error sector; branch coherence additionally depends on recipient overlap.	Appendix G.
Joint comparisons	Assigned tensor states, selected events, setting-conditioned sources, communication and guidance have different premises.	Section 8 and Appendix H.
Physical completion	Autonomous reference loading, analyzer realization, durable external records and the complete two-wing law are not supplied by citation.	Section 10.

The coverage is the retained derivation logic at the declared model level, not every historical numerical sweep or every proposed microscopic source construction. Source-specific results used only as motivation remain attributed rather than silently adopted as proved premises. The one-bit protocol is explicitly identified as an imported comparison theorem; the supplied quantum representation is identified before its algebra is used. Numerical evidence and analytic conclusions have separate roles throughout.

2 One physical model and one energy account

2.1 Source scope and revision discipline

This reconstruction uses the revised T14 history and analyzer work, final T14K, Paper 11, and the T34 record investigations [1, 2, 4, 11, 12, 14]. Pairing and transport results are retained through their stated scope, not promoted from finite ranking or matching into a derived entangled state [3, 5, 6, 7, 8, 9, 10]. The preparation, event-selection, memory, and probe distinctions in T34A–F remain relevant [15, 16, 17, 18, 20, 21, 19]. The actual receiver action comes from the 122BL/T34F line and its receiver supplement [23, 22]. T17 and Paper 38 contribute storage and conditional wave/joint-state constructions, respectively [13, 24].

The bibliography preserves all located identifiers. An all-versions DOI identifies a paper family; an older cataloged version is not asserted to contain a newer working theorem. The standalone identifiers previously unlocated for T34E, T34F and the receiver supplement remain unlocated. T35 has not been assigned a publication DOI by this work. These qualifications concern provenance, not extra physical conditions.

2.2 Occupied geometry, coordinates, and units

A finite point set is chosen in the face-centered-cubic (FCC) lattice, represented by integer coordinates with even coordinate sum. Every pair at squared separation two is a contact, and every triangle of those contacts is a face. Thus no existing contact is deleted to improve an outcome. A sparse point set is a declared finite motif, not an assertion about an arbitrary filled solid.

Orient an edge $e : i \to j$ by increasing site index. It carries real canonical coordinates A_e, E_e. Each occupied site carries two complex surface coordinates $\psi_{s,i}$, with $s = \pm 1$. Let B be node–edge incidence, positive at the tail, and C face–edge incidence; an ordered face $i < j < k$ has curl $A_{ij} + A_{jk} - A_{ik}$. Then $BC^T = 0$. All quantities below are dimensionless model quantities. The signed channel is not assigned measured electric charge, spin, or photon helicity.

The common Hamiltonian is

$$H = H_{\mathrm{hop}} + \frac{1}{2}\|E\|^2 + \frac{\beta}{2}\|CA\|^2, \tag{2.1}$$
$$H_{\mathrm{hop}} = 2t_0 \sum_{e:i\to j} \sum_{s=\pm 1} \mathrm{Re}(\bar{\psi}_{s,i} e^{isA_e} \psi_{s,j}), \qquad t_0 = 0.08, \quad \beta = 0.02.$$

Its positive hopping coefficient makes some aligned states energized preparations; it must not be renamed a universally positive mechanical strain energy. The dynamics are

$$i\dot{\psi}_{s,i} = \partial H/\partial \bar{\psi}_{s,i}, \qquad \dot{A} = E, \qquad \dot{E} = -J - \beta C^T C A, \tag{2.2}$$
$$J_{s,e} = -2t_0 \,\mathrm{Im}(\bar{\psi}_{s,i} e^{isA_e} \psi_{s,j}), \qquad J = J_+ - J_-.$$

A dot denotes model time. There is no damping, external forcing schedule, installed probability rule, or contact switch during a trajectory.

For $n_{s,i} = |\psi_{s,i}|^2$ and $N_s = \sum_i n_{s,i}$,

$$\dot{n}_s = -BJ_s, \quad \dot{N}_s = 0, \quad G := BE - (n_+ - n_-) = \text{constant}, \quad \dot{H} = 0. \tag{2.3}$$

The same Hamiltonian supplies each source reaction. In particular,

$$z_{s,e} = \bar{\psi}_{s,i} e^{isA_e} \psi_{s,j}, \quad h_e = 2t_0 \,\mathrm{Re}(z_{+,e} + z_{-,e}), \quad \partial_{A_e} J_e = -h_e. \tag{2.4}$$

These contact coherences and face fluxes are invariant under the time-independent gauge change $\psi_{s,i} \mapsto e^{is\chi_i}\psi_{s,i}$, $A_{ij} \mapsto A_{ij} + \chi_i - \chi_j$. Equal energies need not imply equal currents, because real and imaginary coherence enter different observables.

2.3 The regional work balance

Let K be a recording core. Define H_K to contain its internal hopping and electric energies and the faces entirely inside it; assign all other terms to $H_{\mathrm{out}} = H - H_K$. This is an explicit allocation, not a unique continuum energy density. Put $N_K = \sum_{s,i\in K} |\psi_{s,i}|^2$. Let $\dot{\psi}^{\partial}$ contain only hopping across its boundary. Direct differentiation gives

$$P_c = 2\,\mathrm{Re} \sum_{s,i\in K} \left(\frac{\partial H_{\mathrm{hop},K}}{\partial \bar{\psi}_{s,i}}\right)^* \dot{\psi}^{\partial}_{s,i},$$

$$P_f = -\beta \sum_{f \not\subset K} (CA)_f \sum_{e \subset K} C_{fe} E_e, \tag{2.5}$$
$$\dot{H}_K = P_c + P_f = -\dot{H}_{\text{out}}, \qquad \dot{N}_K = 2\,\mathrm{Re} \sum_{s,i \in K} \bar{\psi}_{s,i} \dot{\psi}^{\partial}_{s,i}.$$

Internal conversion cancels; exterior faces and boundary hopping do not. Both powers and inventory transfer are calculated from the same state. Energy is not removed when it leaves the core, and exterior hopping energy can be negative. A scalar "heat lost" account is not substituted for the recipient coordinates.

2.4 The retained contact-wave representation

The earlier T17 storage comparison is a different reduced action, not an extra force appended to Equation (2.1). For contact coordinates e, fixed node inventory q, positive storage matrix $\mathcal{C}$, and $\kappa > 0$, it uses

$$U = \tfrac{\kappa}{2} e^T e + \tfrac{1}{2}(q - Be)^T \mathcal{C}^{-1}(q - Be), \qquad M = \kappa I + B^T \mathcal{C}^{-1} B > 0.$$

With $x = e - e_*$, $M e_* = B^T \mathcal{C}^{-1} q$, and lossless memory equations $\dot{x} = -\eta\zeta$, $\dot{\zeta} = Mx$, the variable

$$\Psi = M^{1/2} x - i\sqrt{\eta}\,\zeta \quad \text{satisfies} \quad i\dot{\Psi} = \sqrt{\eta} M^{1/2} \Psi, \qquad \|\Psi\|^2 = 2(H - H_*).$$

Indeed, differentiating the displayed definition gives $i\dot{\Psi} = \sqrt{\eta} M^{1/2} \Psi$ directly, and the cross term in its norm vanishes for the real quadratures, leaving $\|\Psi\|^2 = x^T M x + \eta \zeta^T \zeta$. These identities establish a genuine conservative complex-amplitude representation. They do not identify stored energy with event probability or establish that the generally nonlocal matrix square root is a microscopic local wavefunction [13, 1, 24].

3 What the history square does and does not establish

Let K_h be a primitive nonnegative history operator, with positive reference weights μ_i satisfying detailed balance $\mu_i (K_h)_{ij} = \mu_j (K_h)_{ji}$. If $f, g \geq 0$ are nonzero preparation and terminal weights, summing complete histories through an interior state gives

$$p_i^{m,n} = \frac{\mu_i (K_h^m f)_i (K_h^n g)_i}{\sum_j \mu_j (K_h^m f)_j (K_h^n g)_j}. \tag{3.1}$$

If $K_h h = \rho h$, $h > 0$, both factors tend to positive multiples of h, so

$$p_i^{m,n} \longrightarrow \pi_i = \frac{\mu_i h_i^2}{\sum_j \mu_j h_j^2}. \tag{3.2}$$

The square is the product of two continuation volumes, not a square inserted into each history. One boundary generally gives μh, and a nonreversible operator generally gives distinct left and right Perron modes. The executable checks exact integer counts and the one-boundary distinction. Appendix D supplies the complete path-sum and spectral argument, including the different measure required by a recorder.

If scaled continuation factors are $h(1 + u_i)$ and $h(1 + v_i)$ with $|u_i| \leq \epsilon_f$, $|v_i| \leq \epsilon_g$, put $d = \epsilon_f + \epsilon_g + \epsilon_f \epsilon_g < 1$. Their normalized product obeys

$$\mathrm{TV}(p^{m,n}, \pi) \leq \min(1, d/(1 - d)). \tag{3.3}$$

The normalized correction estimate is proved in Appendix D; it is a finite approximation bound, not experimental accuracy.

The forward transform

$$P^h_{ij} = \frac{(K_h)_{ij} h_j}{\rho h_i} \tag{3.4}$$

has row sums one and stationary law π by detailed balance. This standard transform is proved here in finite dimensions [26]. It demonstrates a forward realization of the squared residence law, but its h-dependent rates are not derived from Equation (2.1). A positive history kernel, a signed complex surface amplitude, and a detector event are not identified by notation.

Counts of disjoint histories are additive. That premise is less restrictive than a squared-amplitude probability law, but it is still a measure premise. Zhang's analysis distinguishes additivity from noncontextuality and identifies its role in five prominent Born-rule derivations [25]. T35 therefore claims a conditional square-law mechanism, not probability from no probabilistic or counting structure.

A useful representation check is the earlier rail density $p_n(x) = 3(n \cdot x)^2/(4\pi)$ on the sphere. It satisfies $p_n = p_{-n}$ and gives one half under every hemispherical sign readout. A readout depending only on that density cannot distinguish opposite spin preparations. Directed history, phase, or another native coordinate must carry the missing information. Likewise, the half-angle eigenline of

$$D(\theta) = \begin{pmatrix} \cos\theta & \sin\theta \\ \sin\theta & -\cos\theta \end{pmatrix} \tag{3.5}$$

is genuine geometry, but it does not derive an arbitrary-axis material analyzer. The full compression, complementary-mode resolvent, angle convention and matched-receiver derivations are given in Appendix C. They retain T14C's distinction between a relative phase and a physical setting rotation [4].

4 The prepared tetrahedral comparator

4.1 A neutral family with independent fractions

Take roots

$$v_0 = (0,0,0), \quad v_1 = (1,1,0), \quad v_2 = (1,0,1), \quad v_3 = (0,1,1), \tag{4.1}$$

and optional equal arms $v_j + \ell d_j$, $1 \le \ell \le L$, with $d_0 = (-1,-1,0)$, $d_1 = (1,1,0)$, $d_2 = (1,0,1)$ and $d_3 = (0,1,1)$. Without the side reader this gives $4(L+1)$ sites, $4L+6$ contacts and four faces. For $k_L = \pi/(2L+3)$ let

$$F_\ell = \frac{(-1)^\ell \cos[k_L(\ell+1/2)]}{\{\sum_{r=0}^{L} \cos^2[k_L(r+1/2)]\}^{1/2}}, \quad \xi_{\pm,j\ell} = \frac{F_\ell}{2} e^{\pm i\pi j/2}. \tag{4.2}$$

Both are ground eigenvectors of zero-field hopping, with $\mu = -2t_0 \cos k_L$. Tetrahedral adjacency has eigenvalue -1 on the zero-sum root space and 3 on the uniform root vector; the resulting radial root diagonals are $-t_0$ and $3t_0$. Increasing the diagonal cannot lower a Rayleigh quotient. This proves that the displayed radial ground value is the full graph minimum.

For signal fraction p and reference fraction r in $[0,1]$, prepare

$$\begin{aligned} \psi_+ &= \sqrt{n}(\sqrt{p}\,\xi_+ + i\sqrt{1-p}\,\xi_-), \\ \psi_- &= \sqrt{n}(\sqrt{r}\,\xi_+ + i\sqrt{1-r}\,\xi_-), \qquad A = E = 0. \end{aligned} \tag{4.3}$$

Each channel has inventory n. Every site has the same local population in both channels, $nF_\ell^2/4$, because the interference term is the real part of an imaginary multiple of $(-1)^j$. Thus $G = 0$ for independently chosen p, r, and $H = 2n\mu$. A common choice of the opposite quadrature sign also has this neutrality property. Fixed quadrature, fixed inventory and the spatial profile remain physical preparation conditions.

4.2 The all-time internal result and its hypotheses

Opposite-root permutation $j \mapsto j+2$ preserves the graph. Antisymmetric surface states and invariant oriented fields remain in that sector. On the core cycle write

$$A_{01} = A_{23} = a, \quad A_{12} = A_{30} = b, \quad A_{02} = A_{13} = 0, \quad f = a + b, \quad g = a - b. \tag{4.4}$$

All four core face fluxes equal f up to orientation. At $f = 0$ the graph phases are pure gauge. Conservation of $H = 2n\mu$ then forces $E = 0$ and both channels back into a gauge-transformed ground space. The divergence-free current is a single core-cycle current; if its signed-channel difference vanished, the state would be a relative equilibrium. Uniqueness prevents a nonstationary trajectory from reaching that equilibrium at finite time. Every zero-circulation return is therefore a turning point, not a crossing. The initial force is

$$f''(0) = 2t_0 n F_0^2 (p - r). \tag{4.5}$$

Consequently the circulation does not reverse its initially selected sign. This proof applies to the stated graph and initial energy, not arbitrary loading or attachment.

The same boundary argument gives a broader retained result on any connected one-cycle graph initialized in its zero-field ground eigenspace: a nonzero initial cycle force cannot reverse its circulation sign. A zero-flux return forces zero field momentum and a gauge-transformed ground state; divergence-free current then has only the one cycle direction. Generic triangle superpositions can nevertheless have nonzero initial conserved Gauss constants. Such a successful ground-energy calculation cannot be claimed as preparation from a fixed zero-Gauss apparatus. The tetrahedral family above avoids that charge restriction for independently specified fractions.

There is also a native current with a stronger pointwise sign property. Write $u_s = \psi_{s,0,0}$, $v_s = \psi_{s,1,0}$ and

$$C_* = \mathrm{Im}(e^{-if/2} z_{+,01}) - \mathrm{Im}(e^{if/2} z_{-,01}), \quad I_\triangle = -(CJ)_{012} = 4t_0 \cos(f/2) C_*. \tag{4.6}$$

Let T_0^g keep tree and gradient phases but remove f, and put $W_0 = \sum_s \psi_s^\dagger T_0^g \psi_s - 2n\mu \geq 0$. The exact energy identity is

$$W_0 + \tfrac{1}{2} \|E\|^2 + 2\beta f^2 = 8t_0 \sin(f/2) C_*. \tag{4.7}$$

Opposite roots give $|C_*| \leq n/2$. If

$$0 < n < \frac{\beta \pi^2}{2t_0}, \tag{4.8}$$

then $|f| = \pi$ is inaccessible. At nonzero f, Equation (4.7) makes C_* have its sign, and the cosine is positive. At a zero turning point, $I_\triangle = f''$ has the same original sign. It cannot vanish there without a relative equilibrium. Thus

$$\mathrm{sgn}\, I_\triangle(t) = \mathrm{sgn}(p - r), \qquad p \neq r, \quad t < \infty. \tag{4.9}$$

With an independently uniform r, this gives a complete conditional native sign law $P(+) = p$, $P(-) = 1 - p$. The ideal tie has zero measure; a finite grid retains ties as nulls.

This is an internal current, not a separately connected instrument. For finite excess energy $H = 2n\mu + \varepsilon$, the right side of Equation (4.7) instead equals its left side minus ε. If $\varepsilon < 2\beta\pi^2 - 4t_0 n$, the π boundary remains inaccessible, and at $2\beta f^2 > \varepsilon$,

$$|I_\triangle| \geq \tfrac{1}{2} \cot(|f|/2)(2\beta f^2 - \varepsilon) > 0. \tag{4.10}$$

This is a state-dependent tolerance, not a general all-time theorem for an attached reader. The new experiment below tests that interface directly.

5 Actual loading and an external reacting signal

5.1 The whole apparatus is present at launch

Use the same tetrahedron and arms with $L \geq 1$. Add two occupied reader sites

$$a_R = (-1, 1, 0), \qquad b_R = (2, 0, 0). \tag{5.1}$$

The first contacts roots 0 and 3, and the second contacts roots 1 and 2. All nearest-neighbor edges and triangles among the listed sites are retained. There are $4(L+1)+2$ sites, $4L+10$ edges and six faces. For $L = 4$ the apparatus has 22 sites and 26 contacts. The reader is coupled from the start; it is not attached by an unaccounted switch after a successful write.

Define the four-component phase texture

$$x_j(w) = \frac{\sqrt{n}}{2}\{\sqrt{w}\, i^j + i\sqrt{1-w}(-i)^j\}, \quad |x_j(w)|^2 = n/4, \quad x_{j+2} = -x_j. \tag{5.2}$$

At $t = 0$ put $x_j(p)$ and $x_j(r)$ in the two signed channels at the first feeder site $v_j + d_j$. Every other surface coordinate, including every core and reader coordinate, is zero. Set $A = E = 0$. The four populated donor sites are not adjacent to one another, so

$$H(0) = 0, \qquad N_+(0) = N_-(0) = n, \qquad G(0) = 0, \qquad N_K(0) = N_R(0) = 0. \tag{5.3}$$

The zero of H is an energy convention: the preparation has energy above negative ground levels, not a zero-cost physical creation claim. No field pulse is supplied. Normalization is used once to specify the input inventory, not to rescale a state during evolution.

The phase data are independently specified for the two channels at the donors. Their transfer is now physical, but their original creation is still a preparation assumption. Both channels share the same four donor sites; independent parameters do not establish two separate emitting instruments. This distinction is retained rather than hidden by source labels.

The opposite-root permutation also swaps a_R, b_R and preserves every contact. Hence Equation (4.4) remains valid on the core, although the two external faces add a second independent field response. Define the actual external signal

$$R(t) = E_{3a_R}(t) - E_{0a_R}(t), \tag{5.4}$$

with both contacts oriented from their root toward a_R. Each E is gauge invariant under the stated gauge convention. This signal uses two external-contact coordinates, not the internal current in Equation (4.6). It is not an extra force or a nonreacting software probe.

5.2 Derived loading, protection, and reading coefficients

Put $\Delta = p - r$. With t measured from the common launch,

$$\psi_{s,j0}(t) = -it_0 x_{s,j} t + \tfrac{1}{2} t_0^2 x_{s,j} t^2 + O(t^3), \tag{5.5}$$

$$f(t) = \frac{n t_0^3}{6}\Delta t^4 + O(t^5), \tag{5.6}$$

$$R(t) = \frac{n t_0^3(\beta - t_0^2)}{30}\Delta t^5 + O(t^6), \tag{5.7}$$

$$Q_K(t) := H_K(t) + t_0 N_K(t) = -\frac{n^2 t_0^6}{9}\Delta^2 t^6 + O(t^7). \tag{5.8}$$

Here $x_{+,j} = x_j(p)$ and $x_{-,j} = x_j(r)$; H_K contains the six core contacts and four internal faces only. The source amplitudes arrive first, their loop currents generate circulation, and a subsequent response occurs on the added contacts. These different powers of time are derived from the actual loading path. They do not constitute a calibrated relativistic propagation speed.

Derivation of the external response and protection coefficient. At zero field, the first two terms of the surface evolution are $\psi(t) = \psi(0) - iT_0\psi(0)t - T_0^2\psi(0)t^2/2 + \cdots$. The donor is one hop from its core root, and the four donor coefficients sum to zero. This gives Equation (5.5). The summed root current then gives $f'' = 2nt_0^3\Delta t^2 + O(t^3)$, proving Equation (5.6).

At the first external site,

$$\psi_{s,a_R}(t) = -\tfrac{1}{2}t_0^2(x_{s,0} + x_{s,3})t^2 - \tfrac{i}{6}t_0^3(x_{s,0} + x_{s,3})t^3 + O(t^4). \tag{5.9}$$

For $j = 0, 3$, the current into that site is

$$\begin{aligned} J_{s,ja_R}(t) = {} & t_0^4 \operatorname{Re}\{\bar{x}_{s,j}(x_{s,0} + x_{s,3})\}t^3 \\ & + \frac{t_0^5}{6} \operatorname{Im}\{\bar{x}_{s,j}(x_{s,0} + x_{s,3})\}t^4 + O(t^5). \end{aligned} \tag{5.10}$$

The t^3 term cancels between these two links because $|x_{s,0}| = |x_{s,3}|$. The remaining signed-channel difference is $J_{3a_R} - J_{0a_R} = nt_0^5\Delta t^4/6 + O(t^5)$. The external face flux $F_R = A_{03} + A_{3a_R} - A_{0a_R}$ has leading term $-nt_0^3\Delta t^4/12$. Its two contact forces give

$$\dot{R} = -(J_{3a_R} - J_{0a_R}) - 2\beta F_R = \frac{nt_0^3(\beta - t_0^2)}{6}\Delta t^4 + O(t^5), \tag{5.11}$$

which proves Equation (5.7). Both the surface reaction and face-stiffness reaction are necessary; omitting either changes the coefficient.

In the opposite-root sector, the zero-flux core hopping operator is $-t_0$ on the relevant root vectors, including its gradient gauge. Consequently the exact core identity is

$$Q_K = \tfrac{1}{2}\,\|E_K\|^2 + 2\beta f^2 - 8t_0 \sin(f/2)C_*. \tag{5.12}$$

The leading four cycle momenta are $nt_0^3\Delta t^3/3$, and $C_* = nt_0^2\Delta t^2/2 + O(t^3)$. Their electric contribution is $2n^2t_0^6\Delta^2t^6/9$; the hopping correction is $-n^2t_0^6\Delta^2t^6/3$. The magnetic contribution is higher order. Their sum gives Equation (5.8). Exterior reaction is already included in these expansions of the complete equations. □

5.3 Protection while the external reader reacts

Lemma 5.1 (Core boundary and exact exchange condition)**.** *In the preserved opposite-root sector, $f = 0$ implies $Q_K \geq 0$, irrespective of the current state of the exterior. If $Q_K(t_w) = -d < 0$, its circulation sign is retained on $[t_w, T]$ whenever*

$$\sup_{t_w \leq t \leq T} \left\{ \int_{t_w}^{t} (P_c + P_f)\, du + t_0[N_K(t) - N_K(t_w)] \right\} < d. \tag{5.13}$$

Proof. At $f = 0$ all core hopping phases are gauge removable. For the four complete-graph vertices, $H_{\mathrm{hop},K,s} + t_0 N_{K,s} = t_0|\sum_{i\in K} z_{s,i}|^2 \geq 0$ in that gauge. Electric energy is nonnegative. Moreover Equation (2.5) gives $\dot{Q}_K = P_c + P_f + t_0\dot{N}_K$. The stated budget keeps $Q_K < 0$; a continuous sign reversal would have to cross the forbidden zero boundary. □

Theorem 5.2 (Connected protected loading and external response)**.** *Use the complete graph and launch state in Equations (5.1) to (5.3), with $n > 0$ and $\beta > t_0^2$. For every $p \neq r$ there is a positive interval $0 < t < T_{p,r}$ on which*

$$Q_K(t) < 0, \qquad \operatorname{sgn} f(t) = \operatorname{sgn} R(t) = \operatorname{sgn}(p - r). \tag{5.14}$$

For any fixed $\delta > 0$, a common positive interval exists for all preparations with $|p - r| \geq \delta$.

Proof. The first nonzero coefficients in Equations (5.6) to (5.8) have the stated signs. All other coordinates, including the reader, solve one smooth finite-dimensional vector field. Taylor remainders are uniform on a sufficiently short interval over the compact family of input amplitudes. Away from a tie, the positive coefficients of f, R and the magnitude of the negative coefficient of Q_K have positive lower bounds. Choose one interval on which each leading term dominates its remainder. The local boundary lemma identifies the negative-Q_K interval as a genuine protection interval, not only a coincidental observed sign. □

The fixed inherited coefficients satisfy $\beta - t_0^2 = 0.0136 > 0$. They were not adjusted to produce the reference counts. The result includes the physical reader reaction and does not require the core to have been initialized in a ground mode. It is an exact short-time existence theorem. It supplies neither an evaluated universal duration nor an all-time protection claim. During this interval loading and exterior exchange continue; a freely retained post-loading memory is not thereby established.

5.4 Finite resolution and complete distributions

For fixed n, L, put $a = nt_0^3/6$, $b = nt_0^3(\beta - t_0^2)/30$, and $c = n^2 t_0^6/9$. Suppose uniform remainder bounds are

$$|f - a\Delta t^4| \le M_f t^5, \quad |R - b\Delta t^5| \le M_R t^6, \quad |Q_K + c\Delta^2 t^6| \le M_Q t^7. \tag{5.15}$$

Finite such constants exist on a sufficiently short compact interval. For $|\Delta| \ge \delta$, it is sufficient that

$$t < \min\left(\frac{a\delta}{2M_f}, \frac{b\delta}{2M_R}, \frac{c\delta^2}{2M_Q}\right), \tag{5.16}$$

with a missing constraint interpreted as infinite if its remainder bound is zero. Then $|R| \ge b\delta t^5/2$ and $Q_K \le -c\delta^2 t^6/2$. If additional observation error is bounded by $\eta < b\delta t^5/4$, a decoder with dead band η classifies every preparation outside that tie band correctly and keeps the other readings as unresolved.

For an independently uniform reference, coupling each actual label to the ideal sign of $p - r$ gives

$$\mathrm{TV}\left((q_+, q_-, q_0), (p, 1-p, 0)\right) \le \min(1, p+\delta) - \max(0, p-\delta) \le 2\delta. \tag{5.17}$$

In the ideal zero-resolution limit, bounded convergence also gives $\lim_{t\downarrow 0} P(R(t) > 0) = p$. This is an external-response law after actual loading, rather than the acceleration of an already populated core. The uniform reference measure is still an assumption. The constants in Equation (5.15) have not been given certified numerical values, and Equation (5.17) does not validate an unspecified electrical circuit. An even smaller unmodeled probe is not presumed to have zero force.

6 Reference generation, phase, and launch timing

6.1 A native fixed-inventory quadrature source

A single occupied contact supplies a useful exact component. Set identical signed channels, $A = E = 0$, and initial amplitudes $(\sqrt{n}, 0)$ on its two sites. The difference current vanishes, so this is an invariant field-free sector of the same Hamiltonian. Its exact motion is

$$u_0(t) = \sqrt{n}\cos(t_0 t), \qquad u_1(t) = -i\sqrt{n}\sin(t_0 t). \tag{6.1}$$

It generates a fixed total inventory and a quadrature phase through reciprocal hopping, without a normalization operation. On the first monotone transfer interval $0 < t < \pi/(2t_0)$,

$$U(t) = |u_0|^2/n = \cos^2(t_0 t), \qquad J_{0\to 1} = -n\dot{U} = nt_0 \sin(2t_0 t). \tag{6.2}$$

Thus a uniform clock-time sample gives the arcsine fraction law

$$F_{\mathrm{clock}}(u) = \tfrac{1}{2} + \pi^{-1} \arcsin(2u-1), \tag{6.3}$$

whereas the measure of transferred inventory is

$$\frac{J_{0\to1}(t)\,dt}{n} = -dU, \qquad F_{\mathrm{transfer}}(u) = u. \tag{6.4}$$

The phase and transfer are genuine native dynamics. The two probability laws refer to different sampling operations. A physical launcher that produces one reference trial per equal amount of transferred inventory has not been constructed. Assigning those timestamps or weights in software would not construct it. Nor has this isolated two-site component been joined to a four-port splitter and the loading experiment. It is therefore a component derivation, not an unnoticed replacement of the missing autonomous preparation.

6.2 What a larger waveform source supplies

On a general occupied graph, identical signed channels with zero field obey $i\dot{u} = T_0 u$. A port can contain a sum of native frequencies, $X(t) = \sum_k a_k e^{-i\omega_k t}$, without external forcing. Earlier T35 source tests found nearly uniform normalized ratios at particular ports, but their total port inventory fluctuated substantially. Those inherited observations are not repeated as a newly connected source experiment.

For two independent, equal-variance circular complex Gaussians, the normalized ratio $U = |X|^2/(|X|^2+|Y|^2)$ is uniform and independent of $S = |X|^2 + |Y|^2$. That conditional calculation follows by the Jacobian change to (S,U): $f_{S,U} = s\exp(-s/\vartheta)/\vartheta^2$. A general proper Gaussian covariance $\left(\begin{smallmatrix} a & z \\ \bar{z} & b \end{smallmatrix}\right)$ instead gives

$$F_U(u) = \frac{1}{2}\left[1 - \frac{a(1-u) - bu}{\sqrt{[a(1-u)-bu]^2 + 4u(1-u)(ab-|z|^2)}}\right]. \tag{6.5}$$

This is obtained by whitening and diagonalizing the indefinite quadratic form $(1-u)|X|^2 - u|Y|^2$. A finite native spectrum is not declared Gaussian or rationally independent just because this formula is useful.

6.3 Inventory and phase cannot be repaired by relabeling

With unequal signal and reference inventories, the comparison force is proportional to

$$n_s(2p-1) - n_r(2r-1), \tag{6.6}$$

not simply $p-r$. For the Gaussian example, the unnormalized reference difference is Laplace distributed. At $n_s/\vartheta = 2$, the positive-direction probabilities at $p = 1/4, 3/4$ are approximately $0.183940, 0.816060$, not $1/4, 3/4$. A passive linear map cannot normalize every input, since $L(az) = aL(z)$.

If an independently uniform fraction has $n_r/n_s \in [1-\epsilon, 1+\epsilon]$, then conditioning on that ratio gives the cutoff $\mathrm{clip}[1/2 + (p-1/2)n_s/n_r]$. Consequently the onset discrepancy is at most $\epsilon|p-1/2|/(1-\epsilon)$. This is a useful physical inventory tolerance, not a normalization device. Under the ideal Gaussian factorization, readiness depending only on S leaves U uniform; its pretrial failures and rate still have to be counted.

The new donor experiment avoids fluctuating input norm by specifying the same n in both channels at launch. It does not derive that preparation. Its relative quadrature is also essential. Changing it generally creates unequal local populations; the compatible longitudinal field must then be retained, with its energy. Delaying one input by placing it one further contact away likewise changes the initial charge distribution and loading history. Both controls are included numerically without deleting their fields. A permanently field-free ground family only undergoes common phase rotation, so simply waiting longer there does not mix the reference fractions.

7 Protected storage and readable events are distinct

7.1 The retained three-path memory

The triangle with three equal arms supplies a separate exact protection mechanism [22]. At zero loop circulation $b_\triangle$, all hopping phases are removable. The sum of squares on the finite paths, including their endpoint terms, gives

$$b_\triangle = 0 \quad \Longrightarrow \quad H + 2t_0 N \geq 0. \tag{7.1}$$

Hence $\Delta_g = -H - 2t_0 N > 0$ protects the sign for all times in that closed graph. Gauging the loop phase onto one edge bounds its hopping change by $2t_0 N|\sin(b_\triangle/2)|$. This yields the quantitative clearance

$$\operatorname{dist}(b_\triangle, 2\pi\mathbb{Z}) \geq 2\arcsin\left(\frac{\Delta_g}{2t_0 N}\right). \tag{7.2}$$

A fixed-circulation probe preserves this certificate if its complete change satisfies $\delta H + 2t_0\delta N < \Delta_g$. The constructed $L = 48, N = 6$ preparation has $\Delta_g \simeq 0.161224584$ and clearance 0.3374838475 radians. The retained code reconstructs that state and its reciprocal probe. Appendix E gives the finite-path square identity, stationary-state construction, clearance proof and exact probe preparation.

The distinct blank-to-written example starts at zero circulation and cannot acquire a negative conserved global value. Its finite written record instead uses the local exchange budget. The native output-path population difference $D = P_1 - P_2$ responds to the written state and to an incoming probe. Writing alone and probing alone give zero D in the symmetric controls. The edition-2.0 computation reproduced that connected example through model time 300; the useful original figure is retained below as an explicitly inherited trajectory.

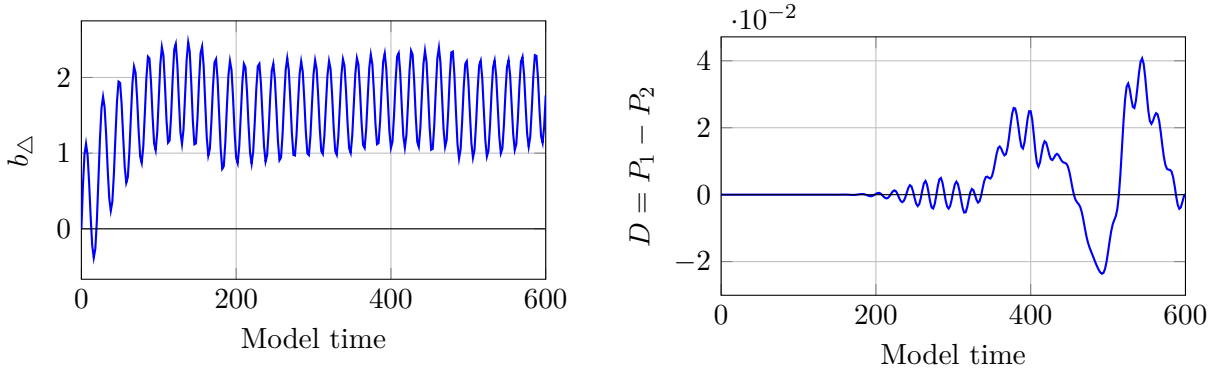


Figure 1: Inherited T34F receiver-supplement trajectory: writing and reciprocal readout in one 147-site system, with $h = 0.02$ [22]. A local pulse establishes circulation before the remote input-path packets give a signed imbalance between the two output paths. Both signals are continuous model observables.

The earlier circulation retention through model times 4000 and 8000 remains an inherited finite-window result. Its detailed late waveform was not fully step-converged. Neither that long-duration sign nor the new short-time loading signal is relabeled a permanent electrical click.

7.2 From complete trajectories to record frequencies

For a full preparation z, its fixed-protocol evolution $\Phi_\theta^t(z)$, and a final record map R_θ including nulls, the actual outcome law is

$$q_a(\theta) = \int \mathbf{1}_{\{R_\theta(z)=a\}}\, d\nu(z). \tag{7.3}$$

Protection constrains trajectories; it does not supply ν. A coupling of actual and ideal labels bounds their total variation by the probability of a preparation, writing, retention, or reading discrepancy. In particular, for normalized kernels,

$$\mathrm{TV}(\nu R, \pi R_*) \le \mathrm{TV}(\nu, \pi) + \sup_z \mathrm{TV}(R(z,\cdot), R_*(z,\cdot)). \tag{7.4}$$

For an initial comparison sign O, final labels $L \in \{+,-,0\}$, and reference CDF F_U, complete counting gives

$$q_+ = F_U(p) - P(O=+, L=-) + P(O=-, L=+) - P(O=+, L=0). \tag{7.5}$$

Every term uses the same launched-trial denominator. No-record events cannot be normalized away.

A stationary state distribution and first-record distribution need not agree. For a provisional Markov state process P and mark probabilities κ_i, stationary marks are proportional to $\pi_i\kappa_i$. For a reset law ν and pre-transition recording, define $Q_{ij} = (1-\kappa_i)P_{ij}$ and $R_{ia} = \kappa_i \mathbf{1}_{\{i \text{ has label } a\}}$. Eventual absorption gives

$$q^{\text{first}} = \nu(I-Q)^{-1}R. \tag{7.6}$$

The full rotor calculation in Appendix F derives a concrete example in which changing stationary crossings to first crossings preserves a correlation and alters a marginal [19]. These observations do not disprove a physical counting mechanism; they identify the sampling operation it must realize.

7.3 Energy response, counting, and conservative repair

A reciprocal pair of stable harmonic coordinates with interaction gqQ has $Q(t) = -gAt^2/2 + \cdots$ and receiver energy $g^2A^2t^2/2 + \cdots$ for a resting receiver and source displacement A. Its interaction energy must be retained. A quadratic energy response is not automatically an exclusive event.

If, separately, actual retained events each consume work ϵ and $W_a = \epsilon N_a + R_a$ with $0 \le R_a < \epsilon$, then

$$\mathrm{TV}\left(\frac{N_a}{\sum N_a}, \frac{W_a}{\sum W_a}\right) \le \frac{\sum R_a}{\sum W_a}. \tag{7.7}$$

The quadratic response and the convex-mixture proof of this count bound are given in Appendix D. Neither identifies a powered detector's amplified output with incoming energy or guarantees one exclusive record per source trial.

Paper 11 instead addresses preservation by explicit export [12]. On a specified correctable error sector, a conservative scattering map with retained block A and outgoing block C obeys $A^\dagger A + C^\dagger C = I$. Across contacts,

$$W_L = \sum_{j=0}^{L-1} \Phi_j^\dagger C_j^\dagger C_j \Phi_j = I - \Phi_L^\dagger \Phi_L, \qquad \Phi_j = A_{j-1}\cdots A_0. \tag{7.8}$$

A uniform lower bound $W_L \ge \eta I$ contracts error energy by $1-\eta$ when exported errors do not return and useful memory is preserved. Appendix G proves the telescoping identity and the precise complementary-contact condition, including the returning-recipient limitation and the separate coherence requirement.

8 Entanglement and locality: the separate joint question

The source-side results in Appendix B establish finite matching, carried phase and conditional mechanical binding at their stated levels. None by itself assigns a tensor-product singlet. Appendix H makes the extra joint-state map explicit, proves the rank distinction, and derives the benchmark and its local statistical alternatives. This is the separate joint step after a single-system record mechanism.

For an explicitly supplied quantum benchmark only, set

$$|\Psi\rangle = \sqrt{p}\,|01\rangle - e^{i\phi}\sqrt{1-p}\,|10\rangle. \tag{8.1}$$

Using the standard Born projectors for coplanar analyzer angles α, β gives

$$\begin{aligned} m_A &= (2p-1)\cos\alpha, & m_B &= -(2p-1)\cos\beta, \\ E &= -\cos\alpha\cos\beta - 2\sqrt{p(1-p)}\cos\phi\sin\alpha\sin\beta, \\ P(s,t) &= \tfrac{1}{4}(1 + sm_A + tm_B + stE). \end{aligned} \tag{8.2}$$

The projector calculation in Appendix H derives these equations from the supplied state. They specify the comparison, not output from Equation (2.1). At $\alpha = \beta = 0$, $E = -1$ independently of ϕ; replacing the correlation by a universally shifted cosine would be incorrect. Both marginals are needed in addition to E.

If a conditional repair exports distinguishable recipient states for two branches, the off-diagonal coherence is multiplied by $\Gamma = \langle e_1|e_0\rangle$. Preserving classical branch labels does not ensure $|\Gamma| = 1$. For the corresponding balanced quantum comparison, the optimized CHSH value is $2\sqrt{1+|\Gamma|^2}$ [32]; this is not a native prediction of the carrier states.

A complete classical common-past state λ, independent settings, and local records give

$$P(A,B \mid a,b) = \int \rho(\lambda) P_A(A \mid a,\lambda) P_B(B \mid b,\lambda)\, d\lambda, \qquad |S_{\mathrm{CHSH}}| \le 2. \tag{8.3}$$

The pointwise bound is $|A_0(B_0 + B_1) + A_1(B_0 - B_1)| \le 2$ for outputs in $[-1, 1]$; zero-coded nulls are included [27, 28]. Local memory, many microstates per label, and nonlinear detectors fit within that premise. Sequential memory requires settings independent of the appropriate prior history and a suitable finite-sample test.

For uniform $\lambda \in S^2$, local responses $A = \mathrm{sgn}(a \cdot \lambda)$ and $B = -\mathrm{sgn}(b \cdot \lambda)$ with Alice acceptance $|a \cdot \lambda|$ yield the singlet correlation among accepted trials. Half the trials are accepted; zero-coding the others yields the standard complete CHSH value $\sqrt{2}$, not $2\sqrt{2}$ [29, 30]. The inherited T34C receiver example likewise distinguishes selected $S \simeq 2.82678$ from complete $S \simeq 1.33203$, with 2048 preparations and 45.46 percent pair retention [17]. These are explicit selected-event mechanisms, not a reanalysis invalidating complete-trial experiments [34, 35, 36].

The proposed experiments could establish a measurement-induced false impression of nonlocality in a specified protocol if detector dynamics affect detection, pairing or retention in a way that invalidates the Bell inference made from the selected records. A calibrated mechanism must predict the relevant history and timing dependence, the apparent violation and the complete outcome/null counts under the actual trial and analysis rules. Demonstrating that connection would identify a measurement or selection explanation for that protocol without contradicting the complete-trial bound. A reduced violation after changing a detector, or a complete-trial statistic consistent with the bound, is insufficient by itself: the intervention may also reduce measurement fidelity or introduce noise. The experimental requirements are developed in Section 10.

Declaring the same cosine-weighted density to be $\rho(\lambda \mid a)$ instead changes the preparation assumption. Sending an actual bit changes the communication assumption [31, 5]. A joint configuration-space guidance law is another completion, with additional equilibrium assumptions [24, 33]. Appendix H supplies the selected-density integral, source-menu normalization, sharp local approximation bound and the exchange/pointer equations of the conditional guidance completion. Their different premises are retained rather than combined into one asserted native mechanism.

Finally, graph locality alone does not prove a strict light cone. Paper 11's conditional event theorem assumes every influence of length ℓ takes at least ℓ/c_* and that causal ancestry is well founded. Summing

those delays proves the endpoint bound. A continuous nearest-neighbor wave equation can instead have arbitrarily early analytic tails. The powers of time in Equations (5.5) and (5.7) describe such model dynamics; no measured causal speed is inferred from them.

9 Calculated results and controls

The retained executable uses one graph builder, one signed-channel vector field, one RK4 integrator, one regional account and one checkpoint format. It imports no earlier research program. Analytical comparisons are separate from native trajectories and from the explicitly supplied quantum benchmark.

This edition restores analytical derivations and their dependencies without changing the Python or PowerShell bytes. The 262-trajectory campaign below originates in edition 2.0. For this edition, the 80 main-grid cases were rerun with identical source and parameters through model time 80, confirming the complete counts in Table 2; the other 182 campaign trajectories were not rerun. The four existing equation/statistical check groups also passed again. Source-specific selector, analyzer and rotor campaigns are not reinstated as duplicate solver branches; their analytical arguments and cited evidence are distinguished from the computations implemented by this executable.

9.1 Discovery and confirmation are distinguished

An exploratory 80-case grid used $p = 0, 1/4, 1/2, 3/4, 1$ and sixteen midpoint references $r = (j + 1/2)/16$, all at $n = 0.5, L = 4$. This exposed an early useful interval and late reversals. The subsequent confirmation used different signal fractions $0.1, 0.3, 0.7, 0.9$ and 32 different midpoint references, with the early reading times 5 and 10 fixed from that exploration. It is internal confirmation, not independent external replication. All cases and all reported late readings remain in the account.

The decoder is fixed as positive for $R > 10^{-10}$, negative for $R < -10^{-10}$, and unresolved otherwise. This model-unit numerical convention is not a laboratory noise specification. No threshold is fitted to a target fraction. The continuous ideal law uses a supplied uniform reference; finite midpoint counts are deterministic quadrature, not random experimental samples or precision estimates of that law.

Signal p	Trials	+ at 5	+ at 10	+ at 20	+ at 80
0	16	0	0	16	16
0.25	16	4	4	12	12
0.5	16	8	8	8	8
0.75	16	12	12	4	4
1	16	16	16	0	0

Table 2: Complete exterior-reader counts on the main grid. There are no unresolved readings at these displayed times; the negative count is 16 minus the positive count. All 80 preparations are retained at every time. Late sign inversion is reported with the same fixed decoder.

At every saved time from 5 through 10, all 80 main-grid preparations have $Q_K < 0$ and the external signal has the comparison sign. These sampled inequalities support the operating interval but are not an interval-arithmetic certificate between samples. The exact theorem establishes a sufficiently short interval without identifying it numerically with 5–10. Reference samples near a tie require progressively finer resolution.

At time 20, the external reading has reversed on the displayed grid even though each core circulation still has its initial sign. Later, some core signs reverse too. The decoder is not retuned at those times. These failures establish why an external waveform and a permanently latched record cannot be equated.

Signal p	Reference nodes	Expected grid +	Read + at 5	Read + at 10	Nulls
0.1	32	3	3	3	0
0.3	32	10	10	10	0
0.7	32	22	22	22	0
0.9	32	29	29	29	0

Table 3: Disjoint confirmation preparations. "Expected grid" counts the stated comparison $r < p$ on these finite nodes, not a sampled Born outcome. The complete trajectory produces the reader label. Finite fractions such as 3/32 are not claimed to equal the continuum value 0.1.

Read or control	f at 10	R at 10	Q_K at 10
Matched loading	0.11573261	0.00289504	-0.00036502
Reference phase zero	-0.01673027	0.03140732	0.00368082
Reference one hop later	0.06235243	0.00153014	-0.00013712

Table 4: Phase and arrival-time controls retain their actual longitudinal preparation fields. The matched launch begins with empty core and readers and zero field; the other controls have additional accounted initial field energy.

9.2 Energy recipients, phase and timing

For $p = 0.75, r = 0.25$, the complete system starts at $H = 0$. At time 10 the core contains about 0.37991955 inventory and has $H_K = -0.03075858$; the explicitly evolved exterior has the opposite energy $+0.03075858$. The external reader sites have about 0.00841905 inventory. The core protection value is approximately -0.0003650181, and $R \simeq 0.0028950434$. These are actual state quantities, not a postulated absorbed-energy fraction or a heat counter.

The matched no-reader trajectory at time 10 has $f \simeq 0.13217942$, while the attached reader gives $f \simeq 0.11573261$. Its reaction is therefore material. In the separate preloaded-ground control, adding the same empty reader sites changes the spectral problem and later reverses a circulation protected in isolation. The earlier all-time theorem is not claimed for that enlarged preparation.

Changing the reference quadrature to zero requires an initial longitudinal-field energy of approximately 0.028125 in the reader geometry. Its core protection value at time 10 is positive. Delaying the reference by one contact requires a different compatible field and an initial energy approximately 0.03125. These controls retain those costs. Neither a phase replacement nor an independently shifted external waveform is hidden inside a successful run.

9.3 Checks, refinement, and inherited results

The reported edition-2.0 execution contains 262 completed trajectories, including the main and confirmation grids, ground-family comparisons, positive/negative/tie controls, phase and arrival controls, host-size and inventory controls, refinement pairs, and five triangle write/read controls. Four groups of equation and statistical checks pass. Completion of a trajectory is not a declaration that it satisfies the desired Born law.

Across the completed campaign, the largest saved energy residual is below 3.0×10^{-11}, the Gauss drift below 1.5×10^{-11}, and the core work-balance residual below 2.4×10^{-11}. The largest core inventory ledger residual is below 1.2×10^{-10}. The three new step-refinement pairs change the external reader by at most 1.29×10^{-10} and the core flux by at most 1.09×10^{-9} at common saved times through 80. These are numerical checks, not certified trajectory enclosures.

The reported triangle computation gives $D(300) \simeq 0.001047479010$ for positive writing plus probe,

its negative for the reversed writing pulse, and zero for the writing-only and probe-only symmetric controls. The prepared protected-state probe gives $D(300) \simeq -0.000162085933$. Stable summation and the exact tree solution for a tree-supported initial Gauss field avoid injecting a roundoff cycle into the symmetric null preparation; no state projection or artificial restoring force is applied during evolution.

The earlier 116-trajectory triangular mode-competition sweeps, the larger waveform-source calculations, and long 4000/8000-time continuations remain inherited supporting comparisons rather than newly rerun campaigns. Their important conclusions are retained: the bare charged doublet and joint neutral completion did not produce the general late Born fractions, software-normalized source ratios had fluctuating inventory, and finite sign retention did not certify a converged late waveform. The common program removes duplicated historical solver branches instead of embedding every obsolete experiment as another independent engine.

10 Physical interpretation and the remaining work

Three levels of autonomy must be kept separate. The newly connected model evolves autonomously after a stated launch: no force is switched, no receiving state is overwritten, and no energy recipient is removed. Its prepared signal and reference are not autonomously manufactured by that evolution. Its observation time and numerical decoder also remain elements of a measurement protocol, not a derived self-triggering electrical register.

The advance is nevertheless physical within the specified model. Information starts outside the recording core; native contact motion loads it; the local energy account enters a sign-protecting region; and external contacts produce a sign-bearing signal with their full reaction included. The short-time theorem proves coexistence of those properties, while the complete grids establish a useful finite operating example and reveal its late limitation. This replaces the earlier unspecified loading/readout gap with a concrete, calculable interaction.

A complete device now needs a source that actually prepares fixed inventory and compatible quadrature at its donor ports, together with a physical event or launch mechanism selecting the reference law. The dimer calculation supplies real quadrature generation and a uniform transferred-inventory measure, but a flux-weighted count cannot be called an emitted fixed-inventory reference without its packetization and backreaction. A mechanical analyzer must map its setting to the incoming mode fractions without inserting the desired angular probability function.

The external signal must then be copied into a persistent readable state before its later oscillation invalidates the chosen interpretation. That copy requires an explicit coupled recipient and a new energy budget; declaring a timestamped sign in software is not the missing register. A later independently chosen measurement time, repeated use, erasure, source renewal, noise, and calibration to electrical quantities must be tested on the complete device. These are specific next physical tasks, not reasons to withdraw the established square-law, protection, loading, and response mechanisms.

For entanglement, even a completed single-system recorder would still need a joint preparation and the complete two-wing law under its named causal assumptions. The present loading result does not alter the Bell bound or convert a conditional quantum benchmark into a native derivation.

A concrete empirical test must first identify the material and readout correspondence and calibrate the predicted detector response independently of the Bell outcome. Controlled variation of prior exposure, waiting time and probe conditions should then test predicted changes in response, detection probability and event timing. The joint test must preserve settings, valid trial identifiers, local outcomes including nulls, event timestamps and relevant detector history. Its trial, pairing and retention rules must be declared in advance, and the mechanism must account for local marginals and joint counts together with any apparent violation, using a statistical analysis that allows memory.

Existing raw records may provide this evidence if they contain the required information and permit a quantitative test under the actual experimental protocol. Where they do not, targeted controlled

measurements are needed. Demonstrating the proposed effect in a model supplies a testable possibility; its operation and explanatory role in an actual Bell experiment require this empirical step.

Consolidated conclusion

T35 now has a connected, reciprocal loading-and-external-reading segment with a proved initial protection interval, in addition to its earlier conditional history law and prepared-record theorems. It does not yet have autonomous generation of the required reference ensemble, permanent external recording, or complete native entanglement statistics. The manuscript and program distinguish those accomplishments and remaining connections without treating every intermediate mechanism as either a complete quantum theory or a failure.

The selected-event comparisons show how measurement and event-selection effects can create a false impression of nonlocality under specified conditions. What remains unestablished is whether they do so in actual Bell experiments, especially those designed to close the relevant loopholes. Calibrated experiments or sufficiently complete raw-data tests could establish that explanation for a specified protocol by quantitatively connecting the detector mechanism to its apparent violation and complete records.

11 Reproduction

Compiling this master writes `T35.py`, `Run_T35.ps1`, the numerical table, and the retained figure. Both complete executable sources are printed below. Python 3.11 or newer and its standard library are sufficient; no prior manuscript, data file, or installed research script is a runtime dependency. The `paper` campaign reproduces the stated schedule; `quick` retains the main controls, while `full` additionally runs a longer reference grid. The budget is wall time, distinct from model time. Completed cases are reused only when source identity and complete case parameters match. Interrupted trajectories resume at saved sample boundaries.

The default Windows output is

```
C:\Users\thile\Downloads\T35_Rebuilt_outputs
```

The launcher uses an adjacent master or program, searches for Python including the user's established interpreter path, and captures both output streams. Typical calls are

```
python T35.py --output-root T35_outputs --campaign paper --workers 18
python T35.py --output-root T35_outputs --campaign paper --resume
python T35.py --output-root T35_outputs --campaign paper --summary
& "C:\Users\thile\Downloads\Run_T35.ps1" -Resume -OpenOutput -NoPause
```

A `STOP.txt` file in the output directory requests a clean checkpoint. Remove it before resuming. A running lock prevents concurrent writes to one output directory; remove a stale lock only after confirming that no process still owns the run. A deliberately interrupted short trajectory was resumed and matched an uninterrupted calculation exactly. The full campaign also resumed after an execution interruption. Windows PowerShell was inspected, not executed under Windows.

The manuscript edition is 2.1; the preserved executable identifies itself as `T35-connected-rebuild-2.0.0`. Its Python and PowerShell source bytes are unchanged from the rebuilt edition. The executable remains one implementation, not a chain of appended entry points. It has one common native state, one integrator, one event/report convention, and one checkpoint schema. Source hashes identify reproducible bytes; they are not digital-signature requirements. Bibliography and source listings are complete, and the original manuscripts remain unchanged.

References

[1] M. J. Sarnowski, *Paper T14: Born Statistics from Angular Coherence Filtering*. Restored angular-history working edition, September 30, 2026. All-versions DOI: https://doi.org/10.5281/zenodo.15777256. Cataloged version (2026-04-01): https://doi.org/10.5281/zenodo.19378511.

[2] M. J. Sarnowski, *Paper T14A: Explicit Triadic Pairing and an Integrated Reduced Entanglement Architecture*. Revised source, joint-state and first-record manuscript, September 30, 2026. All-versions DOI: https://doi.org/10.5281/zenodo.21672902. Cataloged version (2026-07-29): https://doi.org/10.5281/zenodo.21672903.

[3] M. J. Sarnowski, *Paper T14B: Direct Computational Handoff of Triadic Candidate Costs and Radial Phase to Conserved Partner Condensation and Local-Ledger Transport A Target-Free, Intervention-Controlled Audit*. Selector and transfer working revision, September 23, 2026. All-versions DOI: https://doi.org/10.5281/zenodo.21675207. Cataloged version (2026-07-29): https://doi.org/10.5281/zenodo.21675208.

[4] M. J. Sarnowski, *Paper T14C: A Conditional Coplanar Double-Cover Analyzer Basis from an Assigned Two-Role Angular Frame*. Revised local-analyzer manuscript, September 30, 2026; the earlier shifted-angle interpretation is not used. All-versions DOI: https://doi.org/10.5281/zenodo.21682761. Cataloged version (2026-07-29): https://doi.org/10.5281/zenodo.21682762.

[5] M. J. Sarnowski, *Paper T14D: Separate First-Passage Record Encoding under the Toner–Bacon One-Bit Communication Protocol T14C Residual-Shift Interface, Communication Calibration, and Independent 6.3-Million-Trial Hardening*. Finite-recipient and one-bit communication comparison; September 2026 working revision. Supporting content retained through the inspected T14/T34 interfaces; upstream campaigns are not rerun. All-versions DOI: https://doi.org/10.5281/zenodo.21695920. Cataloged version (2026-07-30): https://doi.org/10.5281/zenodo.21695921.

[6] M. J. Sarnowski, *Paper T14E: Whole-VROS Strain-Lowering Pair Formation Coupled Spin Geometry, Nonseparable Relational Minima, and Conditions for Persistence Under Separation*. Revised working manuscript, September 24, 2026; pair-energy, occupied-placement and clearing-work derivations inspected directly. Upstream campaigns are not rerun. All-versions DOI: https://doi.org/10.5281/zenodo.21710512. Cataloged version (2026-07-30): https://doi.org/10.5281/zenodo.21710513.

[7] M. J. Sarnowski, *Paper T14F: Whole-VROS Pair Formation, Separation, and Pair-Created Relational Corridors*. Revised working manuscript, September 24, 2026; geometry-respecting pair comparison and post-separation carrier conditions. All-versions DOI from the supplied index: https://doi.org/10.5281/zenodo.21714724; cataloged version (2026-07-31): https://doi.org/10.5281/zenodo.21714725. The later working revision is not asserted to be that archived version.

[8] M. J. Sarnowski, *Paper T14H: Candidate Native Stage-Current Model of Cyclic Handoff, Functional Reclosure, and Emergent Whole-VROS Circulation A Derivation and Falsification Framework from Nonlinear Quotient Flow and Eight-Mode Stage Order*. Revised discussion of surface-current accounting. Supporting content retained through the inspected T14/T34 interfaces; upstream campaigns are not rerun. All-versions DOI: https://doi.org/10.5281/zenodo.21729304. Cataloged version (2026-08-01): https://doi.org/10.5281/zenodo.21730728.

[9] M. J. Sarnowski, *Paper T14I: Label-Free Whole-History Compatibility and Reproducible Unique Static Partner Selection in a Reduced Two-VROS Strain Model*. Revised discussion of finite partner

energetics. Supporting content retained through the inspected T14/T34 interfaces; upstream campaigns are not rerun. All-versions DOI: https://doi.org/10.5281/zenodo.21763093. Cataloged version (2026-08-02): https://doi.org/10.5281/zenodo.21763094.

[10] M. J. Sarnowski, *Paper T14J: Local Dynamical Accessibility of Frozen T14I Whole-History Minima Depth- and Barrier-Scaled Conservative Relaxation with Finite Retention but No Reproduced Selection Advantage*. Revised discussion of accessibility, retention, and detachment. Supporting content retained through the inspected T14/T34 interfaces; upstream campaigns are not rerun. All-versions DOI: https://doi.org/10.5281/zenodo.21782891. Cataloged version (2026-08-04): https://doi.org/10.5281/zenodo.21782892.

[11] M. J. Sarnowski, *Paper T14K: Toward a Physical Born Rule. Deterministic Preparation, Reciprocal Contacts, and Retained Records*. Final working revision 2.0.0, September 30, 2026. All-versions DOI: https://doi.org/10.5281/zenodo.23074184. Cataloged version (2026-10-01): https://doi.org/10.5281/zenodo.23074185.

[12] M. J. Sarnowski, *Paper 11: Conditional Locality from Angular Coherence and Carrier Exchange. Shared Histories, Corridor Repair, and the Boundary of the Entanglement Claim*. Working revision 1.5.0, October 1, 2026. The supplied catalog family is titled "Time, Causality, and the Emergence of Thermodynamic Directionality in the Holosphere Lattice." All-versions DOI: https://doi.org/10.5281/zenodo.15731361. Cataloged version (2026-02-17): https://doi.org/10.5281/zenodo.18671874.

[13] M. J. Sarnowski, *Paper T17: No Dice Theory: Einstein was Right Run the Corridors: κ_C, σ_R, and ϵ_{aniso} as Drop-In Falsifiers for a Deterministic Cosmos*. Integrated contact-storage working revision, September 25, 2026, used through T14 and Paper 11. All-versions DOI: https://doi.org/10.5281/zenodo.15786448. Cataloged version (2025-12-01): https://doi.org/10.5281/zenodo.17782648.

[14] M. J. Sarnowski, *Paper T34: Local Contact Mechanics, Conditional Born Statistics, and Bell Correlations An Integrated Holosphere Derivation and Locality Audit*. Working revision 2.0, October 13, 2026. All-versions DOI: https://doi.org/10.5281/zenodo.23351715. Cataloged version (2026-10-13): https://doi.org/10.5281/zenodo.23351716.

[15] M. J. Sarnowski, *Paper T34A Local Preparation, Setting Registers, and Finite Receiving Records Advances after T34 and a fresh equation-based computational audit*. 2026 working source in the T34 record-development sequence. All-versions DOI: https://doi.org/10.5281/zenodo.23366519. Cataloged version (2026-10-14): https://doi.org/10.5281/zenodo.23366520.

[16] M. J. Sarnowski, *Paper T34B A Conditional Local Physical Mechanism for Apparent Quantum Nonlocality through Event Selection*. 2026 working source in the T34 record-development sequence. All-versions DOI: https://doi.org/10.5281/zenodo.23374368. Cataloged version (2026-10-14): https://doi.org/10.5281/zenodo.23374646.

[17] M. J. Sarnowski, *Paper T34C Selected Measurements Can Make a Local Detector Appear Nonlocal A Contact Model with Stored Records, Mechanical Readout, and Complete-Trial Tests*. 2026 working source in the T34 record-development sequence. All-versions DOI: https://doi.org/10.5281/zenodo.23378622. Cataloged version (2026-10-14): https://doi.org/10.5281/zenodo.23378623.

[18] M. J. Sarnowski, *Paper T34D Detector Information Loss and Apparent Nonlocality Timing Audits, Strong-Probe Disturbance, and a Safe-Readout Bound*. 2026 working source in the T34 record-development sequence. All-versions DOI: https://doi.org/10.5281/zenodo.23384886. Cataloged version (2026-10-15): https://doi.org/10.5281/zenodo.23384887.

[19] M. J. Sarnowski, *Native Flux, Contact Geometry, and Local Entanglement: A Further Derivation Attempt*. Research supplement to T34, October 14, 2026. Parent-paper all-versions DOI (not a separate supplement DOI): https://doi.org/10.5281/zenodo.23351715.

[20] M. J. Sarnowski, *Paper T34E: Can Detector Dynamics Create a False Impression of Nonlocality? Local Information Loss, Measurement Disturbance, and Testable Predictions*. Supplied working manuscript, October 15, 2026.

[21] M. J. Sarnowski, *Paper T34F: Can Detector Dynamics Create a False Impression of Nonlocality? Environmental Conversion, Remote Triggering, and Joint Field Predictions*. Supplied working manuscript, October 16, 2026.

[22] M. J. Sarnowski, *T34F Receiver-Size and Persistent-Pair Supplement*. Revised working manuscript, October 16, 2026; source file `Pasted text(20261016-030020).txt`. Includes the three-path protection, writing, and reciprocal readout calculations.

[23] M. J. Sarnowski, *Paper 122BL: Stored Strain, Delayed Field Conversion, and Local Release in the Holosphere Lattice*. October 15, 2026 working source, used through T34F. Identifiers supplied in the 122BM and 122AN bibliographies: all versions https://doi.org/10.5281/zenodo.23401422; recorded version https://doi.org/10.5281/zenodo.23401423.

[24] M. J. Sarnowski, *Paper 38: Entanglement Propagation and the Discrete Structure of Spacetime*. Restarted corridor/joint-guidance working edition, September 25, 2026; not identified with the older cataloged deposit. All-versions DOI: https://doi.org/10.5281/zenodo.15655328. Cataloged version (2026-02-20): https://doi.org/10.5281/zenodo.18713994.

[25] J. Zhang, "Summing to uncertainty: On the necessity of additivity in deriving the Born rule," *Physical Review A* **114**, 042208 (2026), DOI: https://doi.org/10.1103/mqy7-s2db. Used here for the scope of the additivity critique, not as a universal impossibility theorem.

[26] J. L. Doob, "Conditional Brownian motion and the boundary limits of harmonic functions," *Bulletin de la Société Mathématique de France* **85**, 431–458 (1957), DOI: https://doi.org/10.24033/bsmf.1494. The finite-state transform used here is proved directly.

[27] J. S. Bell, "On the Einstein Podolsky Rosen paradox," *Physics Physique Fizika* **1**, 195–200 (1964), DOI: https://doi.org/10.1103/PhysicsPhysiqueFizika.1.195.

[28] J. F. Clauser, M. A. Horne, A. Shimony and R. A. Holt, "Proposed experiment to test local hidden-variable theories," *Physical Review Letters* **23**, 880–884 (1969), DOI: https://doi.org/10.1103/PhysRevLett.23.880.

[29] N. Gisin and B. Gisin, "A local hidden variable model of quantum correlation exploiting the detection loophole," *Physics Letters A* **260**, 323–327 (1999), DOI: https://doi.org/10.1016/S0375-9601(99)00455-7.

[30] J. Degorre, S. Laplante and J. Roland, "Simulating quantum correlations as a distributed sampling problem," *Physical Review A* **72**, 062314 (2005), DOI: https://doi.org/10.1103/PhysRevA.72.062314.

[31] B. F. Toner and D. Bacon, "Communication cost of simulating Bell correlations," *Physical Review Letters* **91**, 187904 (2003), DOI: https://doi.org/10.1103/PhysRevLett.91.187904.

[32] R. Horodecki, P. Horodecki and M. Horodecki, "Violating Bell inequality by mixed spin-1/2 states: necessary and sufficient condition," *Physics Letters A* **200**, 340–344 (1995), DOI: https://doi.org/10.1016/0375-9601(95)00214-N.

[33] D. Dürr, S. Goldstein and N. Zanghì, "Quantum equilibrium and the origin of absolute uncertainty," *Journal of Statistical Physics* **67**, 843–907 (1992), DOI: https://doi.org/10.1007/BF01049004.

[34] B. Hensen et al., "Loophole-free Bell inequality violation using electron spins separated by 1.3 kilometres," *Nature* **526**, 682–686 (2015), DOI: https://doi.org/10.1038/nature15759.

[35] M. Giustina et al., "Significant-loophole-free test of Bell's theorem with entangled photons," *Physical Review Letters* **115**, 250401 (2015), DOI: https://doi.org/10.1103/PhysRevLett.115.250401.

[36] L. K. Shalm et al., "Strong loophole-free test of local realism," *Physical Review Letters* **115**, 250402 (2015), DOI: https://doi.org/10.1103/PhysRevLett.115.250402.

A Symbols, units, and equation-to-program map

Symbol or term	Meaning and convention
i, j, s, ℓ	Site, signed-channel, and radial-position indices; $s = \pm 1$ is not assigned physical charge.
t, t_0, β	Model time, hopping coefficient 0.08, and face coefficient 0.02. No physical clock or energy calibration is inferred.
A_e, E_e, B, C	Real edge coordinate and its canonical partner; node–edge and face–edge incidence.
$\psi_s, n_{s,i}, N_s, G$	Complex surface state, local inventory, conserved channel inventory, and conserved Gauss vector.
$z_{s,e}, h_e, J_s, J$	Gauge-invariant contact coherence, hopping energy, channel current, and signed current difference.
$H, H_K, H_{\mathrm{out}}, N_K$	Complete Hamiltonian, allocated core and exterior energies, and core surface inventory.
P_c, P_f, Q_K	Contact and exterior-face inflow powers; local protection functional $H_K + t_0 N_K$.
v_j, d_j, L, n	Core roots, arm directions, arm length, and inventory in each prepared channel.
p, r, Δ	Signal and reference mode fractions and their difference $p - r$.
$F, \xi_\pm, \mu$	Normalized ground radial profile, two ground modes, and zero-field minimum hopping eigenvalue.
a, b, f, g (core chart)	Alternating core link coordinates, active flux $f = a + b$, and gradient coordinate $g = a - b$.
$C_*, I_\triangle, W_0, \varepsilon$	Core coherence contrast, internal loop current, excess zero-flux surface energy, and total preparation excess.
a_R, b_R, R, F_R	Two actual reader sites, external edge-momentum difference, and first external face flux.
$x_j(w), a, b, c$ (loading coefficients)	Donor texture; positive coefficients in the fourth-, fifth-, and sixth-order loading expansions. Context distinguishes these coefficients from core link coordinates.
$M_f, M_R, M_Q, \delta, \eta$	Uniform Taylor remainder bounds, excluded comparison-gap width, and bounded observation error. No numerical noise certificate is inferred.
U, S, ν, π, F_U	Reference fraction, total reference inventory, preparation measure, comparison residence law, and fraction CDF.
K_h, h, ρ, P^h	History operator, its positive Perron mode and eigenvalue, and forward transformed kernel.

Symbol or term	Meaning and convention
Q, R, κ (event formula)	Transient kernel, absorbing-label kernel, and mark probability; distinct from physical reader $R(t)$ and core Q_K.
W_a, N_a, R_a, ϵ (work counting)	Channel work, number of completed records, residual work and work per record.
A_j, C_j, Φ_j, W_L (repair)	Retained and outgoing error maps, retained propagator and extraction matrix.
Γ, α, β (joint benchmark)	Recipient overlap and analyzer angles; the analyzer angle β is not the native face coefficient in that separate calculation.
h_{num}	RK4 step; saved extrema and refinement comparisons are not interval-certified estimates.
$\mathcal{A}, L_{12}, \kappa, \theta, \alpha_i, u, z_i, W_r$	Reduced twelve-slot source generator, ring Laplacian, stiffness, registry angle, site angle, eigenmode, carried amplitude, and lane inventory; distinct from the native link coordinate A.
$\mathcal{V}, r_i, \mu_c, \epsilon_c, C_{ij}, c_j, \tau$	Candidate registry, direction vectors, comparison-cost coefficients, row costs and algorithmic filter budget, not physical flow time.
$\psi^{\mathrm{sel}}, v_j, Z, \bar{c}, \Delta_c, R_c, L_c, \delta_c, \eta_c, m(s)$	Selector coordinate, weight, normalization, mean cost, supported gap, initial odds factor, later odds, leakage target, cost uncertainty, and row minimum.
$\mathcal{R}, \chi_X, \widehat{\chi}_X, d_X, q_c, n_{ij}$	Carried pair-phase relation, actual and recorded path phases, their residual, record quantization unit and retained packet inventory.
$\mathcal{I}, \mathcal{B}, L_B, L_B^+, \kappa_E, g_E, q, E_*, D_X$	Binding-sector and environment constraints, graph Laplacian and pseudoinverse, field stiffness/coupling, neutral profile, least-energy field and profile shape derivative.
$\mathcal{T}_s, \delta_s, H_{zz}, Z, K_{AB}, \mathcal{J}, I_{\mathrm{rel}}$	Bridge overlap and phase, internal Hessian, constraint-tangent basis (not filter normalization), mixed response, conserved angular momentum when present, and relative inertia.
$q_A, q_B, k, A_c, J_c, c_c, f_c, x, \ell_c, R_{\min}, d_{\min}$	Reduced pair-well deformations, coefficients, exponential separation coordinate, range, domain edge and minimum shape denominator; proposed-model quantities.
$P_{\mathrm{cyc}}, u_e, \alpha_e, W_{\min}, \nu_c$	Cycle-space projector, edge unit vector, available cycle norm, least offset-clearing work and separately declared relaxation rate.
$B_a, P_a, Q_a, W_a, p_a, q_a, T_a, C_\lambda, m_a, \widehat{p}_a$	Analyzer harmonic basis, retained/complement projectors, complement basis, block coordinates, coupling/resolvent, retained norm and normalized retained direction.
$D(h), h_z, h_x, \rho_a, \vartheta, \chi, U_a, R_2, w$	Real contrast, its components/magnitude, contrast and physical-axis angles, eigenbasis, planar rotation and contrast winding number.
$m_a^{\mathrm{loc}}, v_a, \varepsilon_a, \gamma_a$	Local population contrast, real coherence, applied relative phase and real analyzer-frame turn.
$Z_\sigma, B_\sigma^{\mathrm{rec}}, C_\sigma^{\mathrm{rec}}, \phi_\sigma, s_\sigma, F_\sigma$	Declared matched-receiver incoming, receiving and rotating-frame amplitudes, readiness phase/action and received inventory.
$\omega_a, \Omega_a, g_a, \nu_a, \Delta_a, d_\pm, X_a$	Matched-receiver frequencies, coupling, oscillation rate, common error, channel detunings and common loading envelope.
$a_\triangle, k_e, v_j, \psi_j, \widetilde{H}$	Frozen triangular receiving frequency, entry coupling, projected bright vector, discrete contact angle and full projected matrix.
$\mu_i, \langle\cdot,\cdot\rangle_\mu, f, g, \rho, h, u_i, v_i, d$ (history)	Reference weights, weighted inner product, boundary weights, principal eigenvalue/mode, relative factor errors and their product-error bound; distinct from native core flux f.
$e_i, w_i, E_c, \Psi, M, M_v, \kappa_i$ (events)	Capacity, loading fraction, fixed total capacity, joint survival, maximum exposure, visit deadline and state-marking probability.
$\delta_{\mathrm{prep}}, \epsilon_{\mathrm{write}}, \epsilon_{\mathrm{ret}}, \epsilon_{\mathrm{read}}$	Complete-law preparation, writing, retention and reading discrepancy bounds, including nulls.
$a_g, b_g, z_g, \Sigma, T_u, D_u, \vartheta_g, r_N$	Gaussian port covariance entries/matrix, quadratic-form trace and eigenvalue separation, intensity scale and physical inventory ratio.

Symbol or term	Meaning and convention
$q_o, p_o, Q_o, P_o, \omega_o, \Omega_o, g_o, A_o$	Separate harmonic-comparison coordinates/momenta, frequencies, reciprocal coupling and source displacement.
$\chi_\pm, \chi_0, c, d, C_s, C_r, \mathcal{Q}_j, \Lambda_L$	Triangular winding/uniform modes, unit coefficient pairs, interference coefficients, arm charges and longitudinal-field geometry factor.
$z_\pm, \kappa_c, a_c, b_c, \delta_c^{\mathrm{amp}}, Q_c, \mu_0$	Neutral-completion coefficients, phase, linear equation coefficients/right side, phase-selection coefficient and uniform-mode expectation.
$C_0, f_\ell, S_f, R_m(x), \mu_*, \epsilon_w, c_p, \alpha_p$	Stored-state normalization, radial profile/norm, finite-chain ratio, frequency, writing-pulse strength, probe center and packet inventory.
$r_p, \eta_p, S_w, \mathcal{D}_w, \delta h_e, u$ (contact probe)	Divergence-free probe direction, strength, central response, written-minus-unwritten response, changed contact energy and elapsed probe time.
$m, \lambda, \nu, a, b, \omega_r, g, \alpha, \mathcal{R}$ (rotor)	Mark normal, free axis, contact normal, two setting directions, rotation speed, crossing surface, circle angle and crossing rate; not the source's pair-phase relation.
$d, q, z, \Delta_r, q_0, \kappa_r, P_\ell, h_r, r_h$ (rotor)	Crossing-frame axis components, preceding crossing interval, conserved mark-axis product, mixture coefficient, Legendre polynomial, patch latitude and radius factor.
n_r, L_r, I_r, h_r, K_r (extended source)	Orientation, angular momentum, inertia, vector torque term and torque matrix; the torque vector is distinct from patch latitude.
$z, \eta, w_\ell, r_\ell, \gamma, G_\ell, b_\ell^{\mathrm{src}}, c_\ell^{\mathrm{src}}, M_x, F_x^{\mathrm{ext}}$	Extended-source amplitudes, contact weights/radii, coupling, cross-product map, source coefficients, emitted-field map and external field.
$\ell_\ell, Q_\ell, J_r, Q_r, Q_g, \epsilon_r, \mathcal{H}, P_\ell$	Contact-linear/quadratic current parts, their sums, guide inventory, relative quadratic norm, hemispherical transform and Legendre degree; distinct from measurement Hamiltonian $\mathcal{H}_{\mathrm{meas}}$.
$x, b_r, y, A_r, B_r, C_r, D_r, \vartheta_r$ (repair)	Retained/incoming/outgoing error vectors, scattering blocks and illustrative lossless rotation angle.
$\lvert e_0\rangle, \lvert e_1\rangle, \Delta_e, \sigma_e, V$	Recipient branch states, Gaussian record separation/width and coherence modulus $\lvert\Gamma\rvert$.
$K, a, b, c_{st}, \sigma_x, \sigma_y, \sigma_z, P_{\mathrm{pop}}$ (joint)	Assigned amplitude matrix, its two packet amplitudes, analyzer coefficients, Pauli operators and shared-population comparison law.
$\eta_A, \eta_B, \pi_i, Z_a, \rho_{\mathrm{source}}, \lambda_1, \lambda_2, c$	Recording efficiencies, setting frequencies, source normalization, source density, shared directions and communicated bit in the stated protocols.
$G, J, E_0, g_A, g_B, \hbar_*, \Theta$ (Paper 38 completion)	Static storage inverse, exchange strength, positive self-energy, endpoint couplings, assumed action scale and accumulated exchange angle.
$x, y, X, Y, u_A, u_B, d_A, d_B, \varphi_\sigma, f_\sigma, j_A, j_B$ (pointers)	Pointer coordinates/actual positions, driving speeds, packet separations, packet amplitude/density and configuration currents.
$z_A, z_B, \lambda_p, L_p, \mu_p, Q_p$	Pointer hyperbolic-tangent coordinates, assumed latch stiffness, minimum location, mobility and exported-energy coordinate.
$\mathbf{1}, e_i, I, \delta(\cdot), [\cdot]_\times, \mathrm{sym}, \dagger, \mathrm{c.c.}$	Constant vector, coordinate unit vector (or explicitly named capacity), identity, Dirac delta, cross-product matrix, symmetric part, conjugate transpose and complex conjugate.

Program component	Derivation implemented
`ContactNetwork`	All FCC contacts/faces; Equations (2.1), (2.2) and (2.5); common observations and RK4 steps.
`prepare`, `radial_ground`	Ground, donor, phase/timing controls, triangle blank and protected preparation; no runtime resetting.
`make_gauss_compatible`	Longitudinal field with an explicit inventory constraint and energy cost.
`native_checks`	Hamiltonian and regional derivatives; Equations (5.6) to (5.8) and (7.2).
`history_checks`	Integer histories, forward transform, and distinct first-record calculation.
`bridge_checks`	Conservative error export, Gaussian fraction control, work-count bound, and native dimer transfer.
`probability_checks`	Supplied quantum projector benchmark and complete versus selected Bell accounting.
`trajectory`, `campaign`	One shared trajectory/checkpoint system and explicit model-time schedules.
`aggregate`, `report`	Complete outcomes, nulls, regional residuals, refinement, and late failures.

The equation-to-program map describes the preserved executable only. The supporting appendices below restore analytical source arguments; they do not claim that every source-specific selector, harmonic scan, rotor campaign or guidance simulation is implemented by `T35.py`. This separation preserves one numerical engine without dropping the derivation logic or relabeling earlier source computations as fresh T35 output.

B Source pairing, carried phase, and mechanical binding

This appendix restores the distinct source-side steps of the revised T14A, T14B and T14E/F accounts [2, 3, 6, 7]. A finite selector, a physical interaction energy, and a two-site quantum representation are different objects. The first two are developed here; the additional joint-state assignment is treated once in appendix H. None of the reduced selector equations below is added to the native Hamiltonian (2.1).

B.1 The retained source and its candidate registry

The fixed-registry source calculation uses twelve surface coordinates and the real generator

$$\mathcal{A}(\theta) = \kappa L_{12} + \operatorname{diag} V_i(\theta), \qquad V_i = 4 - 2\cos\theta - 2\cos(i\pi/3 - \theta), \qquad \kappa = 2 + \cos(\pi/6), \tag{B.1}$$

where $(L_{12}u)_i = 2u_i - u_{i-1} - u_{i+1}$, indices are modulo twelve, and the eigenproblem is restricted to $u_{i+6} = -u_i$. At $\theta = 0$ the additional reflection symmetry gives $u_3 = u_9 = 0$ exactly. The lane inventories $W_r = \sum_{i \equiv r \pmod 3} |u_i|^2$ are positive and sum to one, while each corresponding coherent sum $\sum_{i \equiv r} u_i$ vanishes by antipodal cancellation. Thus a lane inventory cannot be replaced by the square of its summed amplitude. These are coordinates of one reduced field, not yet probabilities or three independently identified particles.

Assign these labels to

$$\mathcal{V} = \{r \in \{-1, 0, 1\}^3 : \ |r|^2 = 2\}, \qquad r_{i+6} = -r_i.$$

The six vectors whose first nonzero entry is positive are ordered lexicographically, followed by their antipodes. This assignment is a registry for comparison; consecutive ring labels are not thereby physical

nearest neighbors. A perfect matching partitions its twelve slots into six pairs. For supplied complex source coordinates z_i, let

$$C_{ij} = \mu_c |r_i + r_j|^2 + \epsilon_{ij}, \qquad \epsilon_{ij} = \epsilon_c \frac{\mathrm{Re}(\bar{z}_i z_j)}{\max_k |z_k|^2}, \quad \mu_c = 8, \quad \epsilon_c = 0.0064. \tag{B.2}$$

This is the declared T14A comparison cost. Its bounded perturbation obeys $|\epsilon_{ij}| \le \epsilon_c$. Every nonantipodal allowed edge has $|r_i + r_j|^2 \ge 2$. An alternative perfect matching must replace $k \ge 2$ antipodal edges and insert k nonantipodal edges. Its geometric cost increases by at least $2k\mu_c$, while the perturbation improves it by at most $2k\epsilon_c$. Therefore the antipodal matching is uniquely minimal whenever $\epsilon_c < \mu_c$, with gap at least $4(\mu_c - \epsilon_c)$. Exclusivity is part of this optimization problem, not a material capture process inferred from enumeration.

A complementary constraint statement does not require a matching algorithm. Fix a source slot s, its antipode $\bar{s}$, nonnegative weights v_i on the other slots with $\sum v_i = 1$, and residual $D = r_s + \sum_{i \ne s} v_i r_i$. Taking $h = r_{\bar{s}}$ gives

$$-h \cdot D = \sum_{i \ne s, \bar{s}} v_i (2 - h \cdot r_i) \ge 1 - v_{\bar{s}}, \qquad 1 - v_{\bar{s}} \le \sqrt{2}\, |D|. \tag{B.3}$$

The inequalities use $h \cdot r_i \le 1$ for competitors and $|h| = \sqrt{2}$. Exact compensation forces the antipode; a small residual bounds the unassigned weight. It does not prescribe the dynamics reaching that constraint.

B.2 Selection without replacing the supplied amplitudes

For a row of fixed real costs $c_j = C_{sj}/\mu_c$ and nonzero candidate support, T14B supplies the complete state $(s, z_s, \{j, c_j, z_j\}_{j \ne s})$. Its normalized filter is

$$\psi_j^{\mathrm{sel}}(\tau) = \frac{z_j e^{-\tau c_j/2}}{Z(\tau)^{1/2}}, \qquad Z(\tau) = \sum_k |z_k|^2 e^{-\tau c_k}, \qquad v_j = |\psi_j^{\mathrm{sel}}|^2. \tag{B.4}$$

Here τ is an algorithmic filtering budget, not elapsed time under (2.2). Since $Z'/Z = -\bar{c}$ with $\bar{c} = \sum_j v_j c_j$, differentiation gives

$$\frac{d\psi_j^{\mathrm{sel}}}{d\tau} = -\tfrac{1}{2}(c_j - \bar{c})\psi_j^{\mathrm{sel}}, \qquad \frac{dv_j}{d\tau} = -(c_j - \bar{c})v_j, \qquad \frac{d\bar{c}}{d\tau} = -\sum_j v_j (c_j - \bar{c})^2. \tag{B.5}$$

Summing the weight equation proves conservation. The multiplier of each supported amplitude is real and positive, so its phase is unchanged; a zero source amplitude remains zero. Successive filters add their budgets because their exponential factors multiply and their intermediate normalizations cancel.

If j_* is the unique minimum on the nonzero support, define

$$\Delta_c = \min_{j \ne j_*,\ z_j \ne 0} (c_j - c_{j_*}) > 0, \qquad R_c = \sum_{j \ne j_*} \frac{|z_j|^2}{|z_{j_*}|^2}.$$

The exact nonwinning-to-winning odds are

$$L_c(\tau) = \sum_{j \ne j_*} \frac{|z_j|^2}{|z_{j_*}|^2} e^{-\tau(c_j - c_{j_*})}.$$

Consequently

$$1 - v_{j_*} = \frac{L_c}{1 + L_c} \le \frac{R_c e^{-\tau\Delta_c}}{1 + R_c e^{-\tau\Delta_c}}, \qquad \tau \ge \max\left(0, \frac{\log[R_c(1-\delta_c)/\delta_c]}{\Delta_c}\right) \implies 1 - v_{j_*} \le \delta_c. \tag{B.6}$$

Here $0 < \delta_c < 1$ is a desired selector leakage. A single supported candidate needs no gap bound. Tied minima retain their original intensity ratios, not a newly invented tie-breaking probability. Perturbing every cost by at most η_c preserves the supported winner when $\Delta_c > 2\eta_c$, with the smaller gap in the same bound.

For prescribed changing costs, subtracting two weight equations yields

$$\log \frac{v_j(\tau)}{v_k(\tau)} = \log \frac{v_j(0)}{v_k(0)} - \int_0^\tau [c_j(u) - c_k(u)]\, du. \tag{B.7}$$

Thus the accumulated differences, not just the latest minimum, determine selection. Their source reaction is absent from a prescribed cost history and would require a coupled material model.

Independent row choices need not be exclusive. For symmetric costs with unique row minima $m(s)$, the additional condition $m(m(s)) = s$ makes the choices a fixed-point-free involution. They then form a perfect matching, and for any other matching M,

$$\sum_{\{s,j\}\in M} c_{sj} = \tfrac{1}{2} \sum_s c_{s,M(s)} \geq \tfrac{1}{2} \sum_s c_{s,m(s)}.$$

Any different matching uses a strictly nonminimal row entry. This proves unique optimality under reciprocity, rather than assuming that separate cheap choices automatically form pairs.

B.3 Transport retains the actual relation and its errors

The selected packet keeps (z_s, z_{j_*}) and its retained inventory; the selector weights do not overwrite those amplitudes. For two nonzero amplitudes define

$$\mathcal{R}(a, b) = -\frac{a\bar{b}}{|a||b|}.$$

The minus sign makes an opposite-sign pair have zero relation angle. Let endpoint $X = A, B$ acquire an actual path phase χ_X and possess an available record $\widehat{\chi}_X$. Its corrected coordinate is

$$a_X^{\text{out}} = a_X e^{id_X}, \qquad d_X = \chi_X - \widehat{\chi}_X, \qquad \frac{\mathcal{R}_{\text{out}}}{\mathcal{R}_{\text{in}}} = e^{i(d_A - d_B)}. \tag{B.8}$$

Magnitudes are unchanged and the principal circular error is bounded by $\min(\pi, |d_A| + |d_B|)$. Rounding each accumulated record to a multiple of q_c gives $|d_X| \leq q_c/2$, hence pair error at most $\min(\pi, q_c)$. Rounding every hop instead requires summing the hop errors. Complete path records preserve an already imperfect incoming pair; they do not reset it to a singlet. The analyzer setting is not a path phase to be subtracted. The physical storage and retrieval of this phase record remain an input to this transport identity.

B.4 From a registry minimum to a physical binding comparison

A native pair calculation must compare fully relaxed states in the same accessible conserved sector $\mathcal{I}$ and environmental conditions $\mathcal{B}$:

$$\Delta E_{\text{bind}} = E_{\text{pair}}^{\min}(\mathcal{I}, \mathcal{B}) - E_{\text{sep}}^{\min}(\mathcal{I}, \mathcal{B}). \tag{B.9}$$

Only factorized constraints and environments justify replacing the second term by two independently minimized self-energies. A closed graph cannot be neutralized differently in the two comparisons. Similarly, freely minimizing a rotating source's angular rate to zero changes its sector; where angular

momentum is actually conserved the relevant energy is $\mathcal{J}^2/(2I)$, with permitted host exchange retained. A static minimum does not certify stability of an unreduced periodic source.

There is an exact held-profile contribution in the contact model. Temporarily restore general field stiffness $\kappa_E > 0$ and phase coupling $g_E > 0$. For $L_B = BB^T$ and a neutral profile q, minimize $\kappa_E\|E\|^2/2$ subject to $BE = g_E q$. If L_B^+ is its inverse on the zero-sum space,

$$E_* = g_E B^T L_B^+ q, \qquad U_* = \frac{\kappa_E g_E^2}{2} q^T L_B^+ q. \tag{B.10}$$

Any other compatible field is $E_* + D$ with $BD = 0$. Their inner product vanishes, proving the minimum by completing the square. For $q = q_A + q_B$, the cross term is $\kappa_E g_E^2 q_A^T L_B^+ q_B$. For fixed geometry and independent shape coordinates, its mixed derivative is $\kappa_E g_E^2 D_A^T L_B^+ D_B$, where $D_X = \partial q_X/\partial y_X$. A negative cross term can lower a positive total energy, but it is not the complete binding energy of all moving source, phase and host coordinates.

The corresponding phase lock must retain its connector. With fixed internal shapes and bridge overlap

$$\mathcal{T}_s = \sum_{e:A\to B} t_e \bar{a}_{s,i} e^{isg_E A_e} b_{s,j}, \qquad \delta_s = \phi_{A,s} - \phi_{B,s},$$

the actual hopping contribution is $2\,\mathrm{Re}(e^{-i\delta_s}\mathcal{T}_s)$. If this phase is free and $\mathcal{T}_s \neq 0$, its minimum is $-2|\mathcal{T}_s|$ at $\delta_s = \arg\mathcal{T}_s + \pi$, with curvature $2|\mathcal{T}_s|$. Zero overlap supplies no lock; a missing bridge supplies no such interaction. This is not a universal imposed opposite phase independent of the contact fields.

B.5 Relaxed stability and a conditional pair well

For equality constraints $C_\alpha(y) = 0$, the relevant Hessian is $Z^T\nabla^2(E + \sum_\alpha \lambda_\alpha C_\alpha)Z$, where Z spans the constraint tangent space. Exact symmetry directions are removed before testing positive definiteness. If internal coordinates z have positive block H_{zz}, differentiating $E_z(R, z_*(R)) = 0$ gives $z_*' = -H_{zz}^{-1}E_{zR}$ and

$$V''(R) = E_{RR} - E_{Rz}H_{zz}^{-1}E_{zR}. \tag{B.11}$$

Holding z fixed would omit the negative relaxation term. A mixed block K_{AB} transforms as $J_A^T K_{AB} J_B$ under separate nonsingular coordinate changes, preserving its rank. Such mechanical nonseparability is a cross-response property, not a tensor-state or Bell theorem.

T14E's explicitly conditional example is

$$E - 2E_0 = \tfrac{k}{2}(q_A^2 + q_B^2) + A_c x^2 - J_c x + c_c x q_A q_B - f_c x(q_A + q_B), \qquad x = e^{-R/\ell_c}. \tag{B.12}$$

The coefficients are a proposed reduced interaction, not derived values of the native receiver. When $k \pm c_c x > 0$, solving the two linear stationarity equations gives $q_A = q_B = f_c x/(k + c_c x)$ and

$$\begin{aligned} V(x) &= A_c x^2 - J_c x - \frac{f_c^2 x^2}{k + c_c x}, \\ V_x &= 2A_c x - J_c - \frac{f_c^2 x(2k + c_c x)}{(k + c_c x)^2}, \qquad V_{xx} = 2A_c - \frac{2f_c^2 k^2}{(k + c_c x)^3}. \end{aligned} \tag{B.13}$$

For $c_c < 0$, $J_c > 0$, $k, \ell_c > 0$, set $x_{\max} = e^{-R_{\min}/\ell_c}$ and $d_{\min} = k + c_c x_{\max}$. The sufficient conditions

$$d_{\min} > 0, \qquad A_c > f_c^2 k^2/d_{\min}^3, \qquad V_x(x_{\max}) > 0$$

make $V_{xx} > 0$ throughout the domain. Since $V_x(0) = -J_c < 0$, there is one interior minimum. Its value is negative because $V(0) = 0$ and its initial slope is negative. At that minimum $V_{RR} = (x/\ell_c)^2 V_{xx} > 0$;

together with the positive shape block, the Schur-complement test proves stability in these three retained coordinates. This does not supply omitted host or moving-contact stability.

The admissible geometry is part of the premise. In the revised T14E/F aligned-source example, the moving region, guide and shell together have 91 sites; translations $(2m, -2m, 0)$ first make two such supports disjoint at $m = 4$, or separation $R = 8$ in its occupied-distance convention. An older small-separation well is not admissible in that particular placement family. The later long-range illustrative well is a conditional example on the corrected domain, not a derived interaction range. Shared sites require a single common host rather than duplicate ownership [6, 7].

B.6 Clearing, opening, and what survives separation

The energy released on capture must remain in internal modes or reach an explicit recipient. Minimization alone supplies no settling trajectory. For detachment, the same field minimum supplies a sharp static cost. Define

$$P_{\mathrm{cyc}} = I - B^T L_B^+ B, \qquad \alpha_e = u_e^T P_{\mathrm{cyc}} u_e,$$

where u_e is the unit coordinate of the contact to be cleared. A compatible increment has $BD = 0$, and clearing requires $D_e = -E_{*,e}$. Since $D_e = (P_{\mathrm{cyc}} u_e)^T D$, Cauchy–Schwarz gives

$$D_{\min} = -\frac{E_{*,e}}{\alpha_e} P_{\mathrm{cyc}} u_e, \qquad W_{\min} = \frac{\kappa_E E_{*,e}^2}{2\alpha_e}, \qquad \alpha_e > 0. \tag{B.14}$$

Orthogonality to E_* identifies this as the exact added offset energy. If $\alpha_e = 0$, a nonzero bridge offset cannot be cleared at fixed source balance. The bound concerns the old graph before opening; geometry, phase work and multiple simultaneous openings require their additional accounting.

For the separately declared triangle-relaxation law in T14E, a clearing increment proportional to a cycle $c_\triangle$ decays as $e^{-\nu_c \|c_\triangle\|^2 t}$. The formerly cleared contact then reloads as $E_e(t) = E_{*,e}[1 - e^{-\nu_c \|c_\triangle\|^2 t}]$. This is why clearing and physical opening must be coordinated; that relaxation law is not silently installed in T35's conservative evolution.

Finally, for an assumed phase potential $-K(R)\cos(m\delta)$, its small-oscillation frequency is $m\sqrt{K/I_{\mathrm{rel}}}$ and phase-slip barrier $2K$. Both vanish when $K(R) \to 0$. Shared past phase, ongoing force, metastable memory and a persistent pair-spanning connector are therefore separate claims. T14F supplies the conditions a proposed connector would have to meet; an energetic pair minimum does not create that connector by definition.

C Analyzer geometry, omitted modes, and matched receiving channels

The revised T14C separates an exact geometric compression from a physically implemented analyzer [4]. The derivation is retained here because neither the source's half-angle eigenline nor a squared receiving inventory alone supplies the native measurement map used in Sections 4 and 5.

C.1 Compression and the term it omits

For (B.1), let $\alpha_i = i\pi/6$ and define the real orthonormal columns

$$f_{c,i} = \cos\alpha_i/\sqrt{6}, \qquad f_{s,i} = \sin\alpha_i/\sqrt{6}, \qquad B_a = (f_c, f_s), \qquad P_a = B_a B_a^T, \quad Q_a = I - P_a.$$

Both first harmonics have ring-Laplacian eigenvalue $2 - 2\cos(\pi/6)$. Multiplication by the nonconstant potential gives

$$-2\cos(2\alpha_i - \theta) f_{c,i} = -\cos\theta f_{c,i} - \sin\theta f_{s,i} - g_{c,i},$$

$$-2\cos(2\alpha_i-\theta)f_{s,i} = -\sin\theta f_{c,i} + \cos\theta f_{s,i} - g_{s,i}, \tag{C.1}$$

where $g_{c,i} = \cos(3\alpha_i-\theta)/\sqrt{6}$ and $g_{s,i} = \sin(3\alpha_i-\theta)/\sqrt{6}$ are orthonormal and perpendicular to B_a. It follows that

$$B_a^T\mathcal{A}B_a = a_0 I - D(\theta), \quad a_0 = \kappa[2-2\cos(\pi/6)] + 4 - 2\cos\theta, \quad Q_a\mathcal{A}B_a = -(g_c, g_s), \tag{C.2}$$

with $D(\theta)$ as defined in Section 3. In particular $\|Q_a\mathcal{A}B_a\|_2 = 1$: the compressed plane is not an invariant subsystem.

Let W_a be an orthonormal odd-sector complement formed from the third and fifth harmonics. For a full eigenpair $\mathcal{A}u = \lambda u$, put $p_a = B_a^T u$, $q_a = W_a^T u$, $T_a = W_a^T\mathcal{A}B_a$, and $C_\lambda = W_a^T\mathcal{A}W_a - \lambda I$. The block equations imply, whenever C_λ is invertible,

$$q_a = -C_\lambda^{-1}T_a p_a, \qquad [B_a^T\mathcal{A}B_a - T_a^T C_\lambda^{-1}T_a]p_a = \lambda p_a. \tag{C.3}$$

The full norm is the sum of the two orthogonal block norms. With $\widehat{p}_a = p_a/\|p_a\|$, the retained inventory is therefore

$$m_a = \|p_a\|^2 = \frac{1}{1+\|C_\lambda^{-1}T_a\widehat{p}_a\|^2}. \tag{C.4}$$

The full eigenvalue appears in this exact elimination. A small angular error of $\widehat{p}_a$ does not bound the omitted inventory, and substituting the uncorrected half-angle eigenvector does not solve the full eigenproblem.

C.2 Half-angle geometry and material angle are not interchangeable

For a nonzero real contrast

$$D(h) = \begin{pmatrix} h_z & h_x \\ h_x & -h_z \end{pmatrix}, \qquad (h_z, h_x) = \rho_a(\cos\vartheta, \sin\vartheta), \quad \rho_a > 0,$$

$D(h)^2 = \rho_a^2 I$. Thus $P_\pm = (I \pm D/\rho_a)/2$, and solving the eigenvector equation gives

$$u_+(\vartheta) = \begin{pmatrix} \cos(\vartheta/2) \\ \sin(\vartheta/2) \end{pmatrix}, \quad u_-(\vartheta) = \begin{pmatrix} -\sin(\vartheta/2) \\ \cos(\vartheta/2) \end{pmatrix}, \quad U_a = (u_+, u_-) = R_2(\vartheta/2). \tag{C.5}$$

Here R_2 is the ordinary real two-dimensional rotation matrix. A closed nonzero contrast loop of winding w changes a continuously followed eigenvector by $(-1)^w$. This is a result of diagonalization, not an assumed spinor probability.

For an actual unoriented axis $n_a = (\cos\chi, \sin\chi)$, however, $2n_a n_a^T - I = D(2\chi)$. A full 2π axis turn winds that contrast twice and the eigenvector returns positively. The registry parameter θ in (B.1) rotates the potential's director by $\theta/2$. These facts prevent identifying every 2π registry loop with a 2π material spin rotation. Moreover a moving basis $x = U_a^T y$ acquires the generator term $-iU_a^T\dot{U}_a$, in addition to the transformed physical generator. Following static eigenvectors is not a time-evolution proof.

For a normalized local two-mode input $q_a = (q_c, q_s)^T$, direct projection gives

$$|u_\pm^T q_a|^2 = \tfrac{1}{2}[1 \pm (m_a^{\mathrm{loc}}\cos\vartheta + v_a\sin\vartheta)], \quad m_a^{\mathrm{loc}} = |q_c|^2 - |q_s|^2, \quad v_a = 2\,\mathrm{Re}(q_c\bar{q}_s). \tag{C.6}$$

For the projected full field the sum is instead $\|B_a^T u\|^2$, not one. Dividing by it defines conditional retained fractions, not capture of the omitted field. A passive change of coordinates rotates both q_a and U_a and leaves the contraction unchanged; a physical analyzer turn holds the field fixed.

The calibration $q_a = (1,-1)^T/\sqrt{2}$ makes the phase/rotation distinction explicit. Applying $\mathrm{diag}(1, e^{i\varepsilon_a})$ to the field gives $w_+ = [1-\cos\varepsilon_a\sin\vartheta]/2$. Turning the real analyzer frame by γ_a instead gives $w_+ = [1-\sin(\vartheta+2\gamma_a)]/2$. A path-phase error cannot in general be renamed an analyzer-angle shift.

C.3 A declared conservative receiver and its exact solution

The matched receiver used in T14A/C is an additional finite apparatus model. For channels $\sigma = \pm 1$, incoming and receiving amplitudes $Z_\sigma, B^{\mathrm{rec}}_\sigma$, and readiness phase/action (ϕ_σ, s_σ), its energy is

$$\begin{aligned} H_{\mathrm{rec}} = \sum_\sigma \{ & \omega_a |Z_\sigma|^2 + (\omega_a + \Omega_a + \sigma\rho_a)|B^{\mathrm{rec}}_\sigma|^2 + \Omega_a s_\sigma \\ & - g_a(\bar{Z}_\sigma e^{i\phi_\sigma} B^{\mathrm{rec}}_\sigma + \mathrm{c.c.})\}. \end{aligned} \tag{C.7}$$

Take $g_a > 0$, $\Omega_a \geq 0$ and positive readiness actions before release. The sufficient positivity condition on the amplitude energy is $\omega_a > \rho_a + g_a$. Hamilton's equations give

$$\begin{aligned} i\dot{Z}_\sigma &= \omega_a Z_\sigma - g_a e^{i\phi_\sigma} B^{\mathrm{rec}}_\sigma, \\ i\dot{B}^{\mathrm{rec}}_\sigma &= (\omega_a + \Omega_a + \sigma\rho_a) B^{\mathrm{rec}}_\sigma - g_a e^{-i\phi_\sigma} Z_\sigma, \\ \dot{\phi}_\sigma &= \Omega_a, \qquad \dot{s}_\sigma = -j^{\mathrm{rec}}_\sigma, \qquad j^{\mathrm{rec}}_\sigma = 2g_a \,\mathrm{Im}(\bar{Z}_\sigma e^{i\phi_\sigma} B^{\mathrm{rec}}_\sigma). \end{aligned} \tag{C.8}$$

Writing $F_\sigma = |B^{\mathrm{rec}}_\sigma|^2$ gives $\dot{F}_\sigma = j^{\mathrm{rec}}_\sigma$, so $|Z_\sigma|^2 + F_\sigma$ and $s_\sigma + F_\sigma$ are conserved, as is the full energy. Readiness reloads on return; it is not a one-way loss variable.

Put $C^{\mathrm{rec}}_\sigma = e^{i\phi_\sigma} B^{\mathrm{rec}}_\sigma$. The actual readiness equation removes Ω_a, leaving the amplitude matrix

$$\begin{pmatrix} \omega_a & -g_a \\ -g_a & \omega_a + \sigma\rho_a \end{pmatrix}.$$

After subtraction of $(\omega_a + \sigma\rho_a/2)I$, its square is $\nu_a^2 I$, with $\nu_a^2 = g_a^2 + \rho_a^2/4$. Exponentiating and using $Z_\sigma(0) = a_\sigma$, $B^{\mathrm{rec}}_\sigma(0) = 0$ yields

$$\begin{aligned} Z_\sigma(t) &= a_\sigma e^{-i(\omega_a + \sigma\rho_a/2)t}[\cos(\nu_a t) + i\sigma\rho_a \sin(\nu_a t)/(2\nu_a)], \\ C^{\mathrm{rec}}_\sigma(t) &= i(g_a/\nu_a) a_\sigma e^{-i(\omega_a + \sigma\rho_a/2)t} \sin(\nu_a t), \\ F_\sigma(t) &= |a_\sigma|^2 X_a(t), \qquad X_a(t) = \frac{g_a^2}{g_a^2 + \rho_a^2/4} \sin^2(\nu_a t). \end{aligned} \tag{C.9}$$

Opposite detunings therefore preserve both input fractions, including during backflow. The common envelope is a derived property of this stated receiver, not a general consequence of conserving total norm.

A common detuning error Δ_a changes the detunings to $d_\pm = \Delta_a \pm \rho_a$ and gives

$$X_\pm = \frac{g_a^2}{g_a^2 + d_\pm^2/4} \sin^2\left(t\sqrt{g_a^2 + d_\pm^2/4}\right), \qquad p_{\mathrm{received}} = \frac{pX_+}{pX_+ + (1-p)X_-}.$$

For nonzero couplings, equality of the two envelopes on an interval forces $g_+^2 = g_-^2$ from the t^2 coefficient and $d_+^2 = d_-^2$ from the t^4 coefficient. Normalization cannot repair a mismatched physical response. The further conversion of matched loading into first records is proved in appendix D, under its separate capacity and retention assumptions.

C.4 What a single occupied receiving contact actually supplies

The revised T14C also projects a specified frozen triangular contact rather than assuming the preceding receiver has already emerged. Let the three-site hopping block be $a_\triangle(\mathbf{1}\mathbf{1}^T - I)$, and attach a carrier of

diagonal frequency $-a_\triangle$ at one site j with entry strength k_e. In its two angular modes, uniform mode, and carrier coordinates, the matrix is

$$\widetilde{H} = \begin{pmatrix} -a_\triangle & 0 & 0 & k_e v_{j,c} \\ 0 & -a_\triangle & 0 & k_e v_{j,s} \\ 0 & 0 & 2a_\triangle & k_e/\sqrt{3} \\ k_e v_{j,c} & k_e v_{j,s} & k_e/\sqrt{3} & -a_\triangle \end{pmatrix}, \qquad v_j = \sqrt{2/3}\begin{pmatrix} \cos\psi_j \\ \sin\psi_j \end{pmatrix}, \quad \psi_j = 2\pi j/3. \tag{C.10}$$

The angular basis has entries $\sqrt{2/3}\cos(2\pi i/3)$ and $\sqrt{2/3}\sin(2\pi i/3)$; the uniform vector is $\mathbf{1}/\sqrt{3}$. Multiplying the original matrix by these columns gives (C.10). Only the angular direction parallel to v_j is driven; its perpendicular direction is dark. The coupling has rank one, whereas (C.9) assumes two nonzero matched input channels.

Inverting the uniform/carrier block of $\lambda I - \widetilde{H}$, where it is invertible, gives

$$H_{\text{eff}}(\lambda) = -a_\triangle I + \frac{k_e^2(\lambda - 2a_\triangle)}{(\lambda - 2a_\triangle)(\lambda + a_\triangle) - k_e^2/3} v_j v_j^T. \tag{C.11}$$

Since $v_j v_j^T = [I + D(2\psi_j)]/3$, the induced contrast is a director contrast with discrete site choices. Changing coordinates cannot raise its input rank or remove its coupled uniform mode. A continuous mechanical setting, two resolved receiving responses, and their actual frequency and kinetic normalization remain physical requirements. This restricted contact calculation identifies those requirements without replacing the native loading theorem in the main text.

D History, preparation, and event measures

The chain of statistical implications is proved here without identifying its different measures by notation. A history count determines how paths are weighted; a preparation law determines what enters; a residence law determines time spent; a first-record law determines what an initialized recorder reports. The history argument is from the restored T14 edition, the matched-capacity result from the separate meter line and revised T14A/K, and the event distinctions are retained in T34 [1, 2, 11, 14].

D.1 Why the two-sided history product becomes a square

Use the finite primitive kernel K_h, positive weights μ_i, and endpoints f, g of (3.1). Give a complete path $x_{-m}, \dots, x_n$ weight

$$\mu_{x_{-m}} f(x_{-m}) \prod_{k=-m}^{n-1} (K_h)_{x_k x_{k+1}}\, g(x_n).$$

Fix $x_0 = i$. Detailed balance reverses the left product: its sum is $\mu_i (K_h^m f)_i$. The right product sums to $(K_h^n g)_i$. Multiplying these independent continuation sums and normalizing proves (3.1). This factorization is a fact about the specified path weights, not an independence assumption about two measured detectors.

In the weighted inner product $\langle u, v\rangle_\mu = \sum_i \mu_i \bar{u}_i v_i$, detailed balance makes K_h self-adjoint. Primitivity gives a simple positive principal eigenvector h and eigenvalue ρ, with all other eigenvalues strictly smaller in modulus. Its spectral decomposition gives

$$\rho^{-m} K_h^m f \longrightarrow \frac{\langle h, f\rangle_\mu}{\langle h, h\rangle_\mu} h,$$

and the same statement for g. Both coefficients are positive for the stated nonzero nonnegative endpoints. Their product cancels on normalization, yielding (3.2). With only one long continuation and a flat

remaining factor, the result is proportional to $\mu_i h_i$, not $\mu_i h_i^2$. Without reversibility, independent left and right principal profiles generally replace the matching two factors.

For the finite estimate in (3.3), write the scaled factors as $h_i(1+u_i)$ and $h_i(1+v_i)$. Let $e_i = u_i + v_i + u_i v_i$, so $|e_i| \le d$, and $\bar{e} = \sum_i \pi_i e_i$. Then

$$p_i - \pi_i = \pi_i \frac{e_i - \bar{e}}{1+\bar{e}}, \qquad \tfrac{1}{2}\sum_i |p_i - \pi_i| \le \frac{d}{1-d}.$$

The estimate concerns the declared history ensemble. It does not control a recorder that samples another ensemble.

For the forward transform (3.4), the eigenvalue equation gives its row sums. Its stationary detailed balance follows from

$$\pi_i P^h_{ij} = \frac{\mu_i (K_h)_{ij} h_i h_j}{\rho \sum_k \mu_k h_k^2} = \pi_j P^h_{ji}.$$

Thus a forward process realizes the same residence measure. The calculation does not derive its h-dependent transition rates from the occupied-contact action. For time-ordered or different continuation operators, the actual left and right propagated profiles must still be multiplied; symmetry of individual factors does not allow replacing their final product by a square.

D.2 Geometry does not by itself choose a record measure

On a sphere, $h_n(x) = n \cdot x$ is the positive first Dirichlet mode of the hemisphere $n \cdot x > 0$, with $-\Delta_{S^2} h_n = 2h_n$. The corresponding two-sided construction has a squared profile there. Combining opposite hemispheres with equal declared weight gives the normalized rail density in Section 3, since $\int_{S^2} (n \cdot x)^2 d\Omega = 4\pi/3$. Its equality under $n \mapsto -n$ is immediate. Its integral over either hemisphere cut through the origin is one half, because $x \mapsto -x$ exchanges the two regions and preserves the density. This proves the stated loss of directed preparation information rather than merely noting a visual resemblance to a squared amplitude.

The complex two-mode reference provides a different measure calculation. Write

$$d = (\sqrt{u}\, e^{i\alpha}, \sqrt{1-u}\, e^{i\beta}), \qquad 0 < u < 1.$$

The induced metric on the unit sphere in $\mathbb{C}^2$ has diagonal entries $[4u(1-u)]^{-1}, u, 1-u$ in (u, α, β), determinant $1/4$, and total surface area $2\pi^2$. Its normalized volume is therefore $du\, d\alpha\, d\beta/(4\pi^2)$. The fraction u is uniform and independent of the relative phase. By contrast, a uniform real unit-circle angle gives the arcsine CDF in (6.3). Neither coordinate-space symmetry establishes that the native source physically prepares that measure. The tetrahedral fixed-quadrature family uses a supplied uniform fraction; it is not a claim to prepare the entire complex sphere while simultaneously fixing its relative phase.

D.3 Matched loading and a general first-release theorem

Suppose an explicitly specified receiver supplies common loading $F_i(t) = w_i X(t)$ in m channels, $w_i \ge 0$, $\sum_i w_i = 1$, and positive initial capacities e_i. Up to the first event, the winner is the least e_i/w_i; zero weights have infinite ratio. This premise is supplied by the matched receiving model in appendix C, not by the history operator. A physical interlock preserving the first release is a further apparatus assumption.

Assume a continuous capacity law with zero-probability ties and joint survival function

$$P(e_i > u_i \text{ for all } i) = \Psi\left(\sum_i u_i\right), \qquad u_i \ge 0, \quad \Psi(0) = 1. \tag{D.1}$$

At exposure y, the flux through channel i's release face is $-w_i\partial_{u_i}\Psi(\sum_j u_j)|_{u_j=w_j y} = -w_i\Psi'(y)$. Integrating to $M = \max_{t\le T} X(t)$ gives

$$P(i \text{ first by } T) = w_i[1-\Psi(M)], \qquad P(\text{no release by } T) = \Psi(M). \tag{D.2}$$

Continuity orders first passages to loading levels even when the envelope later reverses. Independence of capacities is not necessary; the specified sum-form survival is what does the work.

For a uniform capacity simplex $\sum_i e_i = E_c$, translating e_i by u_i leaves a simplex of total $E_c - \sum_i u_i$. Its $(m-1)$-dimensional volume scales as that total to power $m-1$, so

$$\Psi(y) = (1 - y/E_c)_+^{m-1}.$$

For T14A's four joint channels the exponent is three. One can also integrate the winning face directly: set $e_i = w_i y$, $e_j = w_j y + t_j$ for $j \neq i$, with $t_j \ge 0$ and $\sum t_j = E_c - y$. The coordinate Jacobian contributes w_i, leaving exactly the same first-channel fraction. Equal-scale exponential actions conditioned on their sum supply this simplex law in the separate readiness model; a generic thermal or correlated preparation need not do so.

The conclusion has Born form only after the physical receiver supplies $w_i = |(U_a^\dagger a)_i|^2/\|a\|^2$ and the capacity/first-record assumptions are realized. Four channels indexed jointly by both wing outcomes are a global receiver, not two separated local detectors. In particular their amplitudes may depend on both analyzer settings. This proof is retained as a useful conditional connection, not reinstated as native latch or reset dynamics.

D.4 Stationary marks, initialized records, and changes of clock

For the provisional Markov comparison in (7.6), a stationary state i is marked with probability κ_i, giving unnormalized stationary mark frequency $\pi_i\kappa_i$. Starting instead from reset row vector ν, recording before each transition gives probability $\nu Q^k R$ for absorption after exactly k previous missed visits. Summing the geometric series proves (7.6) when $\rho(Q) < 1$. At a finite deadline of M_v visits the recorded law is $\nu\sum_{k=0}^{M_v-1} Q^k R$ and the remaining no-record mass is $\nu Q^{M_v}\mathbf{1}$. If eventual absorption is not certain, that mass must not be normalized away. Reset and marking sensitivities are therefore substantive parts of the measured law.

If model time τ and a measured clock satisfy $dt = w(X)d\tau$, $w > 0$, a stationary residence measure changes to $\pi_t \propto w\pi_\tau$. The event intensity changes inversely, $r_t = r_\tau/w$. Their product, and hence a consistently counted normalized event measure, is unchanged. Altering only the residence density while keeping the old event rate would instead describe a new experiment. A monotone clock change cannot reorder an existing sequence of records; a new deadline or tick-sampling protocol can change the selected observations.

D.5 The Gaussian ratio formula and the inventory tolerance

The larger-source comparison in Section 6 has two logically separate operations: a waveform distribution and an actual fixed-inventory handoff. For independent equal-scale exponential intensities $X_I = |X|^2$, $Y_I = |Y|^2$ of mean ϑ_g, set $S = X_I + Y_I$, $U = X_I/S$. The inverse change is $(X_I, Y_I) = (SU, S(1-U))$ with absolute Jacobian S. Hence $f_{S,U} = Se^{-S/\vartheta_g}/\vartheta_g^2$, proving uniform U independent of S. Readiness depending only on S preserves that fraction under this specific factorized law, although it changes the preparation rate.

For a zero-mean proper complex Gaussian pair with covariance $\Sigma = \left(\begin{smallmatrix} a_g & z_g \\ \bar{z}_g & b_g \end{smallmatrix}\right)$, $\det\Sigma > 0$, the event $U \le u$ is the quadratic-form event $(1-u)|X|^2 - u|Y|^2 \le 0$. Whiten the pair. The Hermitian form then has trace $T_u = a_g(1-u) - b_g u$ and determinant $-u(1-u)\det\Sigma$. Its eigenvalues are $(T_u \pm D_u)/2$,

where $D_u = \sqrt{T_u^2 + 4u(1-u)\det\Sigma}$. They have opposite signs for $0 < u < 1$ and multiply independent unit exponential intensities. Integrating the probability that the positive term is no larger than the negative term gives $(D_u - T_u)/(2D_u)$, exactly (6.5). Equal variances alone do not remove a nonzero coherence z_g.

The signed unnormalized reference intensity $X_I - Y_I$ instead has density $e^{-|v|/\vartheta_g}/(2\vartheta_g)$. With a fixed signal strength $n_s(2p-1)$, its comparison CDF is $\frac{1}{2}e^x$ for $x \le 0$ and $1 - \frac{1}{2}e^{-x}$ for $x \ge 0$, where $x = n_s(2p-1)/\vartheta_g$. This proves the discrepancy cited in Section 6 without any native event simulation. A linear map satisfies $L(az) = aL(z)$ and cannot normalize all nonzero amplitudes to one fixed inventory.

For an actually controlled ratio $r_N = n_r/n_s \in [1-\epsilon, 1+\epsilon]$, conditionally uniform reference fraction has cutoff $\mathrm{clip}_{[0,1]}[1/2 + (p-1/2)/r_N]$. Clipping cannot increase its distance from $p \in [0,1]$, and $|1/r_N - 1| \le \epsilon/(1-\epsilon)$. Averaging proves the inventory tolerance quoted in the main text. This is a bound for a physically controlled band, not a mechanism that produces one.

D.6 Quadratic receiving energy and equal-work counts

For the separate stable harmonic comparison in Section 7, use $H_o = (p_o^2 + \omega_o^2 q_o^2 + P_o^2 + \Omega_o^2 Q_o^2)/2 + g_o q_o Q_o$, with positive frequencies and $g_o^2 < \omega_o^2 \Omega_o^2$. The source begins at $q_o = A_o$, all other coordinates zero. Its receiver equation is $\ddot{Q}_o = -\Omega_o^2 Q_o - g_o q_o$, so $Q_o = -g_o A_o t^2/2 + O(t^4)$ and $\dot{Q}_o = -g_o A_o t + O(t^3)$. The receiver's own quadratic energy begins as $g_o^2 A_o^2 t^2/2 + O(t^4)$. The full energy includes the interaction and source reaction; this response is not an outcome probability.

For actual equal-work records, let $W_a = \epsilon_w N_a + R_a$ with $0 \le R_a < \epsilon_w$. Put $W = \sum_a W_a$, $R = \sum_a R_a$, and assume at least one completed record. If $R > 0$, the normalized work vector is the convex mixture

$$\frac{W_a}{W} = \left(1 - \frac{R}{W}\right)\frac{N_a}{\sum_b N_b} + \frac{R}{W}\frac{R_a}{R}.$$

Total variation between the first distribution and the work distribution is at most R/W, proving the main-text counting bound; $R = 0$ gives equality directly. A powered detector can release reservoir energy after a small trigger, and the equal-work premise still does not ensure one exclusive record per source trial.

D.7 A complete error budget and why rare acceptance matters

Let M_θ be the written label and R_θ the final readable label, both including nulls. Compare an actual preparation ν with an independently specified reference ν_*. If their total variation is at most δ_{prep} and, on the same full trajectories, writing, retention and reading disagree with their respective intended labels only on sets of masses $\epsilon_{\mathrm{write}}, \epsilon_{\mathrm{ret}}, \epsilon_{\mathrm{read}}$, then

$$\mathrm{TV}(q^{\mathrm{read}}, q_*) \le \delta_{\mathrm{prep}} + \epsilon_{\mathrm{write}} + \epsilon_{\mathrm{ret}} + \epsilon_{\mathrm{read}}. \tag{D.3}$$

Here q_* is justified only if the reference writing law has separately been established. Pushforward under a fixed measurable map cannot increase total variation. Coupling successive labels on the same state bounds their distributional distance by disagreement probability; the union bound and triangle inequality prove (D.3). The native theorems control particular terms under their hypotheses, not all terms at once.

If two complete laws differ by δ and each assigns an accepted set probability at least $\alpha > 0$, their conditional accepted laws differ by at most $\min(1, 2\delta/\alpha)$. Separate the changed numerator from the changed normalizing probability to obtain this bound. Thus agreement on a selected subset neither proves the complete law nor makes a missing-record mechanism irrelevant. The transfer identity (7.5) is the exact sign-resolved form of this accounting for the comparison construction.

E Supporting native preparation and memory derivations

This appendix retains the earlier triangular preparation branch and the full three-path memory construction. They use the same occupied-contact action as the main text but different graphs or preparations. The tetrahedral preparation and connected loading proofs remain in Sections 4 and 5; they are not proved again here.

E.1 The conservation identities follow from the actual action

For one edge $i \to j$, the surface equation gives the tail contribution $2t_0 \operatorname{Im}(\bar{\psi}_{s,i} e^{isA_e} \psi_{s,j}) = -J_{s,e}$ to $\dot{n}_{s,i}$ and the opposite contribution at the head. Summing edges proves $\dot{n}_s = -BJ_s$, hence total channel inventory conservation. Differentiating hopping with respect to A_e gives J_e, and differentiating the face term gives $\beta C^T CA$, so the same action gives the displayed field reaction. Then

$$\dot{G} = B(-J - \beta C^T CA) - [-B(J_+ - J_-)] = 0$$

by $BC^T = 0$. The canonical surface and field terms cancel in $\dot{H}$, proving energy conservation. A further derivative of J_e with respect to A_e gives $-2t_0 \operatorname{Re}(z_{+,e} + z_{-,e}) = -h_e$. The regional account in (2.5) follows by the same cancellation on internal contacts; only crossing-surface terms and exterior-face forces remain. These are identities of the declared action, not a derivation of that action from constituent rigid-sphere motion.

E.2 The triangular mode-comparison force and its Gauss cost

On the triangle with three equal arms, use the normalized radial profile F_ℓ of (4.2) and angular modes

$$\chi_{\pm,j\ell} = F_\ell e^{\pm 2\pi i j/3}/\sqrt{3}, \qquad \chi_{0,j\ell} = F_\ell/\sqrt{3}, \qquad j = 0, 1, 2.$$

The two winding modes have zero-field hopping eigenvalue $\mu = -2t_0 \cos k_L$. Their root contribution is $-t_0 F_0$ and the arm recurrence supplies the rest. With unit coefficient pairs $c = (c_1, c_2)$ and $d = (d_1, d_2)$, take their common phases so that $c_1, d_1 \geq 0$ and prepare

$$\psi_+ = \sqrt{n}(c_1\chi_+ + c_2\chi_-), \quad \psi_- = \sqrt{n}(d_1\chi_+ + d_2\chi_-), \quad p = |c_1|^2, \quad r = |d_1|^2. \tag{E.1}$$

The winding signs are distinct from the signed field-channel labels. Angular orthogonality gives

$$\sum_{j=0}^{2} \operatorname{Im}(\bar{\psi}_{s,j0}\psi_{s,j+1,0}) = \tfrac{\sqrt{3}}{2} n F_0^2 (|a_{s,1}|^2 - |a_{s,2}|^2), \qquad a_+ = c, \quad a_- = d.$$

Cross terms cancel in this summed current, not in every local population. Inserting the current in (2.2) at $A = 0$ proves

$$b''_\triangle(0) = 2\sqrt{3}\, t_0 n F_0^2 (p - r). \tag{E.2}$$

With a uniform complex-sphere reference, appendix D therefore gives positive initial direction with fraction p.

If $q_{j\ell} = |\psi_{+,j\ell}|^2 - |\psi_{-,j\ell}|^2$ and $\mathcal{Q}_j = \sum_\ell q_{j\ell}$, zero Gauss constant generally requires a field. With outward arm orientations, its minimum-norm solution is

$$E_{j,\ell-1\to\ell} = -\sum_{u=\ell}^{L} q_{ju}, \qquad E_{i\to j} = (\mathcal{Q}_i - \mathcal{Q}_j)/3 \quad \text{on the core.} \tag{E.3}$$

The arm balances telescope and the core differences complete the root balances. The cycle sum is zero, so neither $b_\triangle$ nor its first derivative is initialized with a signed impulse. Any other compatible field adds the sole divergence-free cycle, orthogonal to this solution.

Put $C_s = \bar{c}_1 c_2$, $C_r = \bar{d}_1 d_2$, and $\Lambda_L = 1/3 + \sum_{\ell=1}^{L} (\sum_{u=\ell}^{L} F_u^2)^2$. Discrete harmonic orthogonality gives $\sum_j \mathcal{Q}_j^2 = 2n^2 |C_s - C_r|^2/3$. The core contribution to $\|E\|^2$ is one third of this quantity, and the arms contribute the indicated radial tail squares. Hence

$$U_E(0) = \frac{n^2 \Lambda_L}{3} |C_s - C_r|^2, \qquad H(0) = 2n\mu + U_E(0). \tag{E.4}$$

Deleting that field deletes a preparation cost and changes a conserved Gauss sector. Pointwise neutrality within the bare doublet requires $C_s = C_r$, hence $r = p$ or $r = 1 - p$ together with the phase condition. It cannot furnish an independently variable reference fraction at zero field in that family. The tetrahedral construction avoids this particular restriction; it does not retroactively remove it from the triangular calculation.

E.3 The exact neutral completion and why it is not autonomous

The earlier T35 branch adds the graph's uniform angular mode:

$$\psi_+ = \sqrt{n}(c_1 \chi_+ + c_2 \chi_- + z_+ \chi_0), \qquad \psi_- = \sqrt{n}(d_1 \chi_+ + d_2 \chi_- + z_- \chi_0), \quad z_- = e^{i\kappa_c} z_+.$$

Equality of the constant population harmonics follows from $|z_-| = |z_+|$. Equality of the remaining complex harmonic is precisely

$$\begin{aligned} a_c \bar{z}_+ + b_c z_+ = \delta_c^{\mathrm{amp}}, \qquad a_c = c_1 - e^{-i\kappa_c} d_1, \\ b_c = \bar{c}_2 - e^{i\kappa_c} \bar{d}_2, \qquad \delta_c^{\mathrm{amp}} = d_1 d_2 - c_1 c_2. \end{aligned} \tag{E.5}$$

Solving this equation together with its conjugate gives

$$z_+ = \frac{\bar{b}_c \delta_c^{\mathrm{amp}} - a_c \bar{\delta}_c^{\mathrm{amp}}}{|b_c|^2 - |a_c|^2}, \tag{E.6}$$

when the determinant is nonzero. The stated preparation rule chooses the larger absolute determinant among $\kappa_c = \arg Q_c$ and $\arg Q_c + \pi$, where $Q_c = c_1 d_1 - \bar{c}_2 d_2$. Indeed

$$|b_c|^2 - |a_c|^2 = 2(1 - p - r) + 2\,\mathrm{Re}(Q_c e^{-i\kappa_c}).$$

If tied, the smaller added inventory is chosen. A zero right-hand side needs no addition. If both determinant extrema vanish, $r = 1 - p$ and $Q_c = 0$, which also give zero right-hand side, including endpoints. This specifies the algebraic completion without choosing its phase from a favorable later outcome.

The resulting local populations agree at every site, so $A = E = 0$ is Gauss compatible. Orthogonality leaves the summed winding force (E.2) unchanged and gives

$$N = 2n(1 + |z_+|^2), \qquad H(0) = 2n\mu + 2n|z_+|^2 \mu_0, \qquad \mu_0 = \mu + 3t_0 F_0^2. \tag{E.7}$$

The added radial uniform component is not an eigenmode and evolves thereafter. This completion depends on both coefficient pairs and pays with real additional inventory. It is not an autonomous independent apparatus preparation. Its earlier numerical improvement in capture did not establish general late Born fractions; those comparisons remain inherited, as stated in Section 9.

E.4 The full three-path protection identity

For the triangle and its three length-L arms, all phases at zero cycle flux are removable by a site gauge. For each channel the exact finite-graph identity is

$$\frac{H_{\mathrm{hop},s}}{t_0} + 2N_s = |z_{0,0} + z_{1,0} + z_{2,0}|^2 + \sum_{j=0}^{2}\sum_{\ell=0}^{L-1} |z_{j,\ell} + z_{j,\ell+1}|^2 + \sum_{j=0}^{2} |z_{j,L}|^2. \tag{E.8}$$

Expanding the squares counts each internal population twice and reproduces each hopping cross term. The endpoint terms supply the missing second contribution at the far ends. Adding nonnegative field energy proves the boundary inequality used in Section 7. Conservation and continuity then protect any preparation with $\Delta_g = -H - 2t_0 N > 0$.

For a general cycle phase, gauge it onto one core edge relative to its nearest 2π multiple. The changed hopping term in channel s has magnitude at most $4t_0|z_{s,i}z_{s,j}|\,|\sin(b_\triangle/2)|$. Summing channels and using $2|z_{s,i}z_{s,j}| \le |z_{s,i}|^2 + |z_{s,j}|^2$ bounds the total by $2t_0 N|\sin(b_\triangle/2)|$. Combining with (E.8) proves the clearance (7.2). A probe at unchanged circulation changes the protected margin to $\Delta_g - \delta H - 2t_0\delta N$, which proves the stated safe-work condition. A continuous intervention changing the circulation needs a positive margin throughout, not only at its endpoint.

E.5 Prepared stationary record, blank, and reciprocal probe

The protected state is constructible rather than specified only by its energy. Take $A = ac_\triangle$, $E = 0$, and

$$\psi_{s,j\ell} = C_0 f_\ell e^{is2\pi j/3}, \quad f_0 = 1, \qquad C_0^2 = \frac{N}{6S_f}, \quad S_f = \sum_{\ell=0}^{L} f_\ell^2. \tag{E.9}$$

Let $R_0(x) = 0$, $R_m(x) = [x - R_{m-1}(x)]^{-1}$. Eliminating the finite arm from its endpoint gives

$$x - R_L(x) = 2\cos(a + 2\pi/3), \quad x < -2, \qquad f_\ell = f_{\ell-1}R_{L-\ell+1}(x). \tag{E.10}$$

The common frequency is $\mu_* = t_0 x$. Differentiating the normalized eigenvalue gives $\mu_*'(a) = -2t_0\sin(a + 2\pi/3)/S_f$. The field stationarity equation is therefore $9\beta a + N\mu_*'(a) = 0$. Solving these scalar equations supplies the $L = 48, N = 6$ preparation and margin reported in Section 7; reflection swaps the two circulation signs.

A distinct blank uses equal channels proportional to

$$w_j(-1)^\ell \cos[k_L(\ell + 1/2)], \qquad (w_0, w_1, w_2) = (1, -1/2, -1/2), \qquad A = E = 0.$$

Its zero root sum and vanished next radial component verify the same stationary frequency $-2t_0\cos k_L$. A cycle pulse $E = \epsilon_w c_\triangle$ adds $3\epsilon_w^2/2$ energy without changing Gauss balance. Because this blank begins at zero circulation, it cannot satisfy the negative conserved global criterion later; its written record instead uses the local exchange budget. This is a different experiment from the unpulsed donor loading in Section 5.

The native probe prepares one packet per signed channel on input arm zero. For center c_p, the nine positions $\ell = c_p - 4, \ldots, c_p + 4$ carry

$$u_\ell = \left[\frac{\alpha_p \cos^2(\pi(\ell - c_p)/10)}{\sum_{v=c_p-4}^{c_p+4}\cos^2(\pi(v - c_p)/10)}\right]^{1/2} e^{i\pi(\ell - c_p)/2}. \tag{E.11}$$

Multiplying u by $i\overline{\langle\psi,u\rangle}/|\langle\psi,u\rangle|$ when the overlap is nonzero makes its added-inventory cross term vanish; otherwise no correction is needed. The resulting actual channel imbalance determines a longitudinal field by cumulative arm balance, whose energy is included. This is a phase-specified preparation, not a reset during the trajectory.

With $\alpha_p = 0.01$, the protected-state probes have centers 10 and 22, while the blank/write/read experiment uses centers 28 and 40. Define $D = P_1 - P_2$ from the two output-arm inventories, excluding their roots. Reflection interchanges arms 1 and 2, fixes the input preparation, and reverses both $b_\triangle$ and D. It therefore supplies the opposite-input relation exactly. It does not require $D(t)$ to have one sign at all times. The inherited trace, fresh edition-2.0 controls and timing qualification are all reported once in Sections 7 and 9.

E.6 A local contact-energy change has a native probe response

The T34F local contact test uses the identity $\partial_{A_e} J_e = -h_e$ in (2.4) [21]. At a fixed wait time, compare written and unwritten complete states. Probe each by $E \mapsto E \pm \eta_p r_p$ with $Br_p = 0$ and define the central response

$$S_w(u) = \frac{E_w^{+\eta_p}(u) - E_w^{-\eta_p}(u)}{2\eta_p}, \qquad \mathcal{D}_w(u) = S_w(u) - S_0(u).$$

At elapsed time zero, $S_w(0) = r_p$ for both histories and $S_w'(0) = 0$, since $\dot{E}$ has no direct E dependence. Differentiating it once more introduces $\partial_A \dot{E} = \mathrm{diag}(h) - \beta C^T C$. The common face term cancels between histories, giving

$$\mathcal{D}_w(0) = \mathcal{D}_w'(0) = 0, \qquad \mathcal{D}_{w,e}''(0) = \delta h_e\, r_{p,e}, \qquad \mathcal{D}_{w,e}(u) = \tfrac{1}{2}u^2 \delta h_e r_{p,e} + O(u^3). \tag{E.12}$$

The coefficient is exact for any finite nonzero central probe; the remainder is not uniform for arbitrarily large probes. This supplies a separate way to distinguish a changed native contact. It does not equate its units to volts or add a permanent readout latch.

F Rotating contacts and the physical choice of an event measure

These are the distinct geometric and native-current arguments of the T34 local-entanglement supplement [19]. They explain why a favorable angular profile does not settle preparation, event timing or the complete joint law. The free rotor is a declared kinematic comparison; the later emitter-current calculation belongs to the supplement's extended source model. Neither is silently substituted for T35's loading apparatus.

F.1 Stationary transverse registrations

Let a material plane on a rotor have unit normal m, let λ be its fixed unit rotation axis, let $\omega_r > 0$ be its speed, and let ν be an occupied-contact normal. Then

$$\dot{m} = \omega_r \lambda \times m, \qquad g = m \cdot \nu.$$

At a transverse registration $g = 0$, define $a = m \times \nu$. It is a unit tangent vector, and the scalar triple product gives

$$\dot{g} = \omega_r \lambda \cdot a. \tag{F.1}$$

Thus a crossing direction supplies a kinematic sign. A marked plane and a record made from that sign remain physical ingredients; an unmarked smooth sphere does not provide them by renaming an amplitude coordinate.

Assume initially independent uniform m, λ on S^2. This law is stationary under free rotation but is not selected by integrable rotation from arbitrary states. The two-direction crossing measure is obtained by multiplying the phase-space density by $\delta(g)|\dot{g}|$. Since $d\Omega_m \delta(m \cdot \nu) = d\alpha$, where α parametrizes the contact circle,

$$d\mathcal{R} = \frac{\omega_r}{16\pi^2} |a \cdot \lambda| \, d\Omega_\lambda d\alpha, \qquad \mathcal{R}_{\text{total}} = \omega_r/4. \tag{F.2}$$

The normalization uses $\int |a \cdot \lambda| d\Omega_\lambda = 2\pi$. Integrating over the circle gives

$$\rho_{\text{event}}(\lambda) = \frac{\sqrt{1-(\lambda \cdot \nu)^2}}{\pi^2}, \quad q(a \mid \lambda) = \frac{|a \cdot \lambda|}{4\sqrt{1-(\lambda \cdot \nu)^2}}, \quad \rho(\lambda \mid a) = \frac{|a \cdot \lambda|}{2\pi}. \tag{F.3}$$

The exceptional parallel axes have zero event measure. The final density is the cosine-weighted source law used in appendix H. Here the observed setting label is generated with the preparation and is correlated with its hidden direction. If instead pairs existed before this crossing test, keeping only crossing pairs would be detection selection. That chronology cannot be decided by the same algebraic posterior alone.

A continuous-setting check avoids choosing a favorable narrow angular subset. For independent uniform circle settings and Bell-local responses, the vector $\int A(a, \lambda) a \, d\alpha/(2\pi)$ has norm at most $2/\pi$: project along any test direction and integrate $|\cos \alpha|$. The corresponding Bob vector has the same bound. Thus

$$|-\mathbb{E}[AB(a \cdot b)]| \leq 4/\pi^2,$$

whereas the supplied singlet curve gives $1/2$. The registration construction changes setting independence, not this pointwise local argument.

F.2 First registrations carry a preceding-interval weight

At a crossing put $d = a \cdot \lambda$, $q = (\nu \times a) \cdot \lambda$, and $z = \nu \cdot \lambda$. In units of rotation angle, Rodrigues' formula starting at that crossing gives

$$g(\tau) = d \sin \tau + qz(1 - \cos \tau).$$

The previous nontrivial root at $\tau = -\Delta_r$ satisfies $-d \sin \Delta_r + qz(1 - \cos \Delta_r) = 0$. Choosing $0 < \Delta_r < 2\pi$ gives $\Delta_r = \pi - 2 \arctan(qz/d)$. A uniformly initialized orbit phase encounters this crossing first in proportion to that preceding interval. The conditional first-registration density is therefore

$$\rho_{\text{first}}(\lambda \mid a) = \frac{|d|}{2\pi} \left[1 - \frac{2}{\pi} \arctan\left(\frac{qz}{d} \right) \right]. \tag{F.4}$$

The zero-d set has zero measure for the continuous preparation. Under $\lambda \mapsto -\lambda$ the correction is odd, whereas the product of two sign responses is even. Hence it integrates to zero in the correlation but need not do so in an individual mean. This proves why an unchanged correlation curve can coexist with changed joint probabilities. The source's conditional probe $b = (a + \nu \times a + \nu)/\sqrt{3}$ has an inherited Bob mean near -0.05132 rather than zero. It is a relative-axis diagnostic, not an independent-setting Bell experiment. A first-event reset cannot inherit the stationary law without its own preparation calculation.

F.3 Conserved rotation labels and an explicit nonunique family

The free motion preserves $q_0 = m \cdot \lambda$. Independent isotropic pre-event orientations make q_0 uniform on $[-1, 1]$, but crossings weight that law by $\sqrt{1 - q_0^2}$:

$$p_{\text{event}}(q_0) = \frac{2}{\pi} \sqrt{1 - q_0^2}.$$

At fixed q_0, write $\lambda = q_0(\nu \times a) + \sqrt{1-q_0^2}(\cos\varphi\, a + \sin\varphi\, \nu)$. The event phase weight is $|\cos\varphi|/4$. For $b = \cos\theta\, a + \sin\theta(\nu \times a)$, the two signs differ at the roots of $\sqrt{1-q_0^2}\cos\theta\cos\varphi + q_0\sin\theta$. Integrating the weighted circle on either side of those roots gives

$$E_{q_0}(\theta) = -\operatorname{sgn}(\cos\theta)\sqrt{\left[\frac{\cos^2\theta - q_0^2}{(1-q_0^2)\cos^2\theta}\right]_+}. \tag{F.5}$$

Degenerate settings require an explicit tie convention. In the smooth mixed ensemble those sets have zero measure. Mixing (F.5) with the event density gives $-\cos\theta$, because the remaining integral for $c = |\cos\theta|$ is $\int_{-c}^{c}\sqrt{c^2-q^2}\,dq = \pi c^2/2$.

Spatial isotropy and stationary motion also allow the pre-event law

$$p_\kappa(q_0) = \tfrac{1}{2}[1 + \kappa_r P_2(q_0)], \qquad P_2(q) = (3q^2-1)/2, \qquad -1 \le \kappa_r \le 2.$$

After crossing weighting, its normalization relative to the uniform mixture is $1 - \kappa_r/8$. The same semicircle integral and its second moment $\int_{-c}^{c} q^2\sqrt{c^2-q^2}\,dq = \pi c^4/8$ yield

$$E_{\kappa_r}(\theta) = -\cos\theta\,\frac{1 - \kappa_r/2 + (3\kappa_r/8)\cos^2\theta}{1-\kappa_r/8}, \qquad S_{\kappa_r} = 2\sqrt{2}\,\frac{1-5\kappa_r/16}{1-\kappa_r/8}. \tag{F.6}$$

The even mixture keeps zero individual means but changes the joint law. The uniform conserved-label mixture is a substantive preparation condition, not a conclusion of isotropy.

There is a native identification check in the extended T34 source model. Its orientation n_r and angular momentum L_r obey $\dot n_r = (L_r/I_r)\times n_r$ and $\dot L_r = n_r \times (h_r - K_r n_r)$. Taking the derivative gives $d(n_r \cdot L_r)/dt = 0$. With its supplied $L_r(0) = 0$, identifying the material mark with n_r and the free axis with $L_r/\|L_r\|$ would restrict it to $q_0 = 0$, not the uniform mixture. This constrains that particular identification; it does not exclude a different separately derived material marker.

F.4 A finite-patch alternative and its distinct predictions

For a patch boundary $m\cdot\nu = h_r$, $|h_r| < 1$, put $r_h = \sqrt{1-h_r^2}$ and $a = (m\times\nu)/r_h$. Then $\dot g = \omega_r r_h(a\cdot\lambda)$. Under independent isotropic mark and axis the extra factor cancels on conditioning, leaving the same cosine posterior but rate $\omega_r r_h/4$.

A different, zero-q_0 free-rotor preparation puts λ on the great circle perpendicular to $m(a) = h_r\nu + r_h(\nu\times a)$. The conditional weight along this circle is $|a\cdot\lambda|/4$. The projection of b onto that circle has norm $\sqrt{1-[m(a)\cdot b]^2}$; integrating the weighted sign response gives

$$E_h(a,b) = -\frac{a\cdot b}{\sqrt{1-[m(a)\cdot b]^2}}, \qquad E_h(\theta) = -\frac{\cos\theta}{\sqrt{\cos^2\theta + h_r^2\sin^2\theta}}. \tag{F.7}$$

For the planar curve its four-angle expression is $4/\sqrt{1+h_r^2}$ and its event rate is $\omega_r\sqrt{1-h_r^2}/\pi$. The planar cosine limit has vanishing per-rotor rate. The oblique probes $(a+\nu\times a)/\sqrt{2}$ and $(a+\nu)/\sqrt{2}$ instead give $-1/\sqrt{1+h_r^2}$ and $-1/\sqrt{2-h_r^2}$. Their maximum discrepancy from $-1/\sqrt{2}$ is at least $\sqrt{2/3} - 1/\sqrt{2}$, by balancing the two denominators at $h_r^2 = 1/2$. Thus the planar limiting agreement is not a full spherical law. For $0 \le h_r < 1$, the initial cap fraction is $(1-h_r)/2$ and the fraction of crossing orbits is r_h. Among first registrations, the initially inside population crosses outward first. Thus the mean crossing sign is $1 - (1-h_r)/r_h = 1 - \sqrt{(1-h_r)/(1+h_r)}$, rather than the stationary zero mean. This is another complete first-event prediction of the stated patch preparation, not a discarded subset. The alternative remains a geometrical comparison, not an independently realized detector.

F.5 Uniform internal phases do not determine a material measure

The source supplement also tests an ordered orientation bridge, not a new microscopic law. With R_x, R_y, R_z the ordinary coordinate-axis rotations, let $R = R_x(\theta_x)R_y(\theta_y)R_z(\theta_z)$. If the three internal angles are independently uniform, then

$$m = Re_z = (\sin\theta_y, -\sin\theta_x\cos\theta_y, \cos\theta_x\cos\theta_y).$$

Direct angle averages give second moments $(1/2, 1/4, 1/4)$, not the $(1/3, 1/3, 1/3)$ of an isotropic direction. Its first-coordinate fourth moment is $3/8$, also different from the cosine-density value $1/3$ despite their matching second moments. The spatial angular velocity of this ordered product is $\dot\theta_x e_x + \dot\theta_y R_x e_y + \dot\theta_z R_x R_y e_z$, not generally the sum of three fixed-axis rates. Thus internal phase counts and a material registration velocity need an actual coordinate map and its induced measure. This preserves the possibility of internal histories without assuming the distribution needed by a measurement.

F.6 Single-system probabilities, hidden ambiguity, and disturbance

Conditioning the cosine preparation on Alice's sign gives the hemisphere law

$$\rho_s(\lambda) = (s\cdot\lambda)_+/\pi, \qquad s = Aa.$$

For a positive sign test at direction b, its probability is the integral of this density over $b\cdot\lambda > 0$. The spherical intersection identity

$$\int_{s\cdot\lambda>0,\ b\cdot\lambda>0} \lambda\, d\Omega = \frac{\pi}{2}(s+b)$$

therefore gives $(1+s\cdot b)/2$ after dotting with s/π. This is the known single-qubit hemisphere comparison retained in the source, not a new Holosphere measurement mechanism. Its equal mixture of opposite s is $|a\cdot\lambda|/(2\pi)$: different hidden ensembles can have the same zero sign means. The hidden mixture still depends on a, so observation alone on one fixed setting-independent source does not supply every such conditional ensemble.

Sequential records require more than relabeling that hidden state. Starting in a positive-z hemisphere, selecting an x-positive result without changing λ leaves the state within positive z; a later z test is then certainly positive. The corresponding quantum projective sequence gives probability one half after the intermediate x measurement. Thus a physical disturbance or state-update law is a separate requirement, even when a single measurement's probability matches the benchmark.

F.7 Uniqueness within the stated one-direction sign class

There is a useful precise target, not just a favorable fitted density. Define the hemispherical transform

$$(\mathcal{H}f)(b) = \int_{S^2} \operatorname{sgn}(b\cdot\lambda) f(\lambda) d\Omega.$$

It annihilates even spherical harmonics. On odd degree $2k+1$ its eigenvalue, obtained by integrating the rotationally invariant kernel against the Legendre polynomial, is

$$\mu_{2k+1} = 4\pi\int_0^1 P_{2k+1}(x)dx = \frac{2\pi(-1)^k}{4^k(k+1)}\binom{2k}{k} \neq 0.$$

Consequently it is injective on odd integrable functions: vanishing transform forces all odd harmonic coefficients to vanish, and polynomial density determines the function almost everywhere. This is the harmonic identity used in the T34 supplement.

Fix a and an integrable source density ρ_a independent of b, keeping the two local sign maps. A zero Bob mean for every b implies $\mathcal{H}\rho_a = 0$, so its odd part vanishes. Hence $g_a = \operatorname{sgn}(a \cdot \lambda)\rho_a$ is odd. The full singlet correlation requires $\mathcal{H}g_a = a \cdot b$. But $g_0 = (a \cdot \lambda)/(2\pi)$ has exactly this transform, by the sphere integral in appendix H. Odd injectivity gives $g_a = g_0$, and therefore $\rho_a = |a \cdot \lambda|/(2\pi)$ almost everywhere. This is a uniqueness statement for these specific sign responses and hidden direction, not a theorem about every possible hidden-state description.

F.8 A native current is not automatically the counted event traffic

For the extended source law in the T34 supplement, define $G_\ell = -[\nu_\ell]_\times$ so that $G_\ell n_r = n_r \times \nu_\ell$. At fixed other coordinates let

$$b_\ell^{\mathrm{src}} = 2w_\ell r_\ell \sum_{s=\pm1} s\ \mathrm{Re}(\bar{z}_{i_\ell s} e^{isA_\ell} \eta_{k_\ell s}),$$
$$c_\ell^{\mathrm{src}} = 2\gamma w_\ell r_\ell \sum_{s=\pm1} \mathrm{Im}(\bar{z}_{i_\ell s} e^{isA_\ell} \eta_{k_\ell s}), \qquad M_x = \sum_{\ell: x_\ell = x} b_\ell^{\mathrm{src}} G_\ell. \tag{F.8}$$

Here z, η are its guide and recipient amplitudes, w_ℓ, r_ℓ its contact weights and radii, and γ its field coupling. Its field is $F_x^{\mathrm{ext}} - \gamma M_x n_r$. The actual current is therefore

$$j_\ell(n_r) = c_\ell^{\mathrm{src}}(G_\ell n_r) \cdot (F_{x_\ell}^{\mathrm{ext}} - \gamma M_{x_\ell} n_r) = \ell_\ell \cdot n_r + n_r^T Q_\ell n_r,$$
$$\ell_\ell = c_\ell^{\mathrm{src}} G_\ell^T F_{x_\ell}^{\mathrm{ext}}, \qquad Q_\ell = -\gamma c_\ell^{\mathrm{src}} \operatorname{sym}(G_\ell^T M_{x_\ell}). \tag{F.9}$$

Summing yields $j(n_r) = J_r \cdot n_r + n_r^T Q_r n_r$. Its guide signed-inventory balance is $\dot{Q}_g = -j(n_r)$, since internal currents cancel in the regional sum. A hypothetical event boundary $Q_g = q_*$ would therefore have flux measure $\rho\, \delta(Q_g - q_*)|j|\, d\Gamma$, or the appropriate one-direction positive part. Neither the boundary, its arriving density, its reset nor its record is supplied by that continuity equation. Net current $|\sum j_\ell|$, resolved traffic $\sum |j_\ell|$, and signed-species traffic also need not agree.

Antipodal folding of the net-current diagnostic obeys the elementary identity

$$\tfrac{1}{2}(|j(n_r)| + |j(-n_r)|) = \max(|J_r \cdot n_r|, |n_r^T Q_r n_r|). \tag{F.10}$$

If $J_r \neq 0$, exact normalized cosine weight requires $Q_r = (J_r v^T + v J_r^T)/2$ with $\|v\| \leq 1$. To see this, the nodal equator forces $PQ_rP = 0$ for $P = I - ee^T$, $e = J_r/\|J_r\|$, so the quadratic form factors as $(J_r \cdot n_r)(v \cdot n_r)$. The maximum is proportional to the linear absolute value only if its factor is one everywhere, which requires $|v \cdot n_r| \leq 1$. The converse follows immediately from (F.10).

For $\epsilon_r = \|Q_r\|_{\mathrm{op}}/\|J_r\| \leq 1$, excess folded weight is supported in $|e \cdot n_r| \leq \epsilon_r$ and bounded there by $\|J_r\|(\epsilon_r - |e \cdot n_r|)$. Integration gives excess at most $2\pi\|J_r\|\epsilon_r^2$, while the pure cosine mass is $2\pi\|J_r\|$. Thus its normalized total-variation discrepancy is at most $\epsilon_r^2/(1+\epsilon_r^2)$. This explains near-cosine diagnostics without identifying them with records.

Resolved linear contacts have weight $\sum_\ell |\ell_\ell \cdot n_r|$. If their coefficient matrix has rank three, it is bounded below by its positive smallest singular value and cannot have a cosine nodal equator. Likewise a positive mixture can vanish on that entire equator only if almost every component vanishes there: apply nonnegativity on a countable dense subset and then continuity. These results preserve the distinction between coherent recombination, resolved traffic and an actual first-record law.

G Conservative repair and preservation of coherence

Paper 11's useful repair statement is about an explicit retained subsystem and explicit outgoing recipients [12]. This is a conditional scattering description of its correctable sector, not a dissipation term appended to (2.2). The energy metric is normalized so that the relevant quadratic energy is half the squared norm.

G.1 Exported error and the telescoping identity

Write one conservative contact as

$$\begin{pmatrix} x' \\ y \end{pmatrix} = \begin{pmatrix} A_r & B_r \\ C_r & D_r \end{pmatrix} \begin{pmatrix} x \\ b_r \end{pmatrix}, \qquad A_r^\dagger A_r + C_r^\dagger C_r = I. \tag{G.1}$$

Here x is retained error, b_r incoming carrier error, and y outgoing error. With a quiet incoming error coordinate, $b_r = 0$,

$$\tfrac{1}{2}\|x'\|^2 = \tfrac{1}{2}\|x\|^2 - \tfrac{1}{2}\|C_r x\|^2.$$

The removed amount is in y, not destroyed. A code or useful-memory sector must separately be invariant or have its own error allowance.

For successive contacts let $\Phi_0 = I$, $\Phi_j = A_{j-1}\cdots A_0$. At contact j,

$$\Phi_j^\dagger C_j^\dagger C_j \Phi_j = \Phi_j^\dagger \Phi_j - \Phi_{j+1}^\dagger \Phi_{j+1}.$$

Summing proves the extraction identity (7.8). If its sum $W_L \geq \eta I$ on the specified error sector, then $\|\Phi_L x\|^2 \leq (1-\eta)\|x\|^2$. Repeating such blocks contracts that sector only while each bound holds and the outgoing errors do not re-enter as new inputs. The finite conservative inverse interaction can return the exported error, so a one-pass improvement is not automatic permanent relaxation.

G.2 Complementary contacts remove different invisible directions

For two passes,

$$W_2 = C_0^\dagger C_0 + A_0^\dagger C_1^\dagger C_1 A_0, \qquad x^\dagger W_2 x = \|C_0 x\|^2 + \|C_1 A_0 x\|^2. \tag{G.2}$$

It is positive definite exactly when

$$\ker C_0 \cap \ker(C_1 A_0) = \{0\}. \tag{G.3}$$

Necessity follows by using a common invisible vector; sufficiency follows because a sum of two nonnegative squares vanishes only when both do. This is the substantive condition behind complementary repair, rather than an appeal to repeated interaction alone.

For example, with $c_r = \cos\vartheta_r$ and $s_r = \sin\vartheta_r \neq 0$, take

$$A_0 = \operatorname{diag}(c_r, 1), \quad C_0 = \operatorname{diag}(s_r, 0), \qquad A_1 = \operatorname{diag}(1, c_r), \quad C_1 = \operatorname{diag}(0, s_r).$$

Each retained/outgoing pair extends to an ordinary lossless rotation with a recipient. One pass leaves a dark coordinate, while the two-pass sum is $s_r^2 I$. Repeating the first direction instead leaves the second coordinate exactly dark. Changing only the sign of its coupling leaves $C_r^\dagger C_r$ unchanged and cannot fix that lack of access.

This access condition is not itself a radiation rate. In the more detailed Paper 11 source analysis, geometrical access, actual host-force access and dynamical transfer into recipient modes remain distinct. An off-band protected linear oscillation does not acquire a resonant secular radiation channel merely because a contact map sees it. Those source-specific spectral calculations are not replaced by the abstract contraction proof.

G.3 A protected classical label can still lose joint coherence

Within the explicitly supplied joint-state comparison, consider

$$|\Xi\rangle = \frac{|01\rangle|e_0\rangle - |10\rangle|e_1\rangle}{\sqrt{2}}, \qquad \Gamma = \langle e_1|e_0\rangle.$$

Expanding $|\Xi\rangle\langle\Xi|$ and tracing the recipients leaves diagonal populations $1/2$ and off-diagonal entries $-\Gamma/2$ and $-\bar{\Gamma}/2$. The two classical branch labels may both survive perfectly while $|\Gamma| < 1$. This calculation explains the extra requirement on a proposed repair of entangled coherence: the outgoing recipients must either remain suitably indistinguishable or their overlap must be included in the predictions.

For independent recipient factors, the overlap multiplies. If their normalized position amplitudes are Gaussian with equal density variance σ_e^2 and branch separation Δ_e, completing the square in their overlap integral gives

$$|\Gamma| = \exp\left[-\sum_e \frac{\Delta_e^2}{8\sigma_e^2}\right].$$

The Gaussian shapes, separations and independence are assumptions of this comparison, not measured properties of the native carriers. After a removable fixed phase is aligned, write $V = |\Gamma|$. The balanced pair has correlation tensor $\mathrm{diag}(-V, -V, -1)$: longitudinal anticorrelation remains even when transverse coherence vanishes.

For the usual coplanar settings this gives $S_{\mathrm{fixed}} = \sqrt{2}(1+V)$. To derive the optimum, write Bob's two unit vectors' sum and difference as orthogonal vectors of lengths $2\cos t$ and $2\sin t$. Optimize Alice's responses along the two corresponding transformed directions, then optimize t. The two available singular values are $1, V$, yielding $S_{\max} = 2\sqrt{1+V^2}$, attained at Bob angles $\pm\arctan V$ with Alice along the two principal axes. This proves the stated result for this particular dephasing family, not an isotropic-noise law or a native prediction of Γ [2, 24, 32].

G.4 Conditional causal reach and graph locality

Paper 11's event argument assumes every physical hop of length ℓ_e takes at least ℓ_e/c_*, that causal ancestry is well founded, and that no separate instantaneous channel bypasses those hops. For any finite influence path,

$$t_{\mathrm{arrival}} - t_{\mathrm{start}} \geq \sum_e \ell_e/c_* \geq |x_{\mathrm{arrival}} - x_{\mathrm{start}}|/c_*.$$

The first inequality is the assumed hop latency and the second is the triangle inequality. This is a conditional propagation theorem. It must not be inferred merely from sparsity of a continuous-time matrix: the exponential of a nearest-neighbor generator can have nonzero analytic terms at arbitrarily early times along longer paths. The short-time powers in T35 are calculations in its stated ODE, not a separately derived relativistic cone.

H Joint representations, Bell accounting, and conditional completions

This appendix supplies the logical steps compressed in Section 8. It keeps three constructions separate: a native source/record mechanism, a declared two-system quantum representation, and classical record protocols with stated causal or selection assumptions. Their conditional successes are not interchangeable premises.

H.1 What must be added between an actual pair and a tensor state

The T14A/B handoff carries two amplitudes on labels of one source field. If their packet inventory is $n_{ij} = |z_i|^2 + |z_j|^2 > 0$, define $a = z_i/\sqrt{n_{ij}}$, $b = z_j/\sqrt{n_{ij}}$. The particular map

$$K = \begin{pmatrix} 0 & a \\ b & 0 \end{pmatrix}, \qquad \|K\|_F^2 = 1 \tag{H.1}$$

assigns them to joint alternatives $(0,1)$ and $(1,0)$ of two systems. This changes the state space: slot oddness and matching alone do not define two local alternatives at each endpoint. When $ab \neq 0$, $\det K = -ab \neq 0$, so the assigned state is not an outer product. That is a mathematical consequence of the assignment, not its derivation from the source.

Even after a tensor space has been supplied, independent local linear evolution obeys

$$i\dot{K} = H_A K + K H_B^T, \qquad K(t) = U_A(t) K(0) U_B(t)^T.$$

Both propagators are invertible and therefore preserve rank. A rank-one product stays rank one. Earlier interacting preparation could create rank two; its law must be supplied separately. This rank argument concerns coherent amplitude transport, not a prohibition on all correlations or on mechanical pair formation.

H.2 Deriving the benchmark joint probabilities

For the normalized benchmark in Section 8, the coplanar measurement operator is $\sigma_z \cos\alpha + \sigma_x \sin\alpha$, with outcome projectors $[I + s(\sigma_z \cos\alpha + \sigma_x \sin\alpha)]/2$. The z operator is diagonal and the x operator interchanges the two local alternatives. Applying them to $\sqrt{p}|01\rangle - e^{i\phi}\sqrt{1-p}|10\rangle$ gives

$$\langle \sigma_z \otimes I \rangle = 2p - 1, \quad \langle I \otimes \sigma_z \rangle = -(2p-1), \quad \langle \sigma_z \otimes \sigma_z \rangle = -1,$$

$$\langle \sigma_x \otimes \sigma_x \rangle = -2\sqrt{p(1-p)} \cos\phi, \qquad \langle \sigma_z \otimes \sigma_x \rangle = \langle \sigma_x \otimes \sigma_z \rangle = 0.$$

Multiplying the two local projectors and taking their expectation proves all parts of (8.2), including both marginals. Equivalently, use the eigenvectors (C.5) and expand $|u_s(\alpha)^T K u_t(\beta)|^2$. The required tensor state, analyzer action and Born projector rule are explicit benchmark inputs. Their algebra does not close the native preparation or recording problem.

Two local statistical controls expose the missing joint content. Independent local preparation gives the product of the two marginals and correlation $-(2p-1)^2 \cos\alpha \cos\beta$. Shared preparation of $(0,1)$ with fraction p and $(1,0)$ otherwise, followed by the stated local overlap transition probabilities, instead gives

$$P_{\mathrm{pop}}(s,t) = p|u_{s0}(\alpha)|^2 |u_{t1}(\beta)|^2 + (1-p)|u_{s1}(\alpha)|^2 |u_{t0}(\beta)|^2,$$

with the same marginals as the benchmark but correlation $-\cos\alpha\cos\beta$. The transverse interference term is absent. In the balanced case, independent, shared-population, and coherent joint preparations have identical single-wing means yet different joint laws. No-signalling marginals alone do not select the coherent law.

H.3 The complete-trial bound and a sharp approximation test

For the setting-independent Bell-local representation (8.3), conditional local means lie in $[-1,1]$. For each full common-past state,

$$|A_0(B_0 + B_1) + A_1(B_0 - B_1)| \leq |B_0 + B_1| + |B_0 - B_1| \leq 2.$$

The last inequality holds for every $B_0, B_1 \in [-1,1]$; averaging proves the bound. Zero-coded nulls are included. Local memory is included in the full prior state, with independence of settings understood relative to that history. This is an expectation/response-law statement, not a claim that every finite empirical estimator lies below two.

At settings $(\alpha_0, \alpha_1) = (0, \pi/2)$ and $(\beta_0, \beta_1) = (\pi/4, -\pi/4)$, the balanced target correlations are $(-1,-1,-1,1)/\sqrt{2}$. Their signed CHSH sum is $-2\sqrt{2}$; every local law has signed sum at least -2. Thus

$$\max_{ij} |E_{ij}^{\mathrm{local}} - E_{ij}^{\mathrm{target}}| \geq \frac{\sqrt{2}-1}{2}, \qquad \max_{ij} \mathrm{TV}(P_{ij}^{\mathrm{local}}, P_{ij}^{\mathrm{target}}) \geq \frac{\sqrt{2}-1}{4}. \tag{H.2}$$

The first follows by distributing the total discrepancy over four correlations. The second uses $|\Delta\mathbb{E}[AB]| \leq 2\,\mathrm{TV}$ for bounded binary products. Both are sharp: equally mix the eight deterministic assignments (A_0, A_1, B_0, B_1) with signed CHSH -2. Simultaneous sign reversal makes their marginals unbiased, and enumeration gives correlations $(-1, -1, -1, 1)/2$. Their individual joint distributions attain the displayed distances. This source-derived diagnostic excludes only the stated class, not every possible Holosphere completion [2].

H.4 Selected cosine records and complete records

Let λ be uniform on S^2, with local signs $A = \mathrm{sgn}(a \cdot \lambda)$, $B = -\mathrm{sgn}(b \cdot \lambda)$ and Alice acceptance $|a \cdot \lambda|$. Its probability is $1/2$ because $\int |a \cdot \lambda| d\Omega = 2\pi$. The accepted posterior is $|a \cdot \lambda|/(2\pi)$. Rotational symmetry and a direct polar integral give

$$\int_{S^2} \lambda\, \mathrm{sgn}(b \cdot \lambda)\, d\Omega = 2\pi b.$$

Therefore its accepted correlation is

$$-\frac{1}{2\pi} \int (a \cdot \lambda)\, \mathrm{sgn}(b \cdot \lambda) d\Omega = -a \cdot b.$$

The accepted individual means vanish by inversion symmetry. Coding rejected Alice events as zero instead multiplies this correlation by $1/2$, giving complete standard CHSH $\sqrt{2}$, not $2\sqrt{2}$. Removing the rejection mechanism is yet another experiment: uniform sign responses give the local complete law. These established comparisons are the mechanism behind a possible false impression of nonlocality from a selected sample; they are not a demonstration that a particular complete-trial experiment made that error [29, 30, 17].

The empirical question is whether the actual detector and analysis implement such a mechanism. The proposed tests could establish that connection for a specified protocol by predicting its apparent violation and complete records from independently calibrated detector behavior. The requirements in Section 10 distinguish that experimental explanation from this conditional selected-density calculation.

For any already specified binary joint law w_{st} and constant local recording fractions η_A, η_B, the complete alphabet includes

$$\begin{aligned} P(s,t) &= \eta_A \eta_B w_{st}, & P(s,0) &= \eta_A(1-\eta_B) w_A(s), \\ P(0,t) &= (1-\eta_A)\eta_B w_B(t), & P(0,0) &= (1-\eta_A)(1-\eta_B). \end{aligned} \tag{H.3}$$

Outcome-dependent efficiencies must instead remain inside the joint sum. T14A's example with a balanced pair, $\alpha = 0$, $\eta_A(+) = 1$, $\eta_A(-) = 1/2$, $\eta_B(+) = 1$, $\eta_B(-) = 1/5$ gives Alice's complete plus-record fraction $1/2$ at both $\beta = 0$ and $\pi/2$, while its coincidence-conditioned fraction changes from $2/7$ to $2/3$. At equal axes only opposite pairs occur; at perpendicular axes all four joint alternatives have equal weight, giving these ratios directly. Selected marginals can change without changing the complete local stream.

H.5 Source–setting dependence has its own normalization

The same cosine density can instead be a pretrial preparation conditioned on Alice's setting. For a finite setting menu a_i with prescribed frequencies π_i, define

$$Z_a(\lambda) = \sum_i \pi_i |a_i \cdot \lambda|, \qquad \rho_{\mathrm{source}}(\lambda) = \frac{Z_a(\lambda)}{2\pi}, \qquad P(i \mid \lambda) = \frac{\pi_i |a_i \cdot \lambda|}{Z_a(\lambda)}. \tag{H.4}$$

Their product is $\pi_i |a_i \cdot \lambda|/(2\pi)$, whose integral is π_i and whose conditional direction law is the required cosine. Zero-Z_a sets have zero source probability. Retaining the last conditional while replacing the

source by a uniform one changes the joint preparation. This is why the normalization cannot be discarded as mere bookkeeping.

The physical question is when and how the source and settings acquire this dependence, and what happens after an independently imposed setting override. A local material mechanism, operational no-signalling and Bell-local factorization are not synonymous. The rotating registrations of appendix F supply one conditional event geometry for this source–setting law, not an independent-setting replacement of it.

For comparison, the T14D/Toner–Bacon protocol uses shared independent unit vectors λ_1, λ_2, Alice output $A = -\operatorname{sgn}(a \cdot \lambda_1)$, communicated bit $c = \operatorname{sgn}(a \cdot \lambda_1)\operatorname{sgn}(a \cdot \lambda_2)$, and Bob output $B = \operatorname{sgn}[b \cdot (\lambda_1 + c\lambda_2)]$. Its singlet expectation is the cited one-bit protocol result [31, 5]. That spherical-average theorem is an imported comparison, not a new native theorem proved by T35. The bit and its travel time are physical inputs, so its successful statistics cannot be borrowed while claiming complete independent-setting Bell locality.

H.6 Paper 38's explicit additional joint evolution

Paper 38 supplies a different conditional completion [24]. First, minimizing the positive contact storage in Section 2 gives

$$U_{\min}(q) = \tfrac{\kappa}{2} q^T G q, \qquad G = (\kappa \mathcal{C} + B B^T)^{-1}.$$

One way to verify it is to set the node residual potential to $v = \mathcal{C}^{-1}(q - Be)$. Stationarity gives $e = B^T v/\kappa$, hence $v = \kappa G q$; substitution into the two quadratic energies gives the result. With port profiles $q = g_A s_A e_A + g_B s_B e_B$, the reciprocal cross coefficient is $J = \kappa g_A g_B G_{AB}$. This is a frozen equilibrium interaction, not an instantaneous propagation law.

Next the completion explicitly promotes two endpoint responses to Pauli channel operators and assumes a joint-amplitude law. Two matched channels give

$$\mathcal{H}_{AB} = E_0 I + \frac{J}{2}(\sigma_x \otimes \sigma_x + \sigma_y \otimes \sigma_y), \quad E_0 = \tfrac{\kappa}{2}(g_A^2 G_{AA} + g_B^2 G_{BB}) \geq |J|. \tag{H.5}$$

The inequality follows from positivity of G and the arithmetic–geometric mean bound. This operator representation and the evolution $i\hbar_* \dot{\Psi} = \mathcal{H}_{AB}\Psi$ are additional constitutive assumptions, not consequences of the static elimination alone.

In the $|01\rangle, |10\rangle$ block the exchange is $J\sigma_x$. Its exponential acting on $|01\rangle$ gives $\cos\Theta|01\rangle - i\sin\Theta|10\rangle$, with $\Theta = \int J(t)dt/\hbar_*$. A fixed local phase $\operatorname{diag}(1, -i)$ at A changes the second coefficient to $-\sin\Theta$. At $\Theta = \pi/4$ the result is the singlet. At $\Theta = \pi/2$ it is again a product, so weakening or cutting preparation is not described by a universal monotone "entanglement strength." A native source would have to realize the declared channel law and phase control.

H.7 Guided pointer records and the precise locality price

The same completion assumes pointer coordinates x, y and impulsive measurement generator

$$\mathcal{H}_{\text{meas}} = -i\hbar_*[u_A(t)(\boldsymbol{\sigma} \cdot a)\partial_x + u_B(t)(\boldsymbol{\sigma} \cdot b)\partial_y].$$

Free pointer spreading is neglected in this regime. Let $d_X(t) = \int_0^t u_X(v)dv$ and let the initial normalized pointer amplitude have density f_σ of Gaussian variance σ^2. In the two analyzer eigenbases, expand the prepared state with coefficients c_{st}. Translation gives

$$\Psi(x, y, t) = \sum_{s,t} c_{st}|s_a, t_b\rangle \varphi_\sigma(x - sd_A)\varphi_\sigma(y - td_B).$$

Orthogonality of the channel labels gives

$$\begin{aligned}\rho &= \sum_{s,t} |c_{st}|^2 f_\sigma(x - sd_A) f_\sigma(y - td_B),\\ j_A &= u_A \sum_{s,t} s|c_{st}|^2 f_\sigma(x - sd_A) f_\sigma(y - td_B),\\ j_B &= u_B \sum_{s,t} t|c_{st}|^2 f_\sigma(x - sd_A) f_\sigma(y - td_B).\end{aligned} \tag{H.6}$$

Differentiating the translated densities proves $\partial_t\rho + \partial_x j_A + \partial_y j_B = 0$. With the additional configuration law $\dot{X} = j_A/\rho$, $\dot{Y} = j_B/\rho$ and an initial equilibrium distribution equal to $\rho(0)$, the transported density satisfies the same continuity equation. This is preservation of a supplied equilibrium law, not autonomous generation of it. Continuity alone does not uniquely choose this guidance law over every possible divergence-free modification.

When the translated packets separate, their branch weights become record frequencies. At finite Gaussian separations, integrating the two pointer signs instead gives, for a singlet,

$$E_{\text{read}} = -a \cdot b \, \operatorname{erf}\!\left(\frac{d_A}{\sqrt{2}\sigma}\right) \operatorname{erf}\!\left(\frac{d_B}{\sqrt{2}\sigma}\right). \tag{H.7}$$

Each factor is the mean sign of a shifted Gaussian; no unresolved trials are discarded in this comparison. A separate effective latch $V(X) = \lambda_p(X^2 - L_p^2)^2/4$, $\dot{X} = -\mu_p V'(X)$, and $\dot{Q}_p = \mu_p[V'(X)]^2$ preserves the nonzero sign and conserves $V + Q_p$. Its heat coordinate and assumed mobility do not constitute T35's native contact apparatus and are not restored as such.

For simultaneous singlet readout, write $z_A = \tanh(Xd_A/\sigma^2)$, $z_B = \tanh(Yd_B/\sigma^2)$. The first guidance velocity becomes

$$\dot{X} = u_A \frac{z_A - (a \cdot b) z_B}{1 - (a \cdot b) z_A z_B}.$$

Its dependence on the remote actual coordinate and setting is explicit. Equilibrium marginals prevent statistical signalling but do not make this trajectory law Bell local. Implementing that dependence by ordinary finite-speed messages would instead be a communication-assisted device whose timing must be accounted for. Closing a preparation corridor after assigning the joint state does not by itself erase the assumed state or its guidance law. These are the additional premises that distinguish Paper 38's constructive comparison from a derivation using only local corridor history.

I Complete Python program

This is the complete source used for the rebuilt calculations. No omitted routine, embedded archive, downloaded code, or earlier research-program import is required.

```
#!/usr/bin/env python3
"""Paper T35: one native solver for loading, storage and reacting readout.

Python 3.11+, standard library only. All ensembles and observation conventions
are explicit. No target-law draws, earlier script imports, downloads, fitted
force, damping or post-outcome rejection. Results are model calculations.

python T35.py --output-root T35_outputs --campaign paper --workers 18
python T35.py --output-root T35_outputs --campaign paper --resume
"""
from __future__ import annotations
import argparse
import cmath
import csv
import hashlib
import itertools
import json
import math
import os
from pathlib import Path
import platform
import random
import shutil
import sys
import time
from concurrent.futures import ProcessPoolExecutor, as_completed
from typing import Any

VERSION = 'T35-connected-rebuild-2.0.0'
HOP, BETA = 0.08, 0.02
ROOTS = ((0,0,0), (1,1,0), (1,0,1), (0,1,1))
DIRECTIONS = ((-1,-1,0), (1,1,0), (1,0,1), (0,1,1))
READERS = ((-1,1,0), (2,0,0))

def check(ok: bool, message: str) -> None:
    if not ok:
        raise AssertionError(message)

def close(x: float, y: float, tol: float = 1e-10) -> None:
    check(abs(x-y) <= tol*max(1., abs(x), abs(y)), f'Mismatch: {x} versus {y}')

def csum(x):
    values=list(x)
    return complex(math.fsum(v.real for v in values),math.fsum(v.imag for v in values))

def norm2(x) -> float:
    return math.fsum(abs(v)**2 for v in x)

def dot(x, y):
    return sum(a*b for a,b in zip(x,y))

def normalize(x):
    total = sum(x)
    check(total > 0, 'Nonpositive normalization.')
    return [v/total for v in x]

def tv(x, y) -> float:
    check(len(x) == len(y), 'Mismatched distributions.')
    return .5*sum(abs(a-b) for a,b in zip(x,y))

def solve(a, b):
    """Pivoted linear solve, with a vector right-hand side."""
    n = len(a)
    m = [list(row)+[b[i]] for i,row in enumerate(a)]
    for k in range(n):
        p = max(range(k,n), key=lambda j: abs(m[j][k]))
        check(abs(m[p][k]) > 1e-14, 'Singular linear system.')
        m[k],m[p] = m[p],m[k]
        scale = m[k][k]
        m[k] = [v/scale for v in m[k]]
        for j in range(n):
```

```
            if j != k:
                z = m[j][k]
                m[j] = [u-z*v for u,v in zip(m[j],m[k])]
    return [row[-1] for row in m]

def bisect(fun, lo: float, hi: float, iterations: int = 80) -> float:
    flo, fhi = fun(lo), fun(hi)
    check(flo*fhi <= 0, 'Root not bracketed.')
    for _ in range(iterations):
        mid = (lo+hi)/2
        fm = fun(mid)
        if flo*fm <= 0:
            hi = mid
        else:
            lo,flo = mid,fm
    return (lo+hi)/2

def atomic_json(path: Path, value: Any) -> None:
    path.parent.mkdir(parents=True, exist_ok=True)
    temp = path.with_suffix(path.suffix+'.pending')
    temp.write_text(json.dumps(value, indent=2, allow_nan=False)+'\n', encoding='utf-8')
    temp.replace(path)

def state_encode(y):
    return [[v.real,v.imag] if isinstance(v,complex) else v for v in y]

def state_decode(y):
    return [complex(*v) if isinstance(v,list) else v for v in y]

def sign(x: float, threshold: float = 1e-10) -> int:
    return int(x > threshold)-int(x < -threshold)

class ContactNetwork:
    """All FCC contacts and triangles; one Hamiltonian and two work integrals.

    State: psi_plus, psi_minus, A, E, integrated core work, integrated core
    inventory influx. The last two entries are observers, not extra forces.
    """
    def __init__(self, geometry: str = 'tetra', length: int = 4,
                 reader: bool = False):
        self.geometry, self.length = geometry,length
        count = 3 if geometry == 'triangle' else 4
        check(length >= 0 and geometry in ('tetra','triangle','dimer'), 'Bad geometry.')
        self.points, self.arms = [],[]
        if geometry == 'dimer':
            self.points = [(0,0,0),(1,1,0)]
            self.arms = [[0],[1]]
        else:
            for v,d in zip(ROOTS[:count],DIRECTIONS[:count]):
                self.arms.append(list(range(len(self.points), len(self.points)+length+1)))
                self.points.extend(tuple(v[k]+ell*d[k] for k in range(3))
                                   for ell in range(length+1))
        self.roots = [arm[0] for arm in self.arms]
        self.reader_sites = []
        if reader:
            check(geometry == 'tetra', 'Reader is defined for the tetrahedron.')
            for p in READERS:
                check(p not in self.points, 'Duplicate occupied site.')
                self.reader_sites.append(len(self.points))
                self.points.append(p)
        self.n = len(self.points)
        self.edges = [(i,j) for i in range(self.n) for j in range(i+1,self.n)
                      if sum((x-y)**2 for x,y in zip(self.points[i],self.points[j])) == 2]
        self.m = len(self.edges)
        self.index = {e:k for k,e in enumerate(self.edges)}
        near = [set() for _ in self.points]
        for i,j in self.edges:
            near[i].add(j); near[j].add(i)
        self.faces, self.face_vertices = [],[]
        for i in range(self.n):
            for j in sorted(v for v in near[i] if v > i):
                for k in sorted(v for v in near[i]&near[j] if v > j):
                    self.face_vertices.append((i,j,k))
                    self.faces.append(((self.index[i,j],1),(self.index[j,k],1),
                                       (self.index[i,k],-1)))
        self.aoff, self.eoff = 2*self.n,2*self.n+self.m
        self.woff = 2*self.n+2*self.m
```

```
    core = set(self.roots)
    self.core_edges = {e for e,(i,j) in enumerate(self.edges) if i in core and j in core}
    self.core_faces = {f for f,v in enumerate(self.face_vertices) if set(v) <= core}
    self.target = (self.face_vertices.index(tuple(self.roots[:3]))
                   if geometry != 'dimer' else None)
    self.core = core
    for face in self.faces:
        boundary = [0]*self.n
        for e,s in face:
            i,j = self.edges[e]; boundary[i] += s; boundary[j] -= s
        check(not any(boundary), 'Boundary of a face is not zero.')
    if geometry != 'dimer':
        expected_edges = count*length + (3 if count == 3 else 6) + (4 if reader else 0)
        expected_faces = (1 if count == 3 else 4) + (2 if reader else 0)
        check(self.m == expected_edges and len(self.faces) == expected_faces,
              'Unexpected contacts in declared occupied geometry.')
    if reader:
        self.read_edges = (self.index[self.roots[0],self.reader_sites[0]],
                           self.index[self.roots[3],self.reader_sites[0]])
        self.read_faces = [f for f,v in enumerate(self.face_vertices)
                           if any(i in self.reader_sites for i in v)]
    else:
        self.read_edges, self.read_faces = None,[]

def zero(self):
    return [0j]*(2*self.n)+[0.]*(2*self.m+2)

def rhs(self, y):
    n,ao,eo = self.n,self.aoff,self.eoff
    dy = self.zero()
    terms=[[] for _ in range(2*n)]
    field_terms=[[] for _ in range(self.m)]
    # Gradients and boundary motion are needed only on the small core.
    grad = [[0j]*n for _ in range(2)]
    outside = [[0j]*n for _ in range(2)]
    for e,(i,j) in enumerate(self.edges):
        u = complex(math.cos(y[ao+e]),math.sin(y[ao+e]))
        uc = u.conjugate()
        pi,pj,mi,mj = y[i],y[j],y[n+i],y[n+j]
        fp,fq = -1j*HOP*u*pj,-1j*HOP*uc*pi
        fm,fn = -1j*HOP*uc*mj,-1j*HOP*u*mi
        terms[i].append(fp); terms[j].append(fq)
        terms[n+i].append(fm); terms[n+j].append(fn)
        dy[ao+e] = y[eo+e]
        field_terms[e].append(2*HOP*((pi.conjugate()*u*pj).imag
                              -(mi.conjugate()*uc*mj).imag))
        if e in self.core_edges:
            grad[0][i] += 1j*fp; grad[0][j] += 1j*fq
            grad[1][i] += 1j*fm; grad[1][j] += 1j*fn
        elif (i in self.core) != (j in self.core):
            if i in self.core:
                outside[0][i] += fp; outside[1][i] += fm
            else:
                outside[0][j] += fq; outside[1][j] += fn
    pface = 0.
    for f,face in enumerate(self.faces):
        flux = math.fsum(s*y[ao+e] for e,s in face)
        for e,s in face:
            field_terms[e].append(-BETA*s*flux)
            if f not in self.core_faces and e in self.core_edges:
                pface -= BETA*s*y[eo+e]*flux
    for i in range(2*n):dy[i]=csum(terms[i])
    for e in range(self.m):dy[eo+e]=math.fsum(field_terms[e])
    pcontact = 2*sum((grad[s][i].conjugate()*outside[s][i]).real
                     for s in range(2) for i in self.roots)
    nin = 2*sum((y[s*n+i].conjugate()*outside[s][i]).real
                for s in range(2) for i in self.roots)
    dy[self.woff],dy[self.woff+1] = pcontact+pface,nin
    return dy

def step(self, y, h):
    a = self.rhs(y)
    b = self.rhs([x+.5*h*z for x,z in zip(y,a)])
    c = self.rhs([x+.5*h*z for x,z in zip(y,b)])
    d = self.rhs([x+h*z for x,z in zip(y,c)])
    return [x+h*(aa+2*bb+2*cc+dd)/6 for x,aa,bb,cc,dd in zip(y,a,b,c,d)]
```

```
    def observe(self, y):
        n,ao,eo = self.n,self.aoff,self.eoff
        h,hc,electric = 0.,0.,0.
        currents = []
        gauss = [-(abs(y[i])**2-abs(y[n+i])**2) for i in range(n)]
        for e,(i,j) in enumerate(self.edges):
            u = complex(math.cos(y[ao+e]),math.sin(y[ao+e]))
            zp = y[i].conjugate()*u*y[j]
            zm = y[n+i].conjugate()*u.conjugate()*y[n+j]
            ee = y[eo+e]**2/2
            he = 2*HOP*(zp.real+zm.real)+ee
            h += he; electric += ee
            if e in self.core_edges: hc += he
            currents.append(-2*HOP*(zp.imag-zm.imag))
            gauss[i] += y[eo+e]; gauss[j] -= y[eo+e]
        fluxes = [math.fsum(s*y[ao+e] for e,s in face) for face in self.faces]
        for f,flux in enumerate(fluxes):
            energy = BETA*flux*flux/2
            h += energy
            if f in self.core_faces: hc += energy
        ns = [norm2(y[s*n:(s+1)*n]) for s in range(2)]
        nc = sum(abs(y[s*n+i])**2 for s in range(2) for i in self.roots)
        nr = sum(abs(y[s*n+i])**2 for s in range(2) for i in self.reader_sites)
        result = dict(H=h,N=sum(ns),Ns=ns,gauss=gauss,Hcore=hc,Ncore=nc,
                      Qcore=hc+HOP*nc,Houtside=h-hc,Nreader=nr,
                      electric_energy=electric,work=y[self.woff],influx=y[self.woff+1])
        if self.target is not None:
            result['flux'] = fluxes[self.target]
            result['current'] = -sum(s*currents[e] for e,s in self.faces[self.target])
        else:
            result.update(flux=0., current=currents[0])
        result['reader'] = (y[eo+self.read_edges[1]]-y[eo+self.read_edges[0]]
                            if self.read_edges else 0.)
        result['reader_fluxes'] = [fluxes[f] for f in self.read_faces]
        if len(self.arms) >= 3:
            totals = [sum(abs(y[s*n+i])**2 for s in range(2) for i in arm[1:])
                      for arm in self.arms]
            result['port_difference'] = totals[1]-totals[2]
        return result

    def make_gauss_compatible(self, y):
        """Minimum-norm longitudinal E. No cycle pulse or population deletion."""
        q = [abs(y[i])**2-abs(y[self.n+i])**2 for i in range(self.n)]
        check(abs(sum(q)) < 1e-11, 'Closed zero-Gauss graph needs equal total channels.')
        # Exact tree solution avoids introducing a roundoff cycle into a symmetric control.
        arm=self.arms[0]
        if len(arm)>1 and all(q[i]==0. for i in range(self.n) if i not in arm):
            for e in range(self.m):y[self.eoff+e]=0.
            for ell in range(1,len(arm)):
                y[self.eoff+self.index[arm[ell-1],arm[ell]]]=-math.fsum(q[i] for i in arm[ell:])
            return
        lap = [[0.]*self.n for _ in range(self.n)]
        for i,j in self.edges:
            lap[i][i] += 1; lap[j][j] += 1
            lap[i][j] -= 1; lap[j][i] -= 1
        v = solve([row[:-1] for row in lap[:-1]], q[:-1])+[0.]
        for e,(i,j) in enumerate(self.edges): y[self.eoff+e] = v[i]-v[j]


def radial_ground(length: int):
    k = math.pi/(2*length+3)
    f = [(-1)**ell*math.cos(k*(ell+.5)) for ell in range(length+1)]
    scale = math.sqrt(norm2(f))
    return [z/scale for z in f],-2*HOP*math.cos(k)


def prepare(model: ContactNetwork, cfg: dict):
    """Prepare coordinates once. No normalizing, resetting or switching later."""
    y = model.zero(); kind = cfg.get('kind','loaded'); n = cfg.get('inventory',.5)
    p,r = cfg.get('signal',.75),cfg.get('reference',.25)
    check(0 <= p <= 1 and 0 <= r <= 1 and n > 0, 'Invalid preparation.')
    if model.geometry == 'dimer':
        y[0] = y[model.n] = math.sqrt(n)
        return y
    if kind.startswith('triangle'):
        if kind == 'triangle_stored':
            length = model.length
```

```
            def ratios(x):
                v=0.; out=[0.]
                for _ in range(length): v=1/(x-v); out.append(v)
                return out
            def radial(a):
                target=2*math.cos(a+2*math.pi/3)
                x=bisect(lambda x:x-ratios(x)[-1]-target,-4.,-2.-1e-10)
                rr=ratios(x);f=[1.]
                for ell in range(1,length+1):f.append(f[-1]*rr[length-ell+1])
                return x,f
            total=cfg.get('total_inventory',6.)
            a=bisect(lambda a:9*BETA*a-total*2*HOP*math.sin(a+2*math.pi/3)/norm2(radial(a)[1]),.55,1.0)
            x,f=radial(a);scale=math.sqrt(total/(6*norm2(f)))
            for s,sgn in enumerate((1,-1)):
                for j,arm in enumerate(model.arms):
                    for ell,i in enumerate(arm): y[s*model.n+i]=scale*f[ell]*cmath.exp(1j*sgn*2*math.pi*j/3)
            for e,s in model.faces[0]: y[model.aoff+e]=s*a
        else:
            k=math.pi/(2*model.length+3)
            for j,arm in enumerate(model.arms):
                for ell,i in enumerate(arm):
                    z=(1.,-.5,-.5)[j]*(-1)**ell*math.cos(k*(ell+.5))
                    y[i]=y[model.n+i]=complex(z)
            scale=math.sqrt(cfg.get('total_inventory',12.)/norm2(y[:2*model.n]))
            y[:2*model.n]=[z*scale for z in y[:2*model.n]]
            for e,s in model.faces[0]:y[model.eoff+e]=s*cfg.get('pulse',.1)
        if cfg.get('probe'):
            centers=cfg.get('centers',[28,40])
            for s,c in enumerate(centers):
                packet=[0j]*model.n
                for ell in range(c-4,c+5):
                    packet[model.arms[0][ell]]=math.cos(math.pi*(ell-c)/10)*cmath.exp(1j*math.pi*(ell-c)/2)
                scale=math.sqrt(.01/norm2(packet));packet=[z*scale for z in packet]
                overlap=sum(y[s*model.n+i].conjugate()*packet[i] for i in range(model.n))
                phase=1j*overlap.conjugate()/abs(overlap) if abs(overlap)>1e-15 else 1.
                for i in range(model.n):y[s*model.n+i]+=phase*packet[i]
            # Preserve the already prepared solenoidal core pulse.
            old=[y[model.eoff+e] for e in range(model.m)]
            model.make_gauss_compatible(y)
            for e in range(model.m): y[model.eoff+e]+=old[e]
        return y
    # Tetrahedral ground or actually incoming donor preparation.
    for channel,w in enumerate((p,r)):
        if kind == 'ground':
            f,_=radial_ground(model.length)
        elif kind in ('loaded','phase_control','delay_control'):
            donor=cfg.get('donor',1)+(1 if kind=='delay_control' and channel==1 else 0)
            check(1 <= donor <= model.length, 'Donor must be outside the core.')
            f=[float(ell==donor) for ell in range(model.length+1)]
        elif kind == 'packet':
            center=cfg.get('donor',2)
            f=[math.cos(math.pi*(ell-center)/6)**2*cmath.exp(1j*math.pi*ell/2)
               if ell>0 and abs(ell-center)<3 else 0j for ell in range(model.length+1)]
            scale=math.sqrt(norm2(f));f=[z/scale for z in f]
        else: raise ValueError('Unknown preparation: '+kind)
        phase=cfg.get('phase',math.pi/2) if channel==1 and kind=='phase_control' else math.pi/2
        for j,arm in enumerate(model.arms):
            phase_factor=1j if phase==math.pi/2 else cmath.exp(1j*phase)
            factor=(math.sqrt(w)*(1j)**j+phase_factor*math.sqrt(1-w)*(-1j)**j)/2
            for ell,i in enumerate(arm):y[channel*model.n+i]=math.sqrt(n)*f[ell]*factor
    if kind in ('phase_control','delay_control'):model.make_gauss_compatible(y)
    return y


def compact_observation(model, y, t):
    o=model.observe(y)
    return dict(t=t, **{k:o[k] for k in ('H','N','Ns','Hcore','Ncore','Qcore','Houtside',
        'Nreader','electric_energy','work','influx','flux','current','reader','port_difference') if k in o})


def trajectory(payload):
    cfg,root_s,digest,resume,deadline=payload
    root=Path(root_s);key=hashlib.sha256(json.dumps(cfg,sort_keys=True).encode()).hexdigest()[:20]
    path=root/'cases'/(key+'.json'); cp=root/'checkpoints'/(key+'.json')
    if resume and path.exists():
        old=json.loads(path.read_text())
        if old.get('source_sha256')==digest and old.get('config')==cfg and old.get('status')=='COMPLETED':return old
```

```
    m=ContactNetwork(cfg.get('geometry','tetra'),cfg.get('length',4),cfg.get('reader',False))
    y=prepare(m,cfg);initial=m.observe(y)
    sample=cfg.get('sample',1.)
    blocks=round(cfg['T']/sample)
    check(abs(blocks*sample-cfg['T'])<1e-10,'Duration must be a multiple of sample interval.')
    per_block=math.ceil(sample/cfg.get('step',.04));h=sample/per_block
    rows=[compact_observation(m,y,0.)];start=0
    errors=dict(energy=0.,inventory=0.,gauss=0.,core_work=0.,core_inventory=0.)
    if resume and cp.exists():
        old=json.loads(cp.read_text())
        if old.get('source_sha256')==digest and old.get('config')==cfg:
            y=state_decode(old['state']);rows=old['rows'];start=old['block'];errors=old['errors']
    for block in range(start,blocks):
        if time.time()>=deadline or (root/'STOP.txt').exists():
            atomic_json(cp,dict(config=cfg,source_sha256=digest,state=state_encode(y),rows=rows,block=block,errors=errors))
            return dict(status='PAUSED',config=cfg,source_sha256=digest)
        for _ in range(per_block):y=m.step(y,h)
        o=m.observe(y)
        errors['energy']=max(errors['energy'],abs(o['H']-initial['H']))
        errors['inventory']=max(errors['inventory'],max(abs(a-b) for a,b in zip(o['Ns'],initial['Ns'])))
        errors['gauss']=max(errors['gauss'],max(abs(a-b) for a,b in zip(o['gauss'],initial['gauss'])))
        errors['core_work']=max(errors['core_work'],abs(o['Hcore']-initial['Hcore']-o['work']))
        errors['core_inventory']=max(errors['core_inventory'],abs(o['Ncore']-initial['Ncore']-o['influx']))
        rows.append(compact_observation(m,y,(block+1)*sample))
        if (block+1)%25==0:
            atomic_json(cp,dict(config=cfg,source_sha256=digest,state=state_encode(y),rows=rows,block=block+1,errors=errors))
    result=dict(status='COMPLETED',source_sha256=digest,config=cfg,
                geometry=dict(sites=m.n,edges=m.m,faces=len(m.faces)),step=h,
                initial_gauss=max(map(abs,initial['gauss'])),initial_energy=initial['H'],
                errors=errors,rows=rows)
    atomic_json(path,result)
    if cp.exists():cp.unlink()
    return result


def history_checks():
    n=21;h=[math.sin(math.pi*(i+1)/(n+1)) for i in range(n)];pi=normalize([x*x for x in h])
    rho=(1+2*math.cos(math.pi/(n+1)))/3
    k=[[float(abs(i-j)<=1)/3 for j in range(n)] for i in range(n)]
    rows=[]
    for depth in (8,32,128,512):
        c=[1]*n
        for _ in range(depth):c=[sum(c[max(0,i-1):min(n,i+2)]) for i in range(n)]
        rows.append(dict(depth=depth,midpoint_TV=tv(normalize([v*v for v in c]),pi),endpoint_TV=tv(normalize(c),pi)))
    p=[[k[i][j]*h[j]/(rho*h[i]) for j in range(n)] for i in range(n)]
    err=max(abs(sum(row)-1) for row in p)
    station=max(abs(sum(pi[i]*p[i][j] for i in range(n))-pi[j]) for j in range(n))
    check(rows[-1]['midpoint_TV']<1e-11 and rows[-1]['endpoint_TV']>.1,'History controls failed.')
    check(max(err,station)<1e-12,'Forward transform failed.')
    # First record, with explicitly stated hazards and reset.
    def first(nu,hazards):
        a=[[float(i==j)-(1-hazards[i])*p[i][j] for j in range(n)] for i in range(n)]
        answer=[]
        for r in range(n):
            col=solve(a,[hazards[i]*float(i==r) for i in range(n)])
            answer.append(dot(nu,col))
        close(sum(answer),1.)
        return answer
    constant=first(pi,[.2]*n)
    variable=[.05+.7*(i/(n-1))**2 for i in range(n)]
    f=first(pi,variable);marks=normalize([pi[i]*variable[i] for i in range(n)])
    check(tv(constant,pi)<1e-12,'Stationary constant-hazard law failed.')
    check(tv(f,marks)>.001,'First events incorrectly replaced by stationary marks.')
    return dict(status='PASS',history=rows,Doob_residual=max(err,station),
                first_vs_stationary_marks_TV=tv(f,marks),
                scope='Declared measures and absorbing-chain formulas, not detector outcomes.')


def probability_checks():
    local=max(abs(a*(b+c)+d*(b-c)) for a,b,c,d in itertools.product((-1,0,1),repeat=4))
    close(local,2.)
    # Independent four-component projector calculation for quantum benchmark.
    maximum=0.
    for p,phase,aa,bb in itertools.product((.1,.5,.9),(0.,.7),(0.,.4),(0.,-.8)):
        ket=[0j,math.sqrt(p),-cmath.exp(1j*phase)*math.sqrt(1-p),0j]
        ma=(2*p-1)*math.cos(aa);mb=-(2*p-1)*math.cos(bb)
        corr=-math.cos(aa)*math.cos(bb)-2*math.sqrt(p*(1-p))*math.cos(phase)*math.sin(aa)*math.sin(bb)
```

```
        for si,ta in itertools.product((-1,1),repeat=2):
            def vector(angle,label):
                return ([math.cos(angle/2),math.sin(angle/2)] if label==1
                        else [-math.sin(angle/2),math.cos(angle/2)])
            u,v=vector(aa,si),vector(bb,ta)
            amp=sum(ket[2*i+j]*u[i]*v[j] for i in range(2) for j in range(2))
            expected=(1+si*ma+ta*mb+si*ta*corr)/4
            maximum=max(maximum,abs(abs(amp)**2-expected))
    check(maximum<1e-12,'Quantum comparator mismatch.')
    # Selected versus complete records: deterministic spherical quadrature.
    count=16384;correlations=[];complete=[];accept=[]
    for aa,bb in ((0.,math.pi/4),(0.,-math.pi/4),(math.pi/2,math.pi/4),(math.pi/2,-math.pi/4)):
        num=den=0.
        for j in range(count):
            z=1-2*(j+.5)/count;phi=j*math.pi*(3-math.sqrt(5));rr=math.sqrt(1-z*z)
            x,y=rr*math.cos(phi),rr*math.sin(phi)
            u=x*math.cos(aa)+y*math.sin(aa);v=x*math.cos(bb)+y*math.sin(bb)
            w=abs(u);num+=w*sign(u,0.)*(-sign(v,0.));den+=w
        correlations.append(num/den);complete.append(num/count);accept.append(den/count)
    chsh=lambda c:abs(c[0]+c[1]+c[2]-c[3])
    return dict(status='PASS',local_bound=local,projector_error=maximum,
                selected_CHSH=chsh(correlations),complete_null_coded_CHSH=chsh(complete),acceptance=accept,
                scope='Separate quantum and selected-event benchmarks; not native entanglement.')


def bridge_checks():
    # Complementary conservative error export; energy includes outgoing carriers.
    angle=.43;c,s=math.cos(angle),math.sin(angle);x=[.7,-.4]
    after=[c*x[0],c*x[1]];export=[s*x[0],s*x[1]]
    close(norm2(x),norm2(after)+norm2(export))
    # Normalized Gaussian fraction and its unequal-inventory force comparison.
    def cdf(u,a=1.,b=1.,coherence=0.):
        if u<=0:return 0.
        if u>=1:return 1.
        tr=a*(1-u)-b*u;disc=math.sqrt(tr*tr+4*u*(1-u)*(a*b-coherence*coherence))
        return .5*(1-tr/disc)
    error=max(abs(cdf(j/1000)-j/1000) for j in range(1001))
    check(error<1e-12,'Gaussian fraction identity failed.')
    rows=[]
    for p in (0.,.25,.5,.75,1.):
        z=2*(2*p-1);actual=.5*math.exp(z) if z<=0 else 1-.5*math.exp(-z)
        rows.append(dict(signal=p,unnormalized_probability=actual))
    # Equal-work count bound is an identity, not a native click model.
    work=[3.7,5.2,1.1];unit=.7;counts=[int(w/unit) for w in work]
    residual=[w-unit*k for w,k in zip(work,counts)]
    close(sum(work),unit*sum(counts)+sum(residual))
    check(tv(normalize(counts),normalize(work))<=sum(residual)/sum(work)+1e-12,'Count bound failed.')
    # Autonomous field-free native dimer generates quadrature and current.
    m=ContactNetwork('dimer',0);y=prepare(m,dict(inventory=.5))
    T=math.pi/(2*HOP);steps=2000;h=T/steps;worst=0.
    for k in range(steps+1):
        t=k*h;expected=(math.sqrt(.5)*math.cos(HOP*t),-1j*math.sqrt(.5)*math.sin(HOP*t))
        worst=max(worst,abs(y[0]-expected[0]),abs(y[1]-expected[1]))
        if k<steps:y=m.step(y,h)
    check(worst<1e-10,'Native dimer transfer failed.')
    # Equal current-flux bins versus clock ticks; neither is called a launcher.
    flux_bins=[1/16]*16
    clock_cdf=lambda u:.5+math.asin(2*u-1)/math.pi
    return dict(status='PASS',repair_energy_contraction=c*c,Gaussian_fraction_error=error,
                unnormalized_reference=rows,dimer_max_amplitude_error=worst,
                clock_fraction_CDF_at_quarter=clock_cdf(.25),flux_fraction_CDF_at_quarter=sum(flux_bins[:4]),
                scope='Native dimer evolution plus conditional measure/counting identities; no packet launch device.')


def native_checks():
    # Hamiltonian derivative, Gauss conservation and regional power independently checked.
    rng=random.Random(35021);m=ContactNetwork('tetra',2,True);y=m.zero()
    for i in range(2*m.n):y[i]=complex(rng.uniform(-.2,.2),rng.uniform(-.2,.2))
    for i in range(m.aoff,m.woff):y[i]=rng.uniform(-.1,.1)
    dy=m.rhs(y);eps=1e-6
    plus=m.observe([a+eps*b for a,b in zip(y,dy)])
    minus=m.observe([a-eps*b for a,b in zip(y,dy)])
    energy=(plus['H']-minus['H'])/(2*eps)
    regional=(plus['Hcore']-minus['Hcore'])/(2*eps)
    close(energy,0.,1e-8);close(regional,dy[m.woff],1e-8)
    regional_error=abs(regional-dy[m.woff])
    # New loading, protection and exterior reader leading coefficients.
```

```
    rows=[];p,r,n=.75,.25,.5
    m=ContactNetwork('tetra',4,True);y0=prepare(m,dict(kind='loaded',signal=p,reference=r,inventory=n))
    k4=n*HOP**3*(p-r)/6
    k5=n*HOP**3*(BETA-HOP**2)*(p-r)/30
    k6=-n*n*HOP**6*(p-r)**2/9
    for T in (.2,.4,.8):
        y=y0[:]
        for _ in range(200):y=m.step(y,T/200)
        o=m.observe(y)
        rows.append(dict(time=T,flux_coefficient=o['flux']/T**4,
                         reader_coefficient=o['reader']/T**5,protection_coefficient=o['Qcore']/T**6))
    check(abs(rows[0]['reader_coefficient']/k5-1)<.001,'Exterior coefficient unresolved.')
    check(abs(rows[0]['protection_coefficient']/k6-1)<.001,'Protection coefficient unresolved.')
    # Core current symmetry and exact tetrahedral ground preparation.
    m0=ContactNetwork('tetra',4,False);y=prepare(m0,dict(kind='ground',signal=p,reference=r,inventory=n))
    ob=m0.observe(y);F,mu=radial_ground(4)
    close(ob['H'],2*n*mu);check(max(map(abs,ob['gauss']))<1e-14,'Ground state not neutral.')
    onset=sum(s*m0.rhs(y)[m0.eoff+e] for e,s in m0.faces[m0.target])
    close(onset,2*HOP*n*F[0]**2*(p-r))
    # Isolated triangle stationary record and clearance.
    mt=ContactNetwork('triangle',48);yt=prepare(mt,dict(kind='triangle_stored'))
    ot=mt.observe(yt);margin=-ot['H']-2*HOP*ot['N']
    check(margin>0,'Prepared triangle is not protected.')
    return dict(status='PASS',energy_derivative_error=abs(energy),regional_power_error=regional_error,
        loading_coefficients=dict(flux=k4,external_reader=k5,local_protection=k6),coefficient_checks=rows,
        triangle_margin=margin,triangle_clearance=2*math.asin(margin/(2*HOP*ot['N'])),
        scope='Differential identities and independently integrated small-time coefficient checks.')


def campaign(name: str):
    """All schedules are specified without consulting an outcome."""
    cases=[]
    def add(**kw):
        c=dict(geometry='tetra',length=4,kind='loaded',reader=True,inventory=.5,
               donor=1,signal=.75,reference=.25,T=80.,step=.04,sample=1.,group='control')
        c.update(kw);cases.append(c)
    if name in ('paper','full'):
        for p in (0.,.25,.5,.75,1.):
            for j in range(16):add(signal=p,reference=(j+.5)/16,group='main_grid')
        # Disjoint reference nodes and signal fractions: post-discovery confirmation.
        for p in (.1,.3,.7,.9):
            for j in range(32):add(signal=p,reference=(j+.5)/32,T=12.,group='confirmation')
    for p,r in ((.75,.25),(.25,.75),(.5,.5),(1.,0.),(0.,1.)):
        for reader in (False,True):
            add(signal=p,reference=r,reader=reader)
    for kind in ('ground','phase_control','delay_control','packet'):
        for reader in (False,True):add(kind=kind,reader=reader,phase=0.,donor=2 if kind=='packet' else 1)
    for p,r in ((.75,.25),(1.,0.),(.25,.21875)):
        add(signal=p,reference=r,step=.02,group='refinement')
        add(signal=p,reference=r,step=.04,group='refinement')
    add(length=8,T=80.,group='host_size')
    add(length=4,donor=2,T=80.,group='distance')
    for n in (.25,1.):add(inventory=n,group='inventory')
    if name in ('paper','full'):
        for p in (0.,.25,.5,.75,1.):
            for r in (.125,.375,.625,.875):
                add(length=0,kind='ground',reader=False,signal=p,reference=r,T=20.,step=.02,group='ground_grid')
        add(length=0,kind='ground',reader=False,signal=1.,reference=0.,inventory=6.,T=40.,step=.01,group='outside_bound')
        for pulse,probe in ((.1,True),(-.1,True),(.1,False),(0.,True)):
            add(geometry='triangle',length=48,kind='triangle_blank',reader=False,
                total_inventory=12.,pulse=pulse,probe=probe,T=300.,group='legacy_write_read')
        add(geometry='triangle',length=48,kind='triangle_stored',reader=False,
            total_inventory=6.,probe=True,centers=[10,22],T=300.,group='legacy_write_read')
    if name=='full':
        for p in (.125,.375,.625,.875):
            for j in range(32):add(signal=p,reference=(j+.5)/32,T=300.,group='extended_grid')
    # Remove exactly duplicated configurations; do not remove unfavorable results.
    unique={json.dumps(c,sort_keys=True):c for c in cases}
    return list(unique.values())


def aggregate(cases,checks):
    done=[c for c in cases if c.get('status')=='COMPLETED']
    tables=[]
    for group,times in (('main_grid',(5.,10.,20.,40.,80.)),('confirmation',(5.,10.,12.)),('ground_grid',(1.,5.,20.))):
        signals=sorted({c['config']['signal'] for c in done if c['config']['group']==group})
        for t in times:
```

```
            for p in signals:
                selected=[c for c in done if c['config']['group']==group and c['config']['signal']==p]
                rows=[next(o for o in c['rows'] if abs(o['t']-t)<1e-9) for c in selected]
                field='current' if group=='ground_grid' else 'reader'
                labels=[sign(o[field]) for o in rows]
                tables.append(dict(group=group,time=t,signal=p,trials=len(rows),positive=labels.count(1),
                    negative=labels.count(-1),unresolved=labels.count(0),
                    positive_circulations=sum(sign(o['flux'])==1 for o in rows),
                    negative_Q=sum(o['Qcore'] < -1e-13 for o in rows),
                    minimum_reader_magnitude=min(abs(o[field]) for o in rows)))
    ref=[]
    for c in done:
        cfg=c['config']
        if cfg['group']=='refinement' and cfg['step']==.04:
            fine=next((z for z in done if z['config']==dict(cfg,step=.02)),None)
            if fine:
                ref.append(dict(signal=cfg['signal'],reference=cfg['reference'],
                    maximum_flux_difference=max(abs(a['flux']-b['flux']) for a,b in zip(c['rows'],fine['rows'])),
                    maximum_reader_difference=max(abs(a['reader']-b['reader']) for a,b in zip(c['rows'],fine['rows'])),
                    maximum_Q_difference=max(abs(a['Qcore']-b['Qcore']) for a,b in zip(c['rows'],fine['rows']))))
    main=[c for c in done if c['config']['group']=='main_grid']
    early_all_Q=sum(all(o['Qcore'] < -1e-13 for o in c['rows'] if 5<=o['t']<=10) for c in main)
    early_all_sign=sum(all(sign(o['reader'])==sign(c['config']['signal']-c['config']['reference'])
                           for o in c['rows'] if 5<=o['t']<=10) for c in main)
    maxima={k:max((c['errors'][k] for c in done),default=0.) for k in ('energy','inventory','gauss','core_work','
     core_inventory')}
    return dict(status='COMPLETED' if len(done)==len(cases) else 'PAUSED',completed=len(done),requested=len(cases),
                checks=checks,maximum_residuals=maxima,complete_tables=tables,refinement=ref,
                main_grid_sampled_protected_5_to_10=early_all_Q,
                main_grid_sampled_correct_reader_5_to_10=early_all_sign,
                scope='All launched preparations counted. Finite grids and sampled intervals are not continuum or interval-
     certified claims.')


def report(root: Path, result: dict):
    lines=['# T35 connected loading and readout','',result['scope'],'',
           'Completed trajectories: '+str(result['completed'])+' / '+str(result['requested']),
           '', '## Complete outcome tables','',
           '| Group | Time | Signal | + | - | Null | Trials | Q < 0 |',
           '|---|---:|---:|---:|---:|---:|---:|---:|']
    for r in result['complete_tables']:
        lines.append(f"| {r['group']} | {r['time']:g} | {r['signal']:g} | {r['positive']} | {r['negative']} | {r['unresolved
     ']} | {r['trials']} | {r['negative_Q']} |")
    lines+=['','## Residuals','',json.dumps(result['maximum_residuals'],indent=2),
            '', '## Step refinement','',json.dumps(result['refinement'],indent=2),
            '', 'The short-time theorem includes loading and reader backreaction. Late reversals are retained.',
            'Initial donor fractions and phases are supplied; an autonomous ensemble generator and electrical register are
     not claimed.']
    (root/'execution_report.md').write_text('\n'.join(lines)+'\n',encoding='utf-8')
    if result['complete_tables']:
        with (root/'complete_counts.csv').open('w',newline='',encoding='utf-8') as f:
            writer=csv.DictWriter(f,fieldnames=list(result['complete_tables'][0]));writer.writeheader();writer.writerows(
     result['complete_tables'])


def main() -> int:
    parser=argparse.ArgumentParser(description=__doc__)
    parser.add_argument('--output-root',type=Path,default=Path('T35_outputs'))
    parser.add_argument('--campaign',choices=('quick','paper','full'),default='paper')
    parser.add_argument('--workers',type=int,default=18)
    parser.add_argument('--hours',type=float,default=2.)
    parser.add_argument('--resume',action='store_true')
    parser.add_argument('--summary',action='store_true')
    parser.add_argument('--checks-only',action='store_true')
    args=parser.parse_args()
    if args.workers<1 or args.hours<0:parser.error('Use positive workers and a nonnegative budget.')
    root=args.output_root.expanduser().resolve();root.mkdir(parents=True,exist_ok=True)
    source=Path(__file__).resolve();digest=hashlib.sha256(source.read_bytes()).hexdigest()
    if args.summary:
        p=root/'execution_report.md'
        if not p.exists():parser.error('No execution report exists in this directory.')
        print(p.read_text());return 0
    manifest=root/'manifest.json';identity=dict(version=VERSION,source_sha256=digest,campaign=args.campaign)
    if manifest.exists():
        old=json.loads(manifest.read_text())
        if any(old.get(k)!=v for k,v in identity.items()):
            parser.error('This output directory belongs to another source/campaign; use a new directory.')
```

```
    lock=root/'RUNNING.lock'
    try:
        fd=os.open(lock,os.O_CREAT|os.O_EXCL|os.O_WRONLY)
        os.write(fd,str(os.getpid()).encode());os.close(fd)
    except FileExistsError:
        parser.error('RUNNING.lock exists. Confirm no process is using the directory before removing it.')
    started=time.monotonic();deadline=time.time()+args.hours*3600
    try:
        for marker in ('COMPLETE.txt','FAILED.json'):
            if (root/marker).exists():(root/marker).unlink()
        atomic_json(manifest,dict(identity,python=platform.python_version(),requested_workers=args.workers))
        if source.parent!=root:shutil.copy2(source,root/'T35.py')
        checks={}
        for name,fn in (('history_and_first_records',history_checks),('joint_and_Bell',probability_checks),
                        ('reference_and_energy',bridge_checks),('native_equations',native_checks)):
            checks[name]=fn();print(name+': PASS',flush=True)
        atomic_json(root/'checks.json',dict(source_sha256=digest,results=checks))
        configs=[] if args.checks_only else campaign(args.campaign)
        workers=min(args.workers,18,os.cpu_count() or 1,max(1,len(configs)))
        print(f'Executing {len(configs)} trajectories with {workers} worker(s).',flush=True)
        cases=[]
        if configs:
            payloads=[(cfg,str(root),digest,args.resume,deadline) for cfg in configs]
            with ProcessPoolExecutor(max_workers=workers) as pool:
                futures=[pool.submit(trajectory,p) for p in payloads]
                for f in as_completed(futures):
                    cases.append(f.result())
                    if len(cases)%20==0 or len(cases)==len(configs):print(f'{len(cases)}/{len(configs)} jobs accounted for.',
     flush=True)
        cases.sort(key=lambda c:json.dumps(c['config'],sort_keys=True))
        result=aggregate(cases,checks)
        result.update(identity,actual_workers=workers,elapsed_seconds=time.monotonic()-started)
        atomic_json(root/'results.json',result);report(root,result)
        if result['status']=='COMPLETED':
            (root/'COMPLETE.txt').write_text(digest+'\n',encoding='utf-8')
        print(result['status']+': '+str(root),flush=True)
        return 0 if result['status']=='COMPLETED' else 2
    except Exception as exc:
        atomic_json(root/'FAILED.json',dict(identity,error=type(exc).__name__+': '+str(exc)))
        print(type(exc).__name__+': '+str(exc),file=sys.stderr);return 1
    finally:
        lock.unlink(missing_ok=True)

if __name__=='__main__':
    raise SystemExit(main())
```

J Complete Windows PowerShell runner

```
[CmdletBinding()]
param(
    [string]$OutputRoot = 'C:\Users\thile\Downloads\T35_Rebuilt_outputs',
    [ValidateSet('quick','paper','full')][string]$Campaign = 'paper',
    [ValidateRange(1,256)][int]$Workers = 18,
    [ValidateRange(0,1000)][double]$Hours = 2,
    [switch]$Resume,
    [switch]$Summary,
    [switch]$ChecksOnly,
    [switch]$OpenOutput,
    [switch]$NoPause
)
$ErrorActionPreference = 'Stop'
$ExitCode = 1
try {
    $Here = if ($PSScriptRoot) { $PSScriptRoot } else { (Get-Location).Path }
    $OutputRoot = [IO.Path]::GetFullPath($OutputRoot)
    [void][IO.Directory]::CreateDirectory($OutputRoot)
    $ExecutableDir = Join-Path $OutputRoot 'executable'
    [void][IO.Directory]::CreateDirectory($ExecutableDir)
    $Master = Join-Path $Here 'Paper_T35.tex'
    $Adjacent = Join-Path $Here 'T35.py'
    $Script = Join-Path $ExecutableDir 'T35.py'
    $Utf8 = New-Object System.Text.UTF8Encoding($false)
    if (Test-Path -LiteralPath $Master) {
        $Text = [IO.File]::ReadAllText($Master)
        $Pattern = '(?s)\\begin\{filecontents\*\}\[overwrite\]\{T35\.py\}\r?\n(.*?)\\end\{filecontents\*\}'
        $Match = [regex]::Match($Text, $Pattern)
        if (-not $Match.Success) { throw 'Complete embedded T35.py was not found in Paper_T35.tex.' }
        [IO.File]::WriteAllText($Script, $Match.Groups[1].Value, $Utf8)
    } elseif (Test-Path -LiteralPath $Adjacent) {
        if ([IO.Path]::GetFullPath($Adjacent) -ne [IO.Path]::GetFullPath($Script)) {
            Copy-Item -LiteralPath $Adjacent -Destination $Script -Force
        }
    } else {
        throw "Place this runner beside Paper_T35.tex or T35.py. Neither was found in $Here."
    }
    $Candidates = @(
        'C:\Users\thile\AppData\Local\Programs\Python\Python311\python.exe',
        (Join-Path $env:LOCALAPPDATA 'Programs\Python\Python311\python.exe'),
        (Join-Path $env:LOCALAPPDATA 'Programs\Python\Python312\python.exe'),
        (Join-Path $env:LOCALAPPDATA 'Programs\Python\Python313\python.exe')
    )
    $Python = $null
    $Prefix = @()
    foreach ($Candidate in $Candidates) {
        if (Test-Path -LiteralPath $Candidate) { $Python = $Candidate; break }
    }
    if (-not $Python) {
        $Command = Get-Command python -ErrorAction SilentlyContinue
        if ($Command) { $Python = $Command.Source }
    }
    if (-not $Python) {
        $Command = Get-Command py -ErrorAction SilentlyContinue
        if ($Command) { $Python = $Command.Source; $Prefix = @('-3') }
    }
    if (-not $Python) { throw 'Python 3.11 or newer was not found. Install Python and run this launcher again.' }
    & $Python @Prefix -c 'import sys; raise SystemExit(0 if sys.version_info >= (3,11) else 1)'
    if ($LASTEXITCODE -ne 0) { throw 'Python 3.11 or newer is required.' }
    $Hash = (Get-FileHash -Algorithm SHA256 -LiteralPath $Script).Hash.ToLowerInvariant()
    [IO.File]::WriteAllText((Join-Path $OutputRoot 'source_sha256.txt'), "$Hash`n", $Utf8)
    $Arguments = @($Prefix) + @($Script, '--output-root', $OutputRoot,
        '--campaign', $Campaign, '--workers', [string]$Workers,
        '--hours', $Hours.ToString([Globalization.CultureInfo]::InvariantCulture))
    if ($Resume) { $Arguments += '--resume' }
    if ($Summary) { $Arguments += '--summary' }
    if ($ChecksOnly) { $Arguments += '--checks-only' }
    $Stamp = Get-Date -Format 'yyyyMMdd_HHmmss'
    $Stdout = Join-Path $OutputRoot "stdout_$Stamp.log"
    $Stderr = Join-Path $OutputRoot "stderr_$Stamp.log"
    # Quote arguments for Windows process creation; no shell command payload.
    $Quoted = $Arguments | ForEach-Object { '"' + ($_ -replace '"','\"') + '"' }
    Write-Host "Program: $Script"
    Write-Host "Output:  $OutputRoot"
```

```
    Write-Host "Logs:    $Stdout and $Stderr"
    Write-Host 'A STOP.txt file in the output directory requests a checkpoint.'
    $Process = Start-Process -FilePath $Python -ArgumentList ($Quoted -join ' ') `
        -NoNewWindow -Wait -PassThru -RedirectStandardOutput $Stdout -RedirectStandardError $Stderr
    $ExitCode = $Process.ExitCode
    if (Test-Path -LiteralPath $Stdout) { Get-Content -LiteralPath $Stdout | Write-Host }
    if (Test-Path -LiteralPath $Stderr) { Get-Content -LiteralPath $Stderr | Write-Host }
    if ($ExitCode -eq 2) {
        Write-Host 'Paused with checkpoints. Remove STOP.txt if present, then repeat with -Resume.'
    } elseif ($ExitCode -ne 0) {
        throw "The calculation reported exit code $ExitCode. Inspect FAILED.json and the logs."
    }
    if ($PSCommandPath) {
        $RunnerCopy = Join-Path $OutputRoot 'Run_T35.ps1'
        if ([IO.Path]::GetFullPath($PSCommandPath) -ne [IO.Path]::GetFullPath($RunnerCopy)) {
            Copy-Item -LiteralPath $PSCommandPath -Destination $RunnerCopy -Force
        }
    }
    if ($OpenOutput) { Start-Process -FilePath explorer.exe -ArgumentList ('"' + $OutputRoot + '"') }
} catch {
    Write-Host $_.Exception.Message -ForegroundColor Red
    $ExitCode = 1
} finally {
    if (-not $NoPause) { [void](Read-Host 'Press Enter to close') }
}
exit $ExitCode
```